Studies on Hydrothermal Mineralization Method for Detoxification of Polluted Water and Resource Recovery

Takeshi Itakura

Contents

Chapter 1. General introduction

1.1. Industrial wastewater and ground water pollution

1.1.1 Environmental water and effluent standards

Currently, human beings produce various structural and functional materials by mining a lot of natural mineral resources. These manufacturing processes discharge a large amount of industrial wastes, which contains harmful elements against human body. Especially, the emission of industrial wastewater containing harmful elements is one of the serious problems, because there is a possibility that they diffuse into the environment and their bioaccumulation will occur through series of food chain. In addition, these harmful elements are generally concentrated in certain area in the world and poisoning due to an overdose of these harmful elements into rainwater and well water is a serious problem. Therefore, fundamental law in order to inhibit water pollution is enacted as the environmental water and effluent quality standard. There are twenty-six environmental water standards, which are set relevant to human health in Japan [1]. These standards were set for the elements or chemical compounds, the toxicity of which had been confirmed against humankind or the environment. WHO also enacted the guideline for some elements and compounds and in drinking water [2]. On the other hand, the effluent standards of harmful compounds and elements discharged from industrial activities are set independently in each country. Generally, the values of effluent standards are enacted at ten times higher value than that of the environmental standard. Table 1-1 shows the Japanese national environmental and effluent standards of inorganic chemicals. These elements have high toxicity against human beings. For example, excess intake of boron causes abnormalities of generative organ, and arsenic causes abnormalities of sensation and cancers. Therefore, the detoxification treatment of wastewater or ground/underground water is a

fundamental approach for environmental conservation. Among these harmful elements, boron, fluorine, arsenic and antimony are especially remarked because of their difficulty to remove toxicity from aqueous media. The effluent standard of antimony has not been set, but the reference value of effluent is set at 0.02 mg/dm^3 and that of drinking water is set at 0.002 mg/dm^3 because of its toxicity. Thus, detoxification of antimony is also investigated in the present work.

Table 1-1. National environmental and effluent standards in Japan

	Environmental water standard (mg/dm^3)	Effluent standard (mg/dm^3)
Cd	0.01	0.1
CN	0.1	1
P	0.1	1
Pb	0.01	0.1
Cr(VI)	0.05	0.5
As	0.01	0.1
Se	0.01	0.1
B	1	10
F	0.8	8

1.1.2. Industrial wastewater pollution by boron, arsenic and antimony

Boric acid is used by the various industrial manufacturers such as in semiconductors, ceramics and glasses. Aqueous solution of boric acid shows excellent buffer capacity so that it is widely used in plating industries as buffer solution. Thus, the wastewater containing very high concentrations of boron with several hundreds to thousands mg/dm^3 is generated in these industrial processes. In addition,

the contamination of boron in wastewater occurs also by combustion of coal. Therefore, contaminated wastewater by boric acid is generated from thermal power plants. Co-existence of boric and fluoride ions forms tetrafluoroboric ion by the reaction between boric and fluoride ions. This ion in aqueous media cannot be removed by the conventional method because of its high stability [3].

The wastewater containing arsenic is exhausted from advanced material manufacturing factories such as GaAs and thermal power plants. The arsenic concentration in the wastewater discharged from these industries is not so high, but it has very high toxicity for human being. Thus, detoxification treatment is necessary even when the concentration of arsenic is very low [4-6].

Recently, other element, for example, antimony has received a growing concern over the adverse effect on human health due to its high toxicity and increasing industrial use. Antimony has been used in large quantities as fire retardants, ceramics and other industrial use [7-9].

1.1.3. Ground water pollution

Ground water pollution by boron and arsenic were reported in several countries. The largest boron resource in the world exists in Turkey, where the contamination of water by boric mines is a common environmental problem [10, 11]. The, existing conformation of borate mineral in Turkey is borax, which is soluble into water (see 1.2.1). Arsenic pollution problems in groundwater emerge mainly in Asian countries in such as Bangladesh, India, and China [12-18], where the concentration of arsenic more than hundred to thousand times higher than that of the standard of environmental water is detected. Besides, the contamination by arsenic species in ground water emerges in Japan from hot spring and mine effluent in such as Toyohira River [19]. Therefore, the system construction for removing these elements from ground water is

strongly desired.

1.2. Mineralogy and chemistry

1.2.1. Mineralogy and chemistry of boron

Boron is found in a variety of similar minerals, which are related to borax, sodium tetra borate ($Na_2B_4O_7 \cdot 10H_2O$) [11]. It is a relatively rare element in the earth's crust, representing only 1 x 10^{-3} % as Clark number. Borax is buried in large amounts in Turkey, United States and South Africa. The production of boron trioxide is the initial processes in the synthesis of all boron compounds. The most common mineral for industrial use for producing boron trioxide is borax, because it is easily soluble in water. However, there are other borate minerals utilized actually. One of the minerals exploited for industrial boron trioxide production is ulexite, $CaB_4O_7 \cdot NaBO_2 \cdot 8H_2O$. The others are colemanite ($Ca_2B_2O_5$) and parasibirskite ($Ca_2B_2O_5 \cdot H_2O$), which are calcium borate minerals formed by alteration of ulexite. The boron trioxide production from these minerals is carried out by the treatment with H_2SO_4 to produce boric acid and evaporating, which is the same process as from borax.

The electron configuration of boron is $1s^2\ 2s^2\ 2p^1$. It has only three electrons to work with, so the ion is unpolarizable, and does not hydrate. For this reason, boron is not eager to donate electrons in an electrovalent bond, and can also not accept them easily. Therefore, most of its bonds are covalent, and even forms half-bonds in which only one electron is shared covalently. This gives boron an apparent valence of +3. The first ionization potential is 8.30 V, which is not unusually high and it classified as metalloid. The commonly used boron compounds are ortho boric acid, or simply boric acid, H_3BO_3, and boron trioxide, B_2O_3. The formula for boric acid can be written $B(OH)_3$, as boron hydroxide.

In aqueous solution, boric acid is a very weak acid. Its first ionization constant is 6.4 x 10^{-10} (pKa = 9.14). Figure 1-1 shows the variation of conformation of boric acid by changing pH of solution [20]. Boric acid in the neutral solution does not have any charge. At lower pH, it can be shown as H_3BO_3 and at higher pH, $H_2BO_3^-$. Thus, aqueous solution containing high concentration of boric acid shows fabulous buffer capacity. In addition, boron shows various types of ions depending on its concentration or composition. Figure 1-2 shows the circularity composition of borax (Figure 1-2-(a)) and the other typical compositions of borates. Tetrafluoroboric ion is formed with co-existence of boric and fluoride ions. Fluoride ion is frequently contained together with boric acid in the wastewater discharged from plating industries and thermal power plant together with boric acid. In this case, certain boric acid form tetrafluoroboric ion by the reaction with fluoride ion. Tetrafluoroboric ion exists not only in the wastewater discharged from plating industry, but also it is used for counter anion to cationic component in the ionic liquid, e.g., $(BMI)BF_4$ (BMI: butyl-methyl-imidazolium). However, the removal or recovery method of tetrafluoroboric ion is not reported elsewhere because of its very high stability in aqueous media.

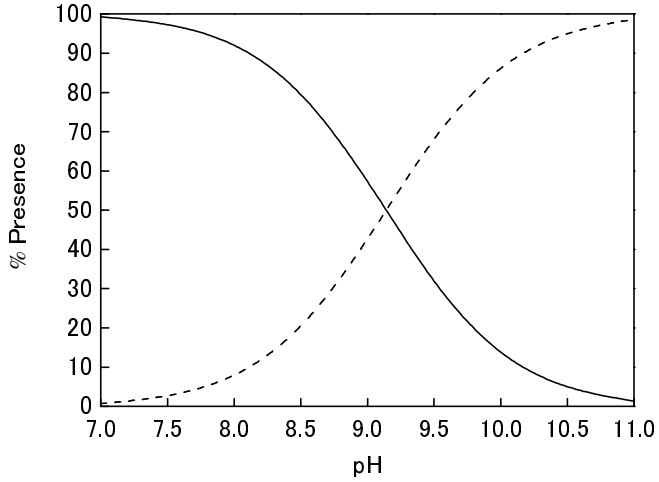

Figure 1-1. Distribution of $H_3BO_3/H_2BO_3^-$ as a function of pH. Solid line: distribution of H_3BO_3 and broken line: $H_2BO_3^-$. Temperature: 25 °C.

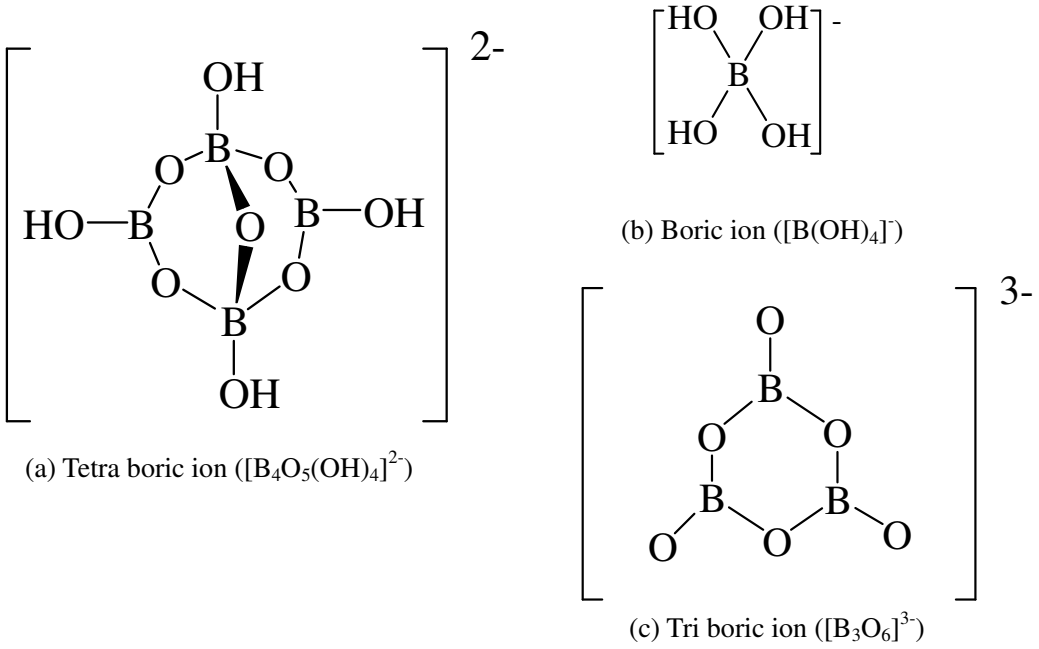

(a) Tetra boric ion ($[B_4O_5(OH)_4]^{2-}$)

(b) Boric ion ($[B(OH)_4]^-$)

(c) Tri boric ion ($[B_3O_6]^{3-}$)

Figure 1-2. Typical conformation of boric ion species.

1.2.2. Mineralogy and chemistry of arsenic

Abundance of arsenic in the earth's crust is estimated as 5 x 10^{-4} %, not much more than that of rare earth metal, and only four times more than that of platinum. Thus, minerals are not mined specifically for arsenic. Arsenic is very frequently accompanied with ore of gold, silver, lead and copper. It is produced as a by-product of refining process of these minerals. It is known that there are some minerals containing arsenic such as sulfide (As_2S_2 or As_2S_3) and arsenopyrite (FeAsS) [13, 14, 21-23]. However, these minerals are not used as industrial resources for production because of their very low concentration in earth's crust. However, chronic arseniasis in some Asian countries as described in 1.1.3 is caused by contamination of arsenic due to the dissolution of these minerals into ground and underground water.

Arsenic has the atomic number 33, so it has 33 electrons in the configuration $1s^2$ $2s^2$ $2p^6$ $3s^2$ $3p^2$ $3d^{10}$ $4s^2$ $4p^3$. The same outer shell s^2p^3 is shared by N, P, Sb and Bi. Thus, the general properties of arsenic are similar to phosphorus and antimony. The outer shell suggests the valences of 3 and 5 for arsenic, and indeed these are observed. The first ionization potential of As is 10.5 V, which is quite high for a metal, but rather low for a nonmetal. Therefore, arsenic is also classified as metalloid. Arsenic has the valence +3 in the trioxide As2O3, while in the pentaoxide As_2O_5 the valence is +5. When these oxides are dissolved in water, they attract H^+ and OH^- ions, and may rearrange their structures. In the case of As_2O_5, we find that

$$As_2O_5 + 3H_2O \rightarrow 2H_3AsO_4$$

The molecule formed by this reaction is ortho arsenic acid, which dissociates to release H^+ ions to form an acidic solution. This ion has similar properties to the ortho phosphoric acid, H_3PO_4. Here, arsenic behaves as a nonmetal and can form some salts with metals called arsenates. Similarly, As_2O_3 hydrolyzes to H_3AsO_3, arsenite acid, whose salts are called as the arsenites. These arsenic oxo ions such as H_3AsO_3 and H_3AsO_4, the oxidation number, the number of hydrogen and charge of each ion are varied by changing pH and the redox potential of solution. Figure 1-3 shows the redox potential versus pH diagram for inorganic arsenic species. Arsenate ion has negative charge at pH range of 2.5 to 14. On the other hand, arsenite ion has not charge at pH values lower than 10. In the groundwater, which is under relatively oxidative conditions, arsenic exists as arsenate ion and it has negative charge. However, under groundwater, which is under relatively reductive conditions, it exists as arsenite ion and it has no charge. Difference in such properties is the cause of difficulty of arsenite ion to remove from aqueous media.

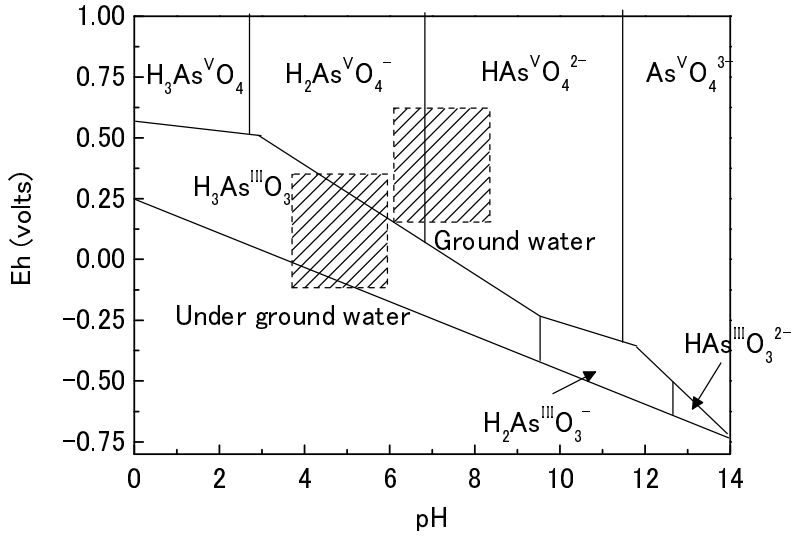

Figure 1-3. The redox potential versus pH diagram for inorganic arsenic species. Temperature: 25 °C.

1.2.3. Mineralogy and chemistry of antimony

The industrial production process of antimonic resources is the same as that of arsenic, i.e., it is by-product of gold, silver and platinum [13, 14, 23]. Thus, the specific mineral for antimony is not mined. Properties of antimony are similar to arsenic because it possesses sharing the same outer shell s^2p^3 as arsenic. In trioxide Sb_2O_3, Sb has the valence +3, while in the pentaoxide Sb_2O_5 the valence state or +5. In aqueous solution, they form H_3SbO_3 or H_3SbO_4 at each valence of +3 and +5 respectively. The first ionization potential of Sb is 8.64 V, and it is classified as metalloid. Figure 1-4 shows the redox potential versus pH diagram for antimonic species[24]. The pentavalent antimonic ion has negative charge in all range of pH. On the other hand, trivalence antimonic ion has no charge at lower pH values than 11.

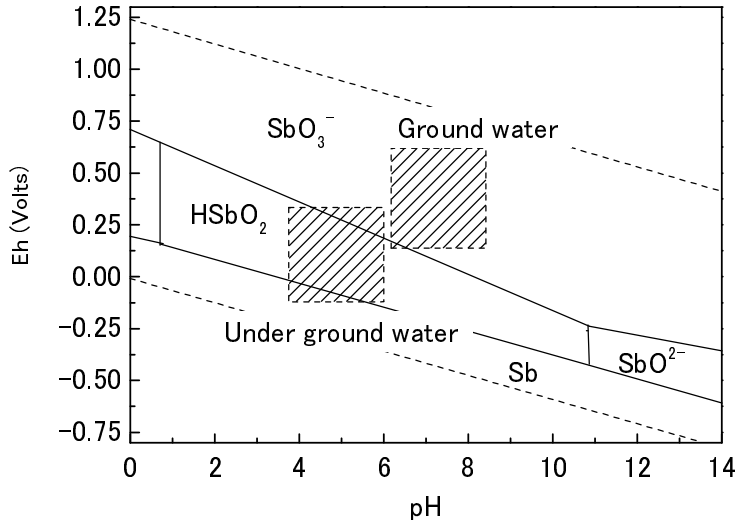

Figure 1-4. The redox potential versus pH diagram for inorganic antimonic species. Temperature: 25 °C.

1.3. Conventional detoxification methods of polluted water

The difficulty of removal of these toxic elements from aqueous media is responsible for formation of very stable oxoanions. These ions have various conformations depending on their concentration and pH values. Furthermore, As, Se and Sb take multiple oxidation numbers by changing pH and redox potential of the solution. Therefore, the traditional precipitation methods of transition metals from aqueous media by changing pH values or by addition of anions (*e.g.*, CO_3^{2-}) cannot be applied to such oxoanions as H_3SbO_4, H_3AsO_4 and H_3BO_3, because they exist as anions with high stability in aqueous media. Hence, alternative methods for removing these ions from aqueous media were investigated in the present work. Co-precipitation, ion exchange, and membrane methods are well known as detoxification methods for aqueous media containing these harmful oxoanions. The features of these methods are described in the following section. However, they have problems such as low removal yield and narrow applicable concentration range of ions.

Additionally, these methods are not developed for resource recovery, but for only detoxification of polluted water. Thus, the establishment of the system for removing and recovering mineral resources such as boron, arsenic and antimony from wastewater will be one of the world-important issues, because the natural mineral resources are finite, and poor especially in Japan. Therefore, the development of new treatment method of wastewater is strongly desired.

1.3.1. Co-precipitation and adsorption method

This treatment is one of the adsorption methods by precipitating various kinds of fine particles of metal oxide or hydroxide in aqueous solution [25, 26]. The important aspects of the adsorbing reagent, such as aluminum hydroxide, iron hydroxide, etc., are their strong interaction with treated matter and high specific surface area. Generally, this treatment method can be applied to removal of almost all harmful oxoanions by choosing the best adsorbent. Advantages of the treatment consist in low cost and effectiveness for the heavily polluted water. However, the removal rate of oxoanions is so low compared with the added amount of adsorbent, especially in case of treating electrically uncharged species like H_3AsO_3. On the other hand, generation of a large amount of polluted adsorbent, which contains very low concentration of hazardous elements, caused the secondary environmental pollution problem. Thus, the disposal treatment for the polluted adsorbent is required followed by the detoxification treatment for polluted water.

1.3.2. Ion exchange and solvent extraction method

Ion exchange method is effective for specific ions and the polluted water with low concentration of pollutants [27, 28]. Shortage of this method is relatively narrow concentration range for the applicable pollutants. It cannot be applied to heavily

polluted water, because high running const was required for the exchange resin due to very short period of re-generation process. Moreover, the dissolution of solvents and resins into the treated-water arouses another serious environmental pollution problem.

1.3.3. Membrane filtration method

Recently, membrane method for detoxifying polluted water is actively investigated [29, 30]. Especially, removing boric acid from seawater by reverse osmosis and ultrafilteration is remarked for desalination. Advantage of this treatment is that the concentrated hazardous waste can be reused as commercially available resources. But, very high pressure (several MPa) is necessary to concentrate pollutants as molecular level, so that this method is actually used only in specific fields. Therefore, modification methods by using surfactants are investigated in order to reduce required pressure for treating arsenic species. However, this method is inefficient in treating trivalent arsenic, because, the modification by using surfactants can be applied only for electrically charged ions.

1.4. Hydrothermal mineralization

It is expected that the recovery of hazardous ions as reusable precipitate from aqueous media is effective for resource circulation and prevention of environmental pollution. However, as mentioned in 1.3, there is no report for precipitation method of boron, arsenic and antimony species. This is attributed to high stability of each oxoanion in aqueous media. Meanwhile, there are a lot of insoluble or hardly soluble compounds or minerals containing high concentration of born, arsenic and antimony in nature e.g., $Ca_2B_2O_5$, $Ca_5(AsO_4)_3(OH)$, etc. Humans have obtained industrial resources from these minerals by a variety of resource production methods as described in 1.2. This fact implies us that there is some mechanism to form these

insoluble minerals in earth's crust. It is well known that the natural mechanism to form minerals from aqueous solution depends on the precipitation of minerals in water at high temperatures and pressure waters (in hydrothermal water). A majority of natural minerals exhibit negative water solubility curve with an increase of temperature [31]. On account of these conditions, hydrothermal mineralization treatment for detoxifying polluted water and recovering resources was investigated in present work by imitating natural mineral forming mechanism. The prospective advantages of this treatment are:

(1) By a theoretical sense, the concentrations of each ion are independent of the initial concentration. The concentration of hazardous ions in treated-water would be dependent on only the solubility of formed minerals.

(2) Formed precipitates by hydrothermal mineralization treatment would be easily reused by the common resource production process, because, recovered precipitate is natural mineral commonly used as industrial resources. Thus, secondary environmental pollution can be solved by reusing recovered precipitate.

Therefore, it is expected that the establishment of hydrothermal mineralization treatment of polluted water would help to solve the problems of conventional detoxification methods, such as narrow concentration range for application, the secondary environmental pollution, etc.

1.5. Purpose of this study

As mentioned above, boric, arsenic, and antimonic oxoanions cannot be effectively removed from polluted water by the conventional methods. Accordingly, the recovery methods of respective resources from water polluted by these oxoanions should be developed in order to achieve resource circulation and solve the problems of conventional methods. The purpose of this study is to establish the hydrothermal

mineralization treatment to recover oxoanion in aqueous media as precipitate of minerals and detoxify the polluted water. Target materials are boric, arsenic, antimonic ions and the conjugated ions such as tetrafluoroboric ion formed in co-existence of boric and fluoride ions, contained in aqueous media. The detoxification of aqueous media containing ionic liquid, which contains some organic-inorganic harmful ions, is also investigated in order to confirm the availability of hydrothermal mineralization treatment for some organic-inorganic harmful element containing solvents. In Chapter 2 and 3, the precipitation recovery of boric ion and tetrafluoroboric ion by using hydrothermal mineralization with $Ca(OH)_2$ mineralizer was described. Then, in-situ solid/liquid separation effect for treating boric and tetrafluoroboric ions is investigated in order to enhance the treatment efficiency, which is shown in Chapter 4. The hydrothermal mineralization treatments for arsenate/arsenite ions and antimonic ion are described in Chapter 5 and 6 to extend the applicable pollutant by hydrothermal mineralization. The detoxification treatments of water containing ionic liquids by using combination of photocatalytic oxidation and hydrothermal mineralization are described in Chapter 7. Finally, Chapter 8 described thermodynamic explanation of hydrothermal mineralization and conclusions the results of each chapter.

References

1. *Handbook of water treatment*, 1998, Maruzen, In Japanese

2. WHO, *Geneva: World Health Organization*, (1993).

3. T. Itakura, R. Sasai, and H. Itoh, *Bulletin of the Chemical Society of Japan* **79**, (8), (2006). 1303-1307

4. *Patty's industrial hygiene and toxicology, 4th ed. volume II*. 1999; In Japanese.

5. *Clinical toxicology*. 2002, WB Saunders, In Japanese.

6. S. Tapio, and B. Grosche, *Mutation Research-Reviews in Mutation Research* **612**, (3), (2006). 215-246

7. N. Khalid, S. Ahmad, A. Toheed, and J. Ahmed, *Applied Radiation and Isotopes* **52**, (1), (2000). 31-38

8. J. Lintschinger, B. Michalke, S. Schulte-Hostede, and P. Schramel, *International Journal of Environmental Analytical Chemistry* **72**, (1), (1998). 11-25

9. M. Patriarca, A. Menditto, B. Rossi, T. D. B. Lyon, and G. S. Fell, *Microchemical Journal* **67**, (1-3), (2000). 351-361

10. M. Badruk, N. Kabay, M. Demircioglu, H. Mordogan, and U. Ipekoglu, *Separation Science and Technology* **34**, (13), (1999). 2553-2569

11. M. S. Celik, M. Hancer, and J. D. Miller, *Journal of Colloid and Interface Science* **256**, (1), (2002). 121-131

12. J. Akai, K. Izumi, H. Fukuhara, H. Masuda, S. Nakano, T. Yoshimura, H. Ohfuji, H. M. Anawar, and K. Akai, *Applied Geochemistry* **19**, (2), (2004). 215-230

13. M. Akcay, H. M. Ozkan, C. J. Moon, and B. Spiro, *Ore Geology Reviews* **29**, (1), (2006). 19-51

14. N. J. Cook, *Ore Geology Reviews* **11**, (5), (1996). 303-338

15. M. A. Hossain, M. K. Sengupta, S. Ahamed, M. M. Rahman, D. Mondal, D. Lodh, B. Das, B. Nayak, B. K. Roy, A. Mukherjee, and D. Chakraborti, *Environ. Sci. Technol.* **39**, (11), (2005). 4300-4306

16. K. S. Murray, D. T. Rogers, and M. M. Kaufman, *Journal of the American Water Resources Association* **42**, (3), (2006). 777-792

17. J. R. Parga, D. L. Cocke, J. L. Valenzuela, J. A. Gomes, M. Kesmez, G. Irwin, H. Moreno, and M. Weir, *J. Hazard. Mater.* **124**, (1-3), (2005). 247-254

18. P. Xu, S. B. Huang, Z. J. Wang, and G. Lagos, *Science of the Total*

Environment **362**, (1-3), (2006). 50-55

19. K. Tatumi, K. Jin, and H. Tachibana, *Journal of Japan Society on Water Environment* **29**, (11), (2006). 671-677

20. J. Redondo, M. Busch, and J. P. De Witte, *Desalination* **156**, (1-3), (2003). 229-238

21. D. G. Rancourt, D. Fortin, T. Pichler, P. J. Thibault, G. Lamarche, R. V. Morris, and P. H. J. Mercier, *American Mineralogist* **86**, (7-8), (2001). 834-851

22. G. C. Allan, and J. T. Woodcock, *Minerals Engineering* **14**, (9), (2001). 931-962

23. V. D. C. Daltry, and A. H. Wilson, *Mineralogy and Petrology* **60**, (3-4), (1997). 185-229

24. M. Kang, T. Kamei, and Y. Magara, *Water Research* **37**, (17), (2003). 4171-4179

25. A. G. Leyva, J. Marrero, P. Smichowski, and D. Cicerone, *Environ. Sci. Technol.* **35**, (18), (2001). 3669-3675

26. M. L. Pierce, and C. B. Moore, *Water Research* **16**, (7), (1982). 1247-1253

27. H. Hosgoren, S. Tural, F. Kahraman, M. Togrul, and M. Karakaplan, *Solvent Extraction and Ion Exchange* **15**, (2), (1997). 249-257

28. F. Kahraman, *Solvent Extraction and Ion Exchange* **13**, (6), (1995). 1025-1036

29. Y. Magara, A. Tabata, M. Kohki, M. Kawasaki, and M. Hirose, *Desalination* **118**, (1-3), (1998). 25-33

30. H. Gecol, E. Ergican, and A. Fuchs, *Journal of Membrane Science* **241**, (1), (2004). 105-119

31. *The Handbook of Hydrothermal Science,* 2000, Gihodo Shuppan, In. Japanese.

Chapter 2 Removal and recovery of boron from aqueous media containing boric ion by hydrothermal mineralization

2.1. Introduction

Boron distributes widely in the environment mainly as boric acid, and it is one of important micronutrients for plants, animals and humans. However, the excess intake of boron has a much greater impact on plants, animals and human bodies. For example, the tolerable limit of boron for citrus and some agricultural crops is 2 or 3 mg/dm^3. Thus, its recommended content for drinking water is 0.3 mg/dm^3 in European Union [1-3]. Recently, the quality standard of discharged water with boron from manufacturing plants has been set at 10 mg/dm^3 in Japan. On the other hand, boric acid is an important industrial resource and is widely used in many kinds of the manufacturing processes, such as in semiconductor and ceramic industries. Thus, the wastewater with several hundred to thousand mg/dm^3 of boron generates in these industrial processes day after day, and an effective removal technique is strongly desired [4].

Some removal methods have been already proposed in the following ways, even though most of them are too difficult to utilize as practical techniques because of some disadvantages. Co-precipitation and adsorption method using metal hydroxide is an inefficient and uneconomical process due to the fatal reasons, i.e. (1) the removal rate is low (2) a large amount of metal hydroxide is required and (3) large amount of unrecyclable wastes are discharged [5-11]. Secondly, evaporation–crystallization process is effective only in the streams with very high boron concentrations more than several thousand mg/dm^3. Thirdly, in the solvent extraction processes, some expensive extractants should be used. Removal of boron from water by this process is easy, but most of extractants are toxic [12, 13]. The fourth ion exchange method is

rather effective in removing boron compounds from wastewater containing several hundred to thousand mg/dm^3 of boron [2, 14-17]. However, the selective ion exchange resins are so expensive and the regeneration process is required so frequently that only small amount of wastewater can be treated [17]. Fifth, removal processes using membrane filter such as the reverse osmosis and polymer enhanced ultrafiltration have been developed [3, 8, 14, 16, 18-24]. However, these techniques are used for desalination process of sea water because, these techniques require high cost for the manufacturing and maintenance. And the other methods such as electro-coagulation method are also investigated [25, 26].

These removal methods, which are solvent extraction, ion exchange and membrane filtration, can be applied only to the wastewater with low boron concentration between several dozen and hundred mg/dm^3. Therefore, the above mentioned removal techniques cannot recover boron element as recyclable compounds, i.e., an appropriate waste treatment will not be available without landfill disposal. Therefore, it is desired to establish the environmentally friendly removal/recovery method of boron from wastewater at lower cost and higher efficiency, especially for boron containing several hundred to thousand mg/dm^3.

In the present study, the recovery method of boron from wastewater containing boric acid was developed to produce reusable borate ore by the hydrothermal treatment, which was analogous to the formation process of borate ore in nature.

2.2. Experimental procedure

Model synthetic wastewaters with 500 or 3000 mg/dm^3 of boron were prepared by dissolving B_2O_3 (Wako Pure Chemical Industries, Ltd.) in distilled and deionized water. These model wastewaters (30 ml) were sealed in a pressure vessel lined with fluorocarbon resin together with reagents. Mineralizer such as $Ca(OH)_2$ or $Mg(OH)_2$

was added into the vessel and in some cases, H_3PO_4 was added in order to prevent re-dissolution of borate ore in the cooling process. Hydrothermal treatments were carried out by leaving the vessel in a dry oven for 2 - 24h at 100 - 200°C. After the hydrothermal treatment, the vessels were cooled down in atmospheric air for 1 hour or in ice water for 5 minutes. Precipitates obtained by the hydrothermal treatment were filtered and collected.

The precipitates were identified by X-ray diffraction (XRD: RIGAKU Rint-2500) using CuKα radiation. The microstructural observation and qualitative elements analysis of the precipitates were performed by scanning electron microscopy (SEM: JEOL JSM-T20) equipped with energy dispersive X-ray spectrometry (EDS: JED-2140). Quantitative elements analysis of the solvent obtained after hydrothermal treatment was carried out by the inductively couple plasma-atomic emission spectrometry (ICP-AES: Perkin-Elmer Optima3300DV).

2.3. Results and discussions

2.3.1. Hydrothermal mineralization of boron in boron containing wastewater

Almost all borate ores were mined as alkali- and/or alkaline earth borates, such as ascharite ($Mg_2B_2O_5 \cdot H_2O$), colemanite ($Ca_2B_6O_{11} \cdot 5H_2O$) and ulexite ($NaCaB_5O_9 \cdot 8H_2O$). The hydrothermal treatments of model wastewater with boron (500 mg/dm^3) and calcium or magnesium hydroxide were carried out at 150^{o}C for 14 hours. As a result, it was found that the boron concentration of model wastewater decreased only in the case when using calcium hydroxide as additives. Figure 2-1 shows the SEM photographs of the precipitates obtained by the hydrothermal treatment of model wastewater added with 1.5 g of $Ca(OH)_2$ at 150°C for 14 hours. The mixture of both needle-like crystals with diameter of 1 - 2μm and plate-like crystals with 10 - 100 μm of grain size was found in the micrographs.

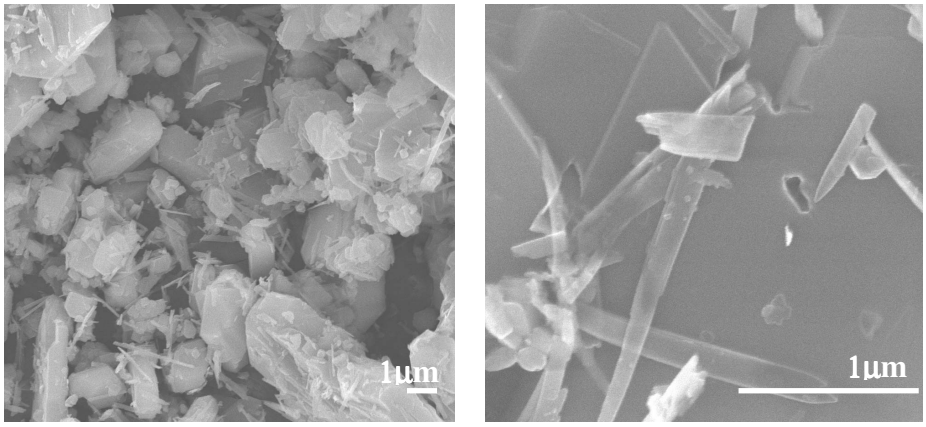

Figure 2-1. SEM photographs of precipitates obtained by the hydrothermal treatment at 150°C for 14 hours ($Ca(OH)_2$: 2.0g, B: 500 mg/dm^3).

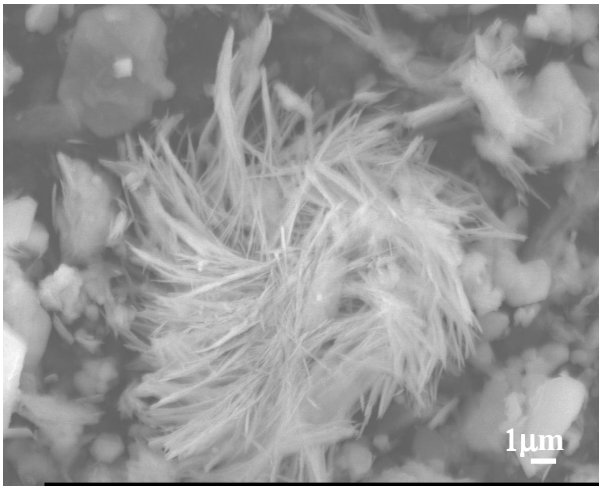

Figure 2-2. SEM photographs of precipitates obtained by the hydrothermal treatment at 150°C for 14 hours ($Ca(OH)_2$: 2.0g, B: 3000 mg/dm^3).

The needle-like crystals were observed only on the surface of the plate-like crystals. This fact suggests that the plate-like crystal would be required for precipitation of the needle-like crystals. In case of the hydrothermal treatment of model wastewater with 3000 mg/dm^3 of boron, the amount of needle-like crystals in the precipitate increased significantly with increasing boron concentration and they aggregated to form bundles of finer needle crystals (cf. Figure 2-2). EDS elemental qualitative analysis of these precipitates showed that the needle-like crystals contained Ca, O and B and plate-like

crystals contained Ca and O. Figure 2-3 shows the XRD pattern of the precipitate obtained from model wastewater with 3000 mg/dm^3 of boron where the diffraction peaks for both $Ca_2B_2O_5 \cdot H_2O$ and $Ca(OH)_2$ were identified. Thus, these results indicate that the needle crystals observed in Figure 2-1 and 2-2 are $Ca_2B_2O_5 \cdot H_2O$ formed by the hydrothermal treatment, and the plate-like crystals are mineralizer $Ca(OH)_2$. This suggests also that $Ca_2B_2O_5 \cdot H_2O$ crystals would be formed by the heterogeneous nucleation on the undissolved $Ca(OH)_2$ crystalline surface. Therefore, the hydrothermal mineralization treatment in the presence of calcium hydroxide could be available method for removal and collection of borate ore from the wastewater containing boric acid.

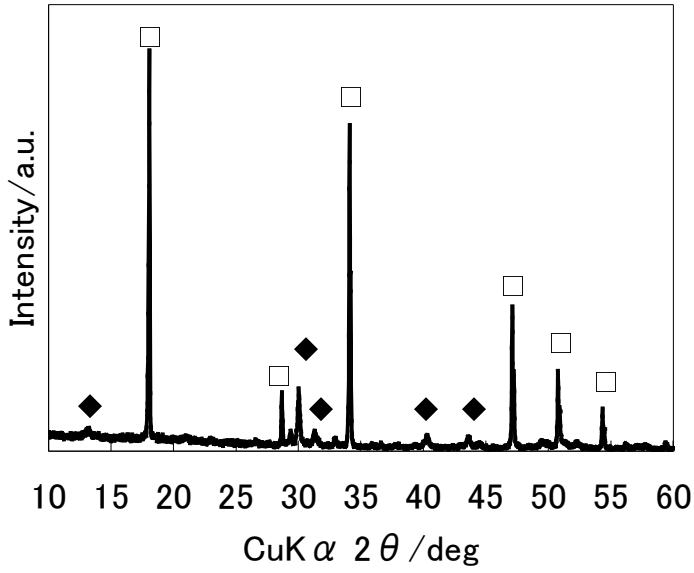

Figure 2-3. XRD pattern of the precipitate obtained by the hydrothermal treatment at 150°C for 14 hours ($Ca(OH)_2$: 2.0g, B: 3000 mg/dm^3). □: $Ca(OH)_2$ and ◆: $Ca_2B_2O_5 \cdot H_2O$.

2.3.2. Optimization of hydrothermal conditions

The boron concentration in the wastewater treated at 150 °C for 14 hours is plotted against the added amount of $Ca(OH)_2$ in Figure 2-4. The residual concentration of

boron decreased with an increase in the amount of added $Ca(OH)_2$, and was constant at ca. 80 mg/dm^3 for the added amount more than 3.0g. This verifies that 3.0 g of added $Ca(OH)_2$ is enough to precipitate the dissolved boron as the calcium borate. Figure 2-5 shows the treatment time dependence of the dissolved boron concentration after the hydrothermal treatment in the solvent added with 3.0g of $Ca(OH)_2$ at 150^{o}C. Residual boron concentration decreased rapidly with an increase in the treatment time and the recovery yield became constant after 6 hours. More than 80 % of dissolved boron was collected as $Ca_2B_2O_5 \cdot H_2O$ by the hydrothermal treatment at 150 °C for 6 hours under the optimal conditions in the presence of calcium hydroxide. However, the boron concentration in the model wastewater was still above 10 mg/dm^3, which is the quality standard value of discharged water in Japan. However, the boron concentration decreased from 80 to 60 mg/dm^3 by rapid cooling of the treated wastewater in the ice bath after hydrothermal treatment. This result indicates the solubility of the $Ca_2B_2O_5 \cdot H_2O$ under hydrothermal condition is lower than ordinary temperature and pressure. In this study, batch type pressure vessels were cooled down at room temperature for 1 h after the treatment. During this cooling process, re-dissolution of $Ca_2B_2O_5 \cdot H_2O$ would be occurred and B concentration increased. On the other hand, rapid cooling prevented re-dissolution of $Ca_2B_2O_5 \cdot H_2O$ by shorter cooling process (typically 10 min). Decrease of B concentration achieved separation of reaction solution from precipitate before re-dissolving large amount of $Ca_2B_2O_5 \cdot H_2O$ into treated-water. From this consideration, all of B concentration after the treatment shown in this study would be higher than that of under hydrothermal condition. Therefore, system construction to prevent re-dissolution would improve efficiency of removal and recovering B by hydrothermal mineralization treatment. In this chapter, re-dissolution preventation method by adding additives to form insoluble

compounds on the surface of precipitate and inhibit contact formed mineral with H_2O during cooling process was introduced.

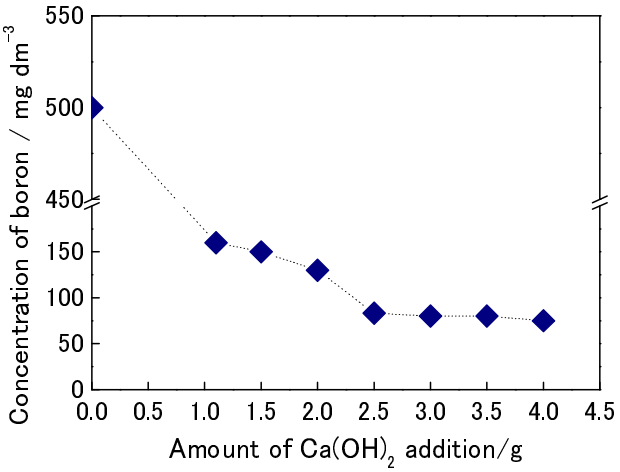

Figure 2-4. Dependence of concentration of boron in the treated water after hydrothermal treatment at 150°C for 14 hours on the amount of added $Ca(OH)_2$ (B: 500mg/dm^3).

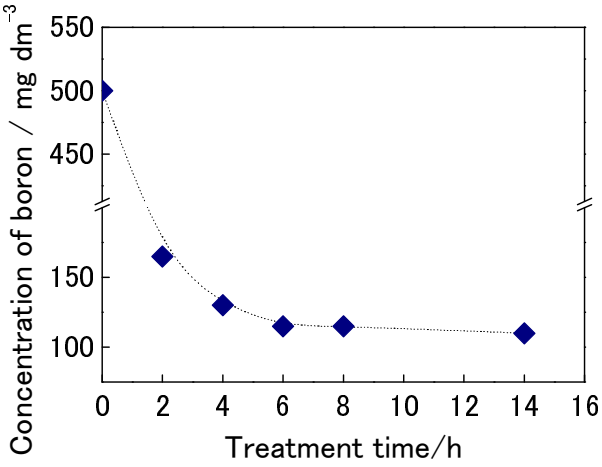

Figure 2-5. Dependence of concentration of boron in the treated water after hydrothermal treatment at 150°C on treatment time ($Ca(OH)_2$ 3.0g, B: 500 mg/dm^3).

2.3.3. Effect of additives on hydrothermal mineralization of dissolved boron

In natural environment, it is well known that calcium borate ore coexists with various calcium salts, which play as reagent for preventing dissolution of calcium

borate ore in aqueous media. The effect of various additives on the hydrothermal mineralization of boron was investigated in the presence of $Ca(OH)_2$ mineralizer for further reduction of boron concentration less than 10 mg/dm^3. As a result of the hydrothermal treatment with calcium hydroxide in the presence of various additives, such as H_2SO_4, $(COOH)_2$, H_3PO_4, and $Mg(OH)_2$, all additives prevented the re-dissolution of calcium borate and reduced the residual boron concentration contained in model wastewater. Detailed investigation to increase the yield was performed using $Ca(OH)_2$ as mineralizer and H_3PO_4 as additive, since H_3PO_4 was the most effective reagent among the above additives. XRD patterns of the precipitates obtained before and after the hydrothermal treatment at 130 °C for 14 hours with 3.0g of $Ca(OH)_2$ and 1.5g of H_3PO_4 are shown in Figure 2-6. The diffraction peaks of $Ca(OH)_2$ and $CaHPO_4 \cdot 2H_2O$ crystals were observed before the hydrothermal treatment (cf. Figure 2-6-b), while the diffraction peaks of $CaHPO_4 \cdot 2H_2O$ crystals disappeared after the hydrothermal treatment, and the new peaks originated from $Ca_{10}(PO_4)_6 \cdot 5H_2O$ (hydroxyl apatite) appeared after the hydrothermal treatment (cf. Figure 2-6-a). This XRD pattern predicted that $CaHPO_4 \cdot 2H_2O$ formed by addition of H_3PO_4 into the synthetic wastewater containing $Ca(OH)_2$ before hydrothermal treatment, and then, $CaHPO_4 \cdot 2H_2O$ converted to hydroxy apatite during the hydrothermal treatment. Thus, the improvement of removal rate of boron from model wastewater could be achieved by the formation of hydroxy apatite. SEM photograph of the precipitate is shown in Figure 2-7. The needle-like crystals wrapped with a number of microcrystals can be observed. Such microcrystals were not observed on the surface of needle-like crystals obtained by the hydrothermal treatment using only $Ca(OH)_2$ (cf. Figure 2-1). The microcrystals on the needle-like crystal might be synthesized by the addition of H_3PO_4. Result of EDS analysis of the microcrystals demonstrated that they consisted of Ca and P, while the needle-like crystals contained Ca and B in case of

the hydrothermal treatment with only $Ca(OH)_2$. Therefore, it is concluded that a thick film of $Ca_{10}(PO_4)_6 \cdot 5H_2O$ precipitated on the surface of needle-like calcium borate crystal. As a result, the removal rate of the boron from model wastewater increased, because the re-dissolution of calcium borate crystals was prevented by the overlayer of $Ca_{10}(PO_4)_6 \cdot 5H_2O$ microcrystals.

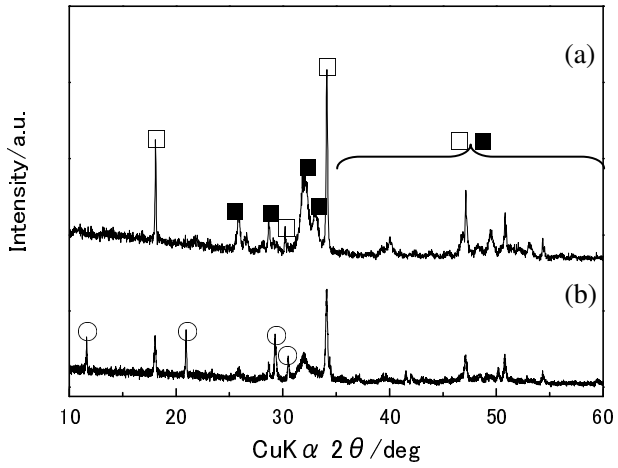

Figure 2-6. XRD patterns of precipitates (a) after hydrothermal treatment at 130°C for 14 hours and (b) before the treatment ($Ca(OH)_2$: 3.0g, H_3PO_4: 1.5g, B: 500 mg/dm^3). ○: $CaHPO_4 \cdot 2H_2O$, □: $Ca(OH)_2$, and ■: $Ca_{10}(PO_4)_6(OH)_2$ (Hydroxy apatite).

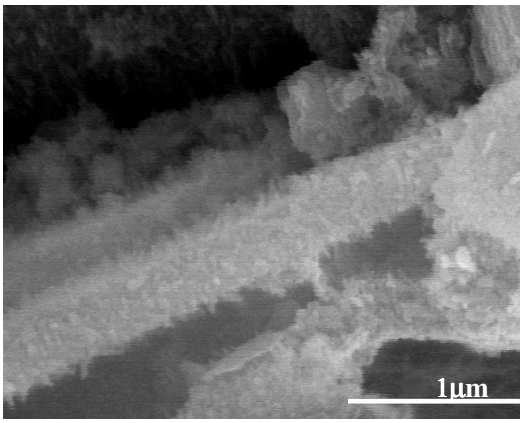

Figure 2-7. SEM photograph of precipitate obtained by the hydrothermal treatment at 130°C for 14 hours ($Ca(OH)_2$: 3.0g, H_3PO_4:1.5g, B: 500 mg/dm^3).

2.3.4. Optimization of hydrothermal conditions in the presence of both calcium hydroxide and phosphoric acid

Figure 2-8 shows the residual boron concentration in the model wastewater plotted against the added amounts of H_3PO_4 and $Ca(OH)_2$. A concave curve was drawn as a function of H_3PO_4 added amount at any $Ca(OH)_2$ addition. It is also noticed that the optimal amount of the H_3PO_4 addition is dependent on the amount of $Ca(OH)_2$ addition. The decrease of boron concentration in the low range of the phosphoric acid concentration on the left side in Figure 2-8 was caused by inhibition of re-dissolution of calcium borate due to the formation of the hydroxy apatite microcrystals. On the other hands, the increase in boron concentration on the right side of the figure can be explained by equilibrium relationship shown in Scheme 2-1. This means that the probability of collision between boron and $Ca(OH)_2$ decreases by the consumption of $Ca(OH)_2$ before the treatment. Moreover, the minimal concentration of residual boron decreased with an increase in the added amounts of $Ca(OH)_2$, and then, became a constant value of ca. 6 mg/dm^3 at more than 3.0g of $Ca(OH)_2$. Therefore, it is found that the optimal amounts of added $Ca(OH)_2$ and H_3PO_4 are 3.0g and 1.5g, respectively. At this optimal condition, the residual concentration of boron in the model wastewater could be less than the quality standard value of discharged water in Japan (10 mg/dm^3).

$$Ca(OH)_2 \leftrightarrow Ca^{2+} + 2OH^-$$

$$Ca^{2+} + HPO_4^{2-} + 2H_2O \rightarrow CaHPO_4 \cdot 2H_2O$$

Scheme 2-1. Chemical reactions in the sample solution before hydrothermal treatment.

The treatment time dependence of the residual boron concentration in the treated water obtained by the hydrothermal treatment under the optimal $Ca(OH)_2$ and H_3PO_4 conditions at 130 °C is shown in Figure 2-9. The residual boron concentration

decreased exponentially with an increase in the treatment time and became a constant value of ca. 6 mg/dm^3 after 12 hours. Then, the optimal treatment time was

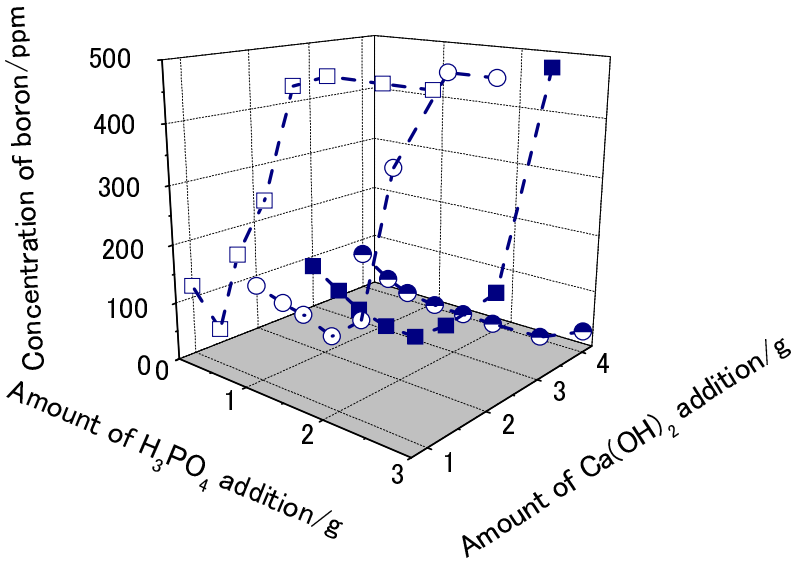

Figure 2-8. Dependence of the concentration of boron in the treated water after the hydrothermal treatment at 130°C for 14 hours on the added H_3PO_4 and $Ca(OH)_2$ (B: 500mg/dm^3).

determined to be 12 hours.

The treatment temperature dependence of the residual boron concentration in the model wastewater hydrothermally treated under the optimal $Ca(OH)_2$ and H_3PO_4 conditions for 14 hours is shown in Figure 2-10. The optimum treatment temperature was found at 130°C, when the boron concentration in the model wastewater attained the smallest value. The XRD patterns of the precipitates obtained by the hydrothermal treatment at various treatment temperatures were examined to clarify the reason for this treatment temperature dependence of the residual boron concentration, as shown in Figure 2-11. The precipitate obtained at lower temperature (90 - 110°C) gave the diffraction peaks of $Ca(OH)_2$, $CaHPO_4$, and $Ca_{10}(PO_4)_6 \cdot 5H_2O$. In contrast,

the peaks for $CaHPO_4$ could not be observed in the XRD patterns of precipitates obtained at higher temperatures (130 – 150°C). From these results, crystallization of $Ca_{10}(PO_4)_6 \cdot 5H_2O$, which plays a role of re-dissolution suppressor of calcium borate, will require the hydrothermal treatment at more than 130°C in the present system. Therefore, in the case of the model wastewater with 500 mg/dm^3 of boron, the optimal hydrothermal condition for reducing residual boron concentration less than 10 mg/dm^3 is summarized as shown in Table 2-1.

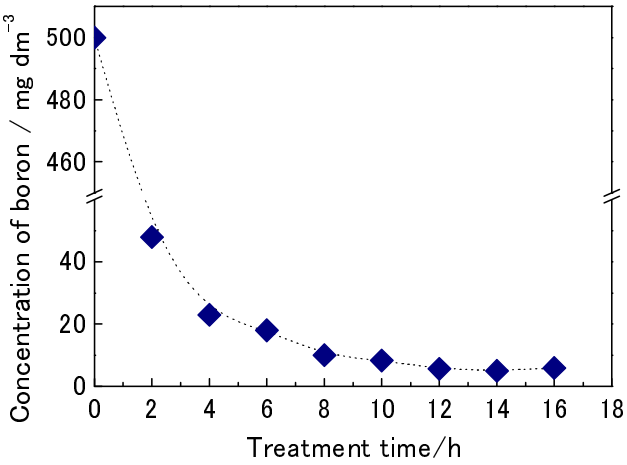

Figure 2-9. Dependence of the concentration of boron in the treated water after the hydrothermal treatment at 130°C on the treatment time ($Ca(OH)_2$: 3.0g, H_3PO_4: 1.5g, B: 500 mg/dm^3).

Table 2-1. Optimal hydrothermal conditions

Temperature/°C	Time/h	$Ca(OH)_2$/g	H_3PO_4/g
130	12	3.0	1.5

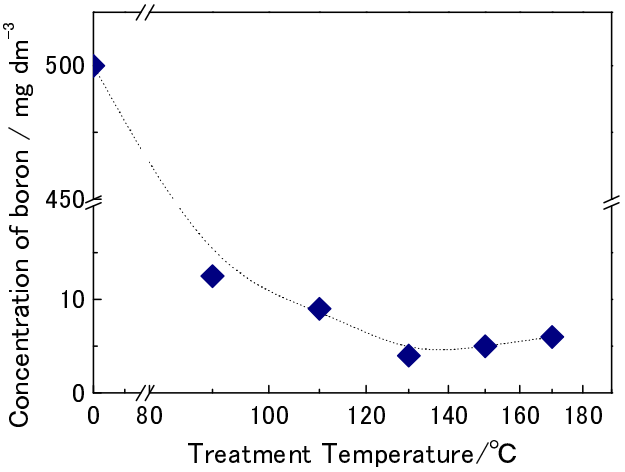

Figure 2-10. Dependence of the concentration of boron in the treated water after the hydrothermal treatment for 14 hours on the treatment temperature ($Ca(OH)_2$: 3.0g, H_3PO_4: 1.5g, B: 500 mg/dm^3).

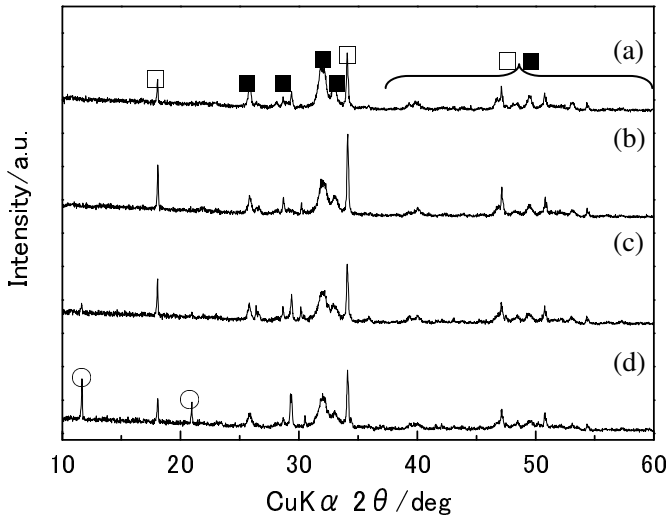

Figure 2-11. XRD patterns of precipitates obtained by hydrothermal treatment at (a): 150°C, (b): 130°C, (c): 110°C and (d): 90°C for 14 hours ($Ca(OH)_2$: 3.0g, H_3PO_4: 1.5g, B: 500 mg/dm^3). ○: $CaHPO_4 \cdot 2H_2O$, □: $Ca(OH)_2$, and ■: $Ca_{10}(PO_4)_6(OH)_2$ (Hydroxy apatite).

2.3.5. Mechanism of hydrothermal mineralization

To clarify the crystallization mechanism of calcium phosphate, the variation of diffraction patterns during hydrothermal treatment was examined (cf. Figure 2-12).

Diffraction peaks of $CaHPO_4 \cdot H_2O$ observed before the treatment (Figure 2-12(c)) gradually disappeared with an increase in the treatment time. New diffraction peaks of both $CaHPO_4$ and $Ca_{10}(PO_4)_6 \cdot 5H_2O$ appeared after the hydrothermal treatment for 6 hours (Figure 2-12(b)). The diffraction pattern of the only $Ca_{10}(PO_4)_6 \cdot 5H_2O$ was observed, when treatment time became longer more than 12 hours (Figure 2-12(a)). These results reveal that the $CaHPO_4 \cdot H_2O$ contained in the precipitate before the treatment convert into $Ca_{10}(PO_4)_6 \cdot 5H_2O$ via $CaHPO_4$ by the hydrothermal treatment with longer time, which is analogous to the facts reported in other papers, even though the boric acid coexists in this solution[27-30]. On the other hands, the required treatment time to crystallize the $Ca_2B_2O_5 \cdot H_2O$ from boron contained in the model wastewater by hydrothermal treatment using only $Ca(OH)_2$ was 6 hours (cf. Figure 2-5), which is shorter than that for the formation of $Ca_{10}(PO_4)_6 \cdot 5H_2O$. Thus, the mechanism of mineralization of calcium borate and the re-dissolution inhabitation of calcium borate could be explained as illustrated in Figure 2-13.

(1) $Ca_2B_2O_5 \cdot H_2O$ is formed by the dehydration reaction between $B(OH)_4^-$ anion in the model wastewater and $Ca(OH)_2$ on the surface of the $Ca(OH)_2$ plate-like crystal.

(2) $CaHPO_4 \cdot H_2O$ is converted to $CaHPO_4$ due to the hydrothermal dehydration together with step (1).

(3) Part of $CaHPO_4$ produced in (2) is steadily converted to $Ca_{10}(PO_4)_6 \cdot 5H_2O$, which will be formed on the surface of $Ca_2B_2O_5 \cdot H_2O$ precipitates.

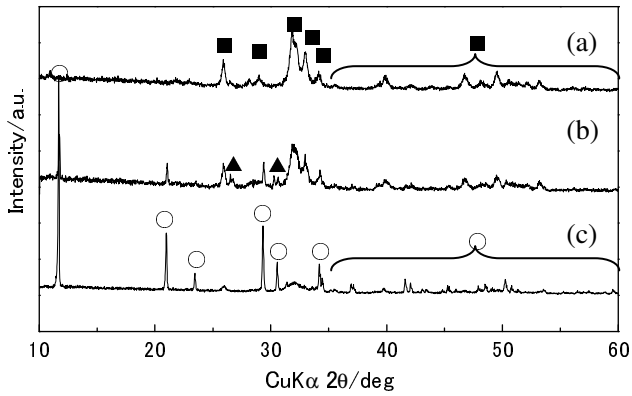

Figure 2-12. XRD patterns of calcium phosphate obtained by hydrothermal treatment at 130°C for (a): 12 hours, (b): 6 hours and (c): before treatment ($Ca(OH)_2$: 3.0g, H_3PO_4: 1.5g, B: 500 mg/dm^3). ▲: $CaHPO_4$, ○: $CaHPO_4 \cdot 2H_2O$, and ■: $Ca_{10}(PO_4)_6(OH)_2$ (Hydroxy apatite).

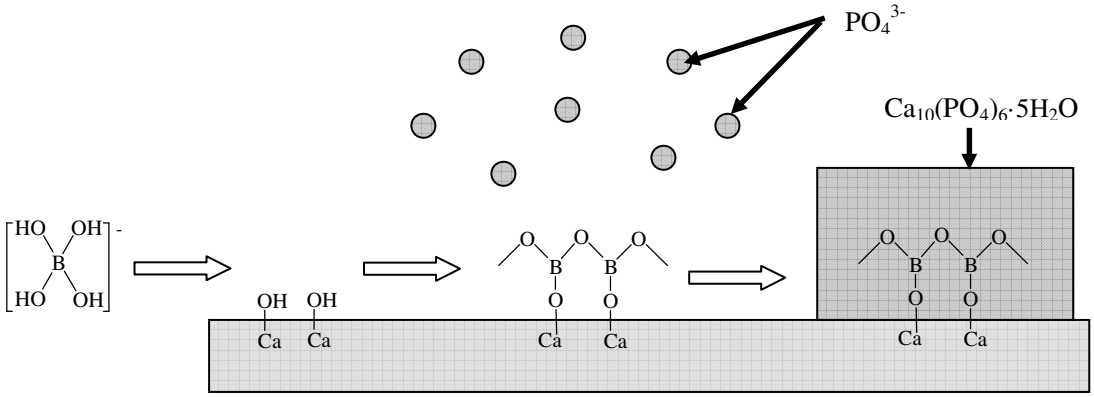

Figure 2-13. A schematic reaction mechanism on $Ca(OH)_2$ surface during the hydrothermal treatment.

2.4. Conclusions

We succeeded in the development of a novel technique for removing boron species from wastewater by hydrothermal mineralization. The present technique makes it possible not only to remove the dissolved boron species from wastewater, but also to recover the calcium borate mineral by the addition of $Ca(OH)_2$ and/or H_3PO_4 to

wastewater, where $Ca(OH)_2$ and H_3PO_4 are mineralizer and redissolution suppressor of the calcium borate mineral, respectively. More than 99% of boron dissolved in the model wastewater (boron concentration: 500 mg/dm^3) was recovered as the precipitate of $Ca_2B_2O_5 \cdot H_2O$ by the hydrothermal treatment at 130 °C for 14 hours with 3.0g of $Ca(OH)_2$ and 1.5g of H_3PO_4.

The recovered $Ca_2B_2O_5 \cdot H_2O$ precipitate in the present treatment is not calcium borate ore (colemanite) that has been found in nature. However, this precipitate can be used in the borax production process along with the natural ore of boron, because this compound has a similar crystal structure to colemanite. Therefore, this technique will be effective on the cost and environmental aspects compared with the conventional removal techniques of boron.

References

1. C. Dilek, H. O. Ozbelge, N. Bicak, and L. Yilmaz, *Separation Science and Technology* **37**, (6), (2002). 1257-1271

2. M. O. Simonnot, C. Castel, M. Nicolai, C. Rosin, M. Sardin, and H. Jauffret, *Water Research* **34**, (1), (2000). 109-116

3. Y. Magara, A. Tabata, M. Kohki, M. Kawasaki, and M. Hirose, *Desalination* **118**, (1-3), (1998). 25-33

4. M. S. Celik, M. Hancer, and J. D. Miller, *J. Colloid Interface Sci.* **256**, (1), (2002). 121-131

5. S. Karahan, M. Yurdakoc, Y. Seki, and K. Yurdakoc, *J. Colloid Interface Sci.* **293**, (1), (2006). 36-42

6. M. D. D. Garcia-Soto, and E. M. Camacho, *Sep. Purif. Technol.* **48**, (1), (2006). 36-44

7. N. Ozturk, and D. Kavak, *J. Hazard. Mater.* **127**, (1-3), (2005). 81-88

8. L. Melnyk, V. Goncharuk, I. Butnyk, and E. Tsapiuk, *Desalination* **185**, (1-3), (2005). 147-157

9. M. D. D. Garcia-Soto, and E. M. Camacho, *Solvent Extr. Ion Exch.* **23**, (6), (2005). 741-757

10. G. Rodriguez-Lopez, M. D. Marcos, R. Martinez-Manez, L. Sancenon, J. Soto, L. A. Villaescusa, D. Beltran, and P. Amoros, *Chemical Communications*, (19), (2004). 2198-2199

11. O. P. Ferreira, S. G. de Moraes, N. Duran, L. Cornejo, and O. L. Alves, *Chemosphere* **62**, (1), (2006). 80-88

12. H. Hosgoren, S. Tural, F. Kahraman, M. Togrul, and M. Karakaplan, *Solvent Extraction and Ion Exchange* **15**, (2), (1997). 249-257

13. F. Kahraman, *Solvent Extraction and Ion Exchange* **13**, (6), (1995). 1025-1036

14. Z. Yazicigil, and Y. Oztekin, *Desalination* **190**, (1-3), (2006). 71-78

15. D. D. Garcia-Soto, and E. M. Camacho, *Desalination* **181**, (1-3), (2005). 207-216

16. H. F. Ayyildiz, and H. Kara, *Desalination* **180**, (1-3), (2005). 99-108

17. M. Badruk, N. Kabay, M. Demircioglu, H. Mordogan, and U. Ipekoglu, *Separation Science and Technology* **34**, (13), (1999). 2553-2569

18. M. Turek, R. Dydo, J. Ciba, J. Trojanowska, J. Kluczka, and B. Palka-Kupczak, *Desalination* **185**, (1-3), (2005). 139-145

19. N. Nadav, M. Priel, and P. Glueckstern, *Desalination* **185**, (1-3), (2005). 121-129

20. P. Dydo, M. Turek, J. Ciba, J. Trojanowska, and J. Kluczka, *Desalination* **185**, (1-3), (2005). 131-137

21. K. Van Hege, M. Verhaege, and W. Verstraete, *Water Research* **38**, (6), (2004). 1550-1558

22. J. Redondo, M. Busch, and J. P. De Witte, *Desalination* **156**, (1-3), (2003). 229-238

23. M. Taniguchi, M. Kurihara, and S. Kimura, *Journal of Membrane Science* **183**, (2), (2001). 259-267

24. D. Prats, M. F. Chillon-Arias, and M. Rodriguez-Pastor, *Desalination* **128**, (3), (2000). 269-273

25. A. E. Yilmaz, R. Boncukcuoglu, M. M. Kocakerim, and B. Keskinler, *J. Hazard. Mater.* **125**, (1-3), (2005). 160-165

26. N. Bektas, S. Oncel, H. Y. Akbulut, and A. Dimoglo, *Environmental Chemistry Letters* **2**, (2), (2004). 51-54

27. M. Ni, and B. D. Ratner, *Biomaterials* **24**, (23), (2003). 4323-4331

28. J. B. Liu, X. Y. Ye, H. Wang, M. K. Zhu, B. Wang, and H. Yan, *Ceramics International* **29**, (6), (2003). 629-633

29. S. Jinawath, D. Pongkao, and M. Yoshimura, *Journal of Materials Science-Materials in Medicine* **13**, (5), (2002). 491-494

30. S. Jinawath, D. Polchai, and M. Yoshimura, *Materials Science & Engineering C-Biomimetic and Supramolecular Systems* **22**, (1), (2002). 35-39

Chapter 3 Removal and recovery of boron and fluorine from aqueous media containing tetrafluoroboric ion

3.1. Introduction

Fluoride and boric ions can be found in wastewaters derived from plating, semiconductor production, metal processing and glass-manufacturing industries. Discharge of such wastewater into the surface water would lead to the contamination of groundwater. Excess intake of these elements results in great impact on plants, animals and human bodies [1, 2]. In chapter 2, it was found that the hydrothermal mineralization using $Ca(OH)_2$ as a mineralizer could collect boron from wastewater as precipitate of boron containing mineral [3]. However, it is often the case that actual wastewater contains other ions, especially, fluoride ion. An acceptable limit of fluoride ion in potable water is 1.5 ml/L according to the WHO standard [4, 5]. Several defluorination methods for wastewater have been intensively investigated, which are known as adsorption [5-9], chemical precipitation [10, 11], ion exchange, membrane [2, 6, 12-16] and electrochemical method [11, 17-20]. Lime precipitation method is commonly used to remove fluorine in the wastewater. However, this technique cannot reduce the fluorine concentration in wastewater less than approximately 20 mg/dm^3, because the theoretical solubility of fluorite in water is 17 mg/dm^3 at 25 °C [21-23]. Furthermore, tetrafluoroboric ion, which generates in coexistence with boric ion and fluoride ion in aqueous solution, cannot be removed by general chemical precipitation method because of its extremely high stability. Consequently, there is no effective method to remove or recover both boron and fluorine from wastewater containing fluoride or tetrafluoroboric ions. Therefore, a new technique to recover boron and fluorine concurrently from wastewater containing tetrafluoroboric acid is desired.

The first objective of this study is to develop a new method to collect fluoride ion contained in wastewater by a novel hydrothermal mineralization technique. The second objective is to establish the precipitation method of boron and fluorine from aqueous media containing tetrafluoroboric acid.

3.2. Experimental procedure

3.2.1. Hydrothermal mineralization treatment

Model wastewaters were prepared by diluting hydrofluoric acid (48 wtpercent, Wako Pure Chemical Industries, Ltd.), fluoroboric acid (48 wtpercent, Wako Pure Chemical Industries, Ltd.) into distilled and deionized water. Each of the model wastewaters contain fluoride ion (368 mmol/L, F; 7000 mg/L) or fluoroboric ion (92 mmol/L, B; 1000 mg/L, F; 7000 mg/L). Thirty milliliters of these model wastewaters, which contain 11.0 mmol of fluoride ions or 2.76 mmol of fluoroboric ions, were sealed in a pressure vessel lined with a fluorocarbon resin along with 0.5 - 1.0 g of $Ca(OH)_2$ (6.41 – 12.8 mmol). Hydrothermal treatment was carried out by placing the vessel in a dry oven controlled over a temperature range of 100 – 200 °C for 2 – 48 h. After the hydrothermal treatment, the vessel was cooled in air for 1 h. The precipitates obtained by hydrothermal treatment were collected by using membrane filter (0.2 μm) and dried at 50 °C for 24 h.

3.2.2. Analytical methods

The precipitates were identified by using X-ray diffraction (XRD: RIGAKU RINT-2500) using CuKα radiation. The microstructural observation and qualitative elemental analysis of the precipitates were performed by using scanning electron microscopy (SEM: JEOL, JSM-T20) equipped with energy dispersive X-ray spectrometry (EDS: JED-2140). Quantitative elemental analysis of boron in the solvent, obtained after hydrothermal treatment, was carried out by using the

inductively coupled plasma-atomic emission spectrometry (ICP-AES: Perkin-Elmer, Optima3300DV). Concentration of fluoride ion remaining in the treated-water was measured by using ion chromatograph (Shimadzu, CTO-10AC. Mobile phase; Bis-Tris 0.067 wt % and p-Hydroxybenzoic acid 0.11 wt % aqueous solution, Column; Shim-Pack IC-A3) with conductivity detector (Shimadzu, CDD-10A).

3.3. Results and discussions

3.3.1. Recovery of fluorine from wastewater containing fluoride ion

Figure 3-1 shows the ion chromatograms of the model wastewater before and after the hydrothermal treatment. The concentration of fluoride ion in the wastewater before the treatment was 18 mg/dm^3. On the other hand, no chromatogram peak of fluoride ion was observed in the wastewater after the treatment. This suggested that the fluoride ion in the wastewater was completely consumed to form precipitates under the hydrothermal conditions using $Ca(OH)_2$ mineralizer. XRD patterns of the precipitates before and after the treatment shown in Figure 3-2 exhibited that they consisted of CaF_2. It was considered that all fluoride ions in the model wastewater were precipitated as solid CaF_2 with its low solubility under hydrothermal conditions. Additionally, crystallinity and crystal radius of CaF_2 increased, because the peaks are changed sharpen by the hydrothermal treatment. Figure 3-3 shows SEM photographs of the precipitates obtained before and after the hydrothermal treatment. This result shows that the crystallinity and crystal radius of CaF_2 increased dramatically by the hydrothermal treatment. This result consists with the result of XRD measurement. Thus, the recovery of fluorine from wastewater was achieved by decreasing dissolution rate of CaF_2 at room temperature because of increase of crystallinity and crystal radius. Therefore, the present hydrothermal mineralizing treatment can recover fluorine completely from wastewater using the minimum amount of $Ca(OH)_2$ required to form

CaF_2.

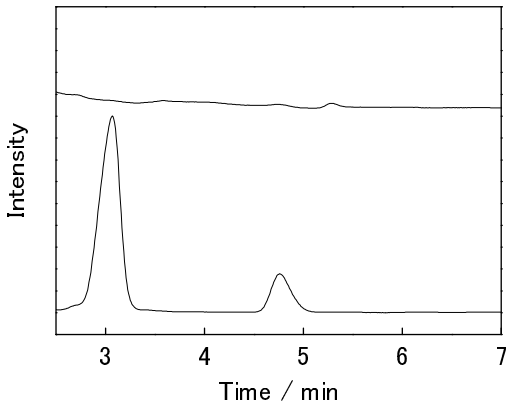

Figure 3-1. Ion chromatograms of the wastewater before and after the hydrothermal treatment. a; before the treatment, b; after the treatment (F-; 7000 mg/dm^3, $Ca(OH)_2$; 0.5g, 200°C, 4 hours).

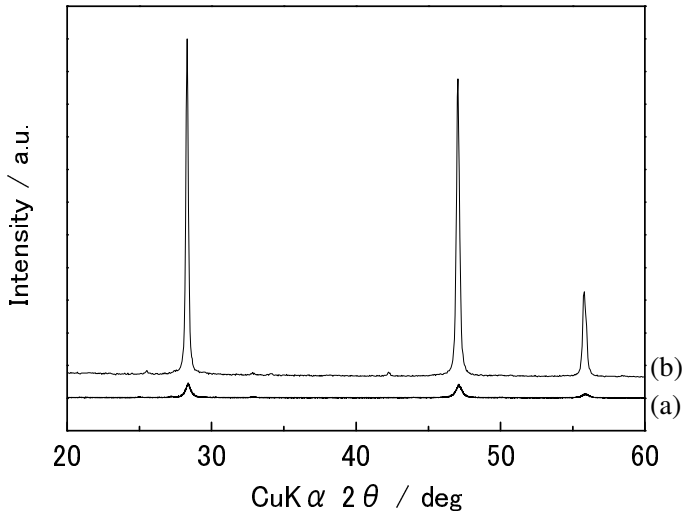

Figure 3-2. XRD patterns of the precipitates before and after the hydrothermal treatment. a; before treatment, b; 4 hours (F^-: 7000 mg/dm^3, $Ca(OH)_2$: 0.5 g). All peaks were derived from fluorite.

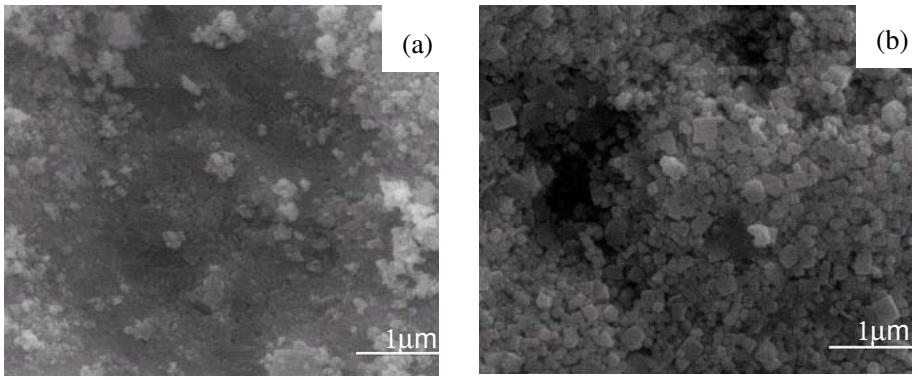

Figure 3-3. SEM photographs of the precipitates obtained by (a) before and (b) after the hydrothermal treatment (F-; 7000 mg/dm^3, $Ca(OH)_2$; 0.5g, 200°C, 4 hours).

3.3.2. Recovery of boron and fluorine from wastewater containing tetrafluoroboric acid

Figure 3-4 shows the XRD patterns of precipitates before and after hydrothermal treatment of tetrafluoroboric acid containing solution. Only the diffraction peaks of $Ca(OH)_2$ were observed before the treatment (Figure 3-4-a). On the other hand, the diffraction peaks of CaF_2 and $Ca_2B_2O_5 \cdot H_2O$ were observed after the treatment (Figure 3-4-b, c, d) and the intensities of diffraction peaks of $Ca_2B_2O_5 \cdot H_2O$ increased up to 24 hours. Figure 3-5 shows the treatment time dependence of the residual B and F concentrations in the wastewater treated at 200 °C. The significant enhancement of recovery yield of fluorine was observed at 2 hours and it was completed by 4 hours. On the other hand, the recovery yield of boron was only 30 % at 2 hours and it gradually increased. It is expected that the removal of F and B would be achieved by forming CaF_2 and $Ca_2B_2O_5 \cdot H_2O$ in the same manner as the case of wastewater containing fluoride or boric ion only, according to the precipitation reaction between Ca^{2+}, and F^- / $B(OH)_4^-$ generated in the thermal decomposition of BF_4^- at the initial stage of treatment. The decomposition of BF_4^- would be completed by 4 hours, after

which the mineralization of boron and fluorine could be accomplished.

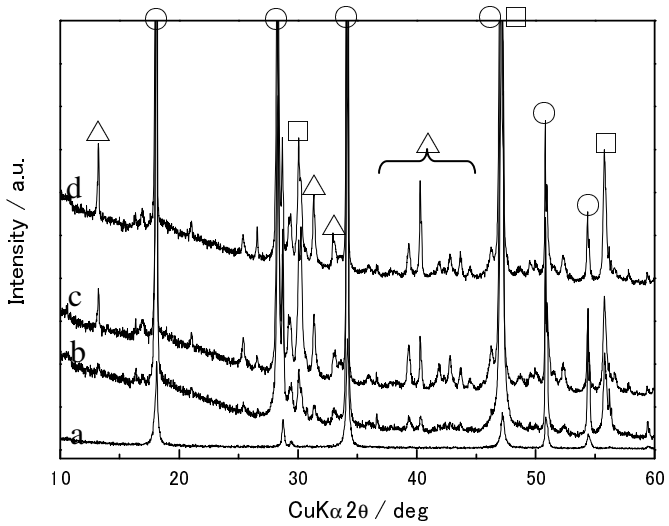

Figure 3-4. XRD patterns of the precipitates before and after the hydrothermal treatment. a; before treatment, b; 2 hours, c; 10hours, d; 24 hours (BF_4^-: 8000 mg/dm^3, $Ca(OH)_2$: 1.0g). ○: $Ca(OH)_2$, □: CaF_2, △$Ca_2B_2O_5 \cdot H_2O$.

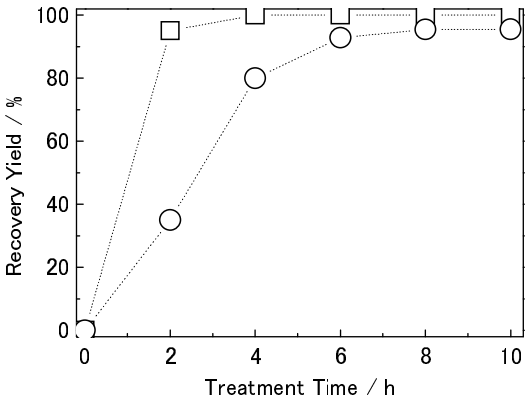

Figure 3-5. Dependence of recovery yield of B and F in the treated-water on treatment time at 150 °C (BF_4^-: 8000 mg/dm^3, $Ca(OH)_2$: 1.0g). ○: B, □: F.

Figure 3-6 shows the B and F concentrations in the treated-water plotted against the treatment time in the temperature range of 100 to 200 °C. Treatment time required to remove B and F decreased greatly with an increase in treatment

temperature. The optimal conditions to recover both F and B from model wastewater containing 8000 mg/dm^3 tetrafluoroboric ion were at 200°C for 36 hours, when the concentrations of F and B were 0.3 mg/dm^3 and 20 mg/dm^3, respectively. Chapter 2 described that $Ca_2B_2O_5 \cdot H_2O$ generated by the hydrothermal mineralization was redissolved in aqueous solution at the cooling process, so that the boron concentration in the treated-water was approximately 100 mg/dm^3. Thus, the H_3PO_4 was added in this model wastewater to prevent the re-dissolution of $Ca_2B_2O_5 \cdot H_2O$ by coating the precipitate with hydroxy apatite formed in the previous hydrothermal treatment conditions. However, the boron concentration in the present study reduced down to 20 mg/dm^3 without adding the re-dissolution inhibition reagent.

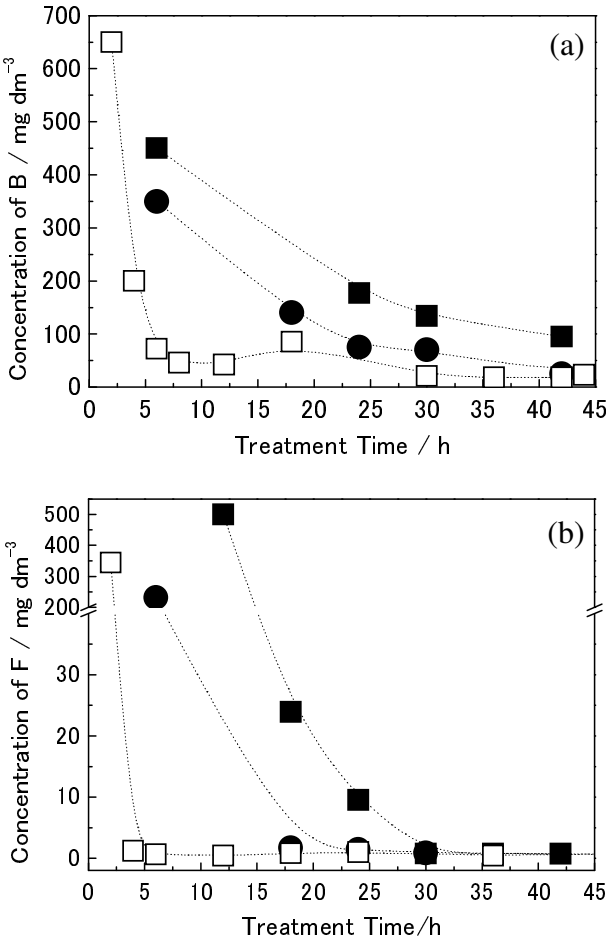

Figure 3-6. Dependence of concentration of B (a) and F (b) in the treated-water on treatment time (BF_4^-: 8000 mg/dm^3, $Ca(OH)_2$: 1.0g). ■: 100°C, ●: 150°C, □: 200°C.

3.3.3. Behavior of tetrafluoroboric ion under hydrothermal condition

SEM photographs of precipitates obtained by the hydrothermal treatment were shown in Figure 3-7. Three layers were observed in the overview photograph (Figure 3-7-a). By the results of EDS and XRD analyses, the first layer (Figure 3-7-b) was CaF_2, the second layer (Figure 3-7-c) was the mixture of CaF_2 and $Ca_2B_2O_5 \cdot H_2O$, and the third layer (Figure 3-7-d) was the mixture of $Ca_2B_2O_5 \cdot H_2O$ and residual $Ca(OH)_2$. Very fine particles were observed as suspended particulates in model wastewater after hydrothermal treatment at 200°C for more than 4 hours. Then, the amount of

particulates seemed gradually to decrease after 8 hours with an increase in the treatment time and completely settled down for 20 hours. XRD pattern shown in Figure 3-8 indicated that these particles were CaF_2. Figure 3-9 shows the schematic diagram of the mechanism to recover boron and fluorine by the hydrothermal mineralization treatment. The decomposition of BF_4^- completed for ca. 4 hours, subsequently the fine particles of CaF_2 formed and grown in the model wastewater (Figure 3-9-(a) and (b)). Finally, they settled down slowly up to 20 hours (Figure 3-9-(e)). Chapter 2 described that the formation of $Ca_2B_2O_5 \cdot H_2O$ from $B(OH)_4^-$ completed for 6 hours. The formation of $Ca_2B_2O_5 \cdot H_2O$ in this study would have started at 2 – 4 hours after and completed by 8 – 10 hours (Figure 3-9-(c)). After that, $Ca_2B_2O_5 \cdot H_2O$ were wrapped with suspended particles. Figure 3-10 shows the SEM photographs of CaF_2 particle obtained by the hydrothermal treatment at 200 °C for 8 and 30 hours. Precipitates obtained at 200°C for 30 hours formed very dense layer (Figure 3-10-b) compared with those for 8 hours (Figure 3-10-a). Possibly this dense layer would play a role to inhibit the re-dissolution of $Ca_2B_2O_5 \cdot H_2O$ into aqueous media by wrapping the precipitate surface. Therefore, the resource recovery of boron and fluorine was attained by collecting them as CaF_2 and $Ca_2B_2O_5 \cdot H_2O$, respectively from fluoroboroic acid solution by the hydrothermal mineralization method, which needed no addition of precipitation agents such as phosphoric acid. However, B concentration after the treatment was not stabilized (see Figure 3-6) than re-dissolution preventation by using H_3PO_4 shown in Chapter 2. The cause of this tendency is difference of re-dissolution preventation mechanism. Re-dissolution preventation mechanism by formation of CaF_2 is not encapsulation of the precipitate, but only settle down. Therefore, it cannot completely inhibit contact of H_2O to precipitate.

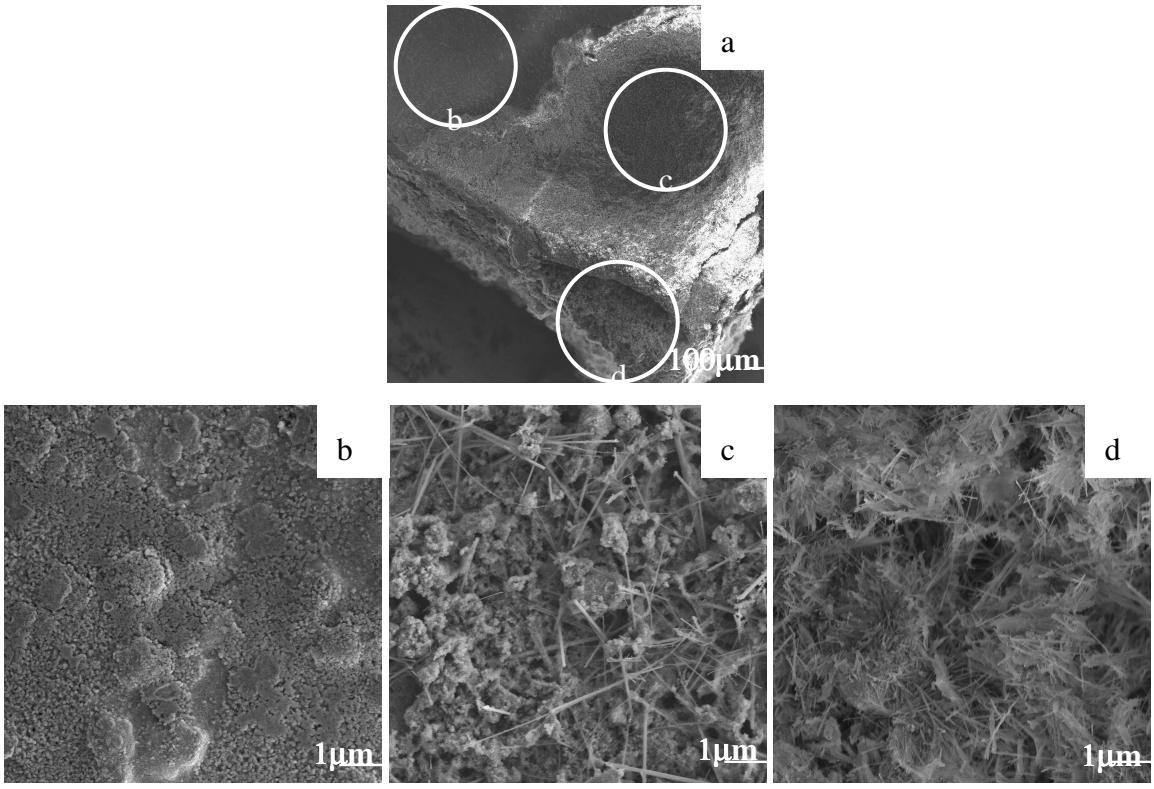

Figure 3-7. SEM photographs of the precipitates obtained by the hydrothermal treatment. a; over view of precipitate, b; first layer, c; second layer, d; third layer.

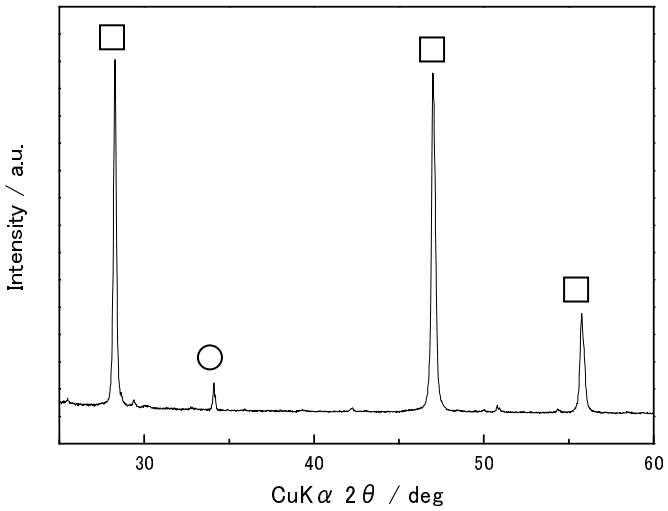

Figure 3-8. XRD patterns of the precipitates before and after the hydrothermal treatment for 4 hours (BF_4^-: 8000 mg/dm^3, $Ca(OH)_2$: 1.0 g). ○: $Ca(OH)_2$, □: CaF_2.

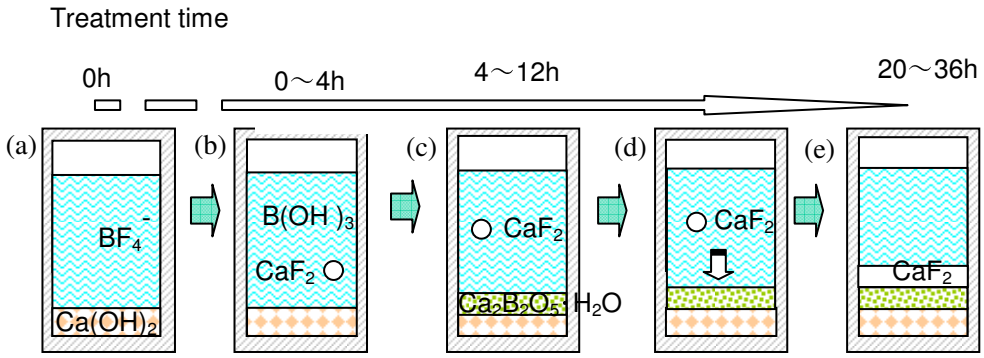

Figure 3-9. Schematic diagram of the hydrothermal mineralization treatment for aqueous media containing BF_4^-.

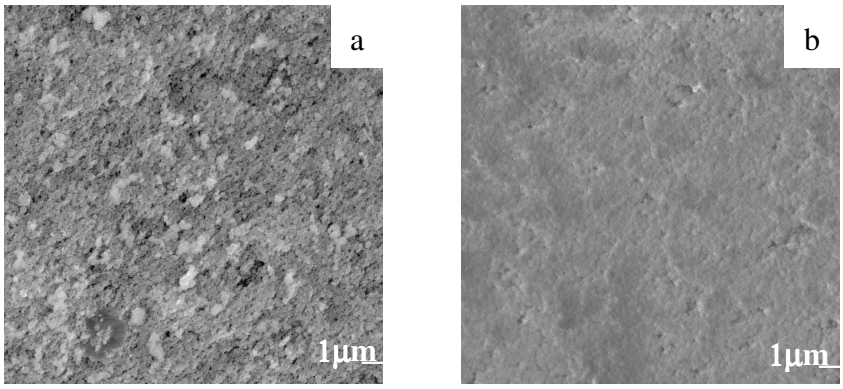

Figure 3-10. SEM photographs of the CaF_2 particles obtained by hydrothermal treatment at 200 °C. a; 8 hours, b; 30 hours.

3.4. Conclusions

Fluoride ion included in the model wastewater was collected completely by hydrothermal treatment with $Ca(OH)_2$ at 150 °C for 4 hours. The amount of added $Ca(OH)_2$ was much lower than the conventional lime precipitation method. Recovery of boron and fluorine from model wastewater containing tetrafluoroboric ion was successfully accomplished by hydrothermal mineralization at 150 °C for more than 36 hours. Formation of fine particles of CaF_2 by decomposition of BF_4^- had an effect for inhibiting re-dissolution of borate mineral by settling down and forming dense layer on the surface of precipitate. The recovery yield of fluorine and boron was 99.9 % and

98 %, respectively.

References

1. C. Dilek, H. O. Ozbelge, N. Bicak, and L. Yilmaz, *Sep. Sci. Technol.* **37**, (6), (2002). 1257-1271

2. M. O. Simonnot, C. Castel, M. Nicolai, C. Rosin, M. Sardin, and H. Jauffret, *Water Res.* **34**, (1), (2000). 109-116

3. T. Itakura, R. Sasai, and H. Itoh, *Water Res.* **39**, (12), (2005). 2543-2548

4. WHO, *Geneva: World Health Organization*, (1993).

5. Meenakshi, and R. C. Maheshwari, *J. Hazard. Mater.* **137**, (1), (2006). 456-463

6. L. N. Ho, T. Ishihara, S. Ueshima, H. Nishiguchi, and Y. Takita, *J. Colloid Interface Sci.* **272**, (2), (2004). 399-403

7. Y. Cengeloglu, E. Kir, and M. Ersoz, *Sep. Purif. Technol.* **28**, (1), (2002). 81-86

8. W. W. Choi, and K. Y. Chen, *Journal American Water Works Association* **71**, (10), (1979). 562-570

9. M. G. Sujana, R. S. Thakur, and S. B. Rao, *J. Colloid Interface Sci.* **206**, (1), (1998). 94-101

10. E. J. Reardon, and Y. X. Wang, *Environ. Sci. Technol.* **34**, (15), (2000). 3247-3253

11. F. Shen, X. M. Chen, P. Gao, and G. H. Chen, *Chem. Eng. Sci.* **58**, (3-6), (2003). 987-993

12. T. Ishihara, Y. Shuto, S. Ueshima, H. L. Ngee, H. Nishiguchi, and Y. Takita, *Journal of the Ceramic Society of Japan* **110**, (9), (2002). 801-803

13. M. Hichour, F. Persin, J. Molenat, J. Sandeaux, and C. Gavach, *Desalination* **122**, (1), (1999). 53-62

14. P. I. Ndiayea, P. Moulin, L. Dominguez, J. C. Millet, and F. Charbit, *Desalination* **173**, (1), (2005). 25-32

15. H. S. Mehta, V. B. Parikh, U. Pal, and S. K. Menon, *J. Fluorine Chem.* **127**, (9), (2006). 1228-1234

16. K. Hu, and J. M. Dickson, *J. Membr. Sci.* **279**, (1-2), (2006). 529-538

17. V. A. Joshi, and M. V. Nanoti, *Annali Di Chimica* **93**, (9-10), (2003). 753-760

18. M. Yang, Y. Zhang, B. Shao, R. Qi, and H. Myoga, *Journal of Environmental Engineering-Asce* **127**, (10), (2001). 902-907

19. C. Y. Hu, S. L. Lo, and W. H. Kuan, *J. Colloid Interface Sci.* **283**, (2), (2005). 472-476

20. C. Y. Hu, S. L. Lo, W. H. Kuan, and Y. D. Lee, *Water Res.* **39**, (5), (2005). 895-901

21. N. Parthasarathy, and J. Buffle, *Water Res.* **19**, (1), (1985). 25-36

22. N. Parthasarathy, J. Buffle, and W. Haerdi, *Water Res.* **20**, (4), (1986). 443-448

23. A. Toyoda, and T. Taira, *Ieee Transactions on Semiconductor Manufacturing* **13**, (3), (2000). 305-309

Chapter 4 In situ solid/liquid separation effect for high yield recovery of boron and fluorine from aqueous media containing boric or tetrafluoroboric ions.

4.1. Introduction

Boron distributes widely in the environment mainly as boric acid. The largest boron sources in the world exist in Turkey, and so, boron contamination to water is a common environmental problem [1]. Recently, the quality standard of discharged water with boron from manufacturing plants has been set at 10 mg/dm^3 in Japan. On the other hand, boric acid is an important industrial resource and is widely used in many kinds of the manufacturing processes, such as in semiconductor, ceramic and plating industries. Thus, the wastewater containing several hundred to thousand mg/dm^3 of boron generates in these industrial processes. Additionally, it is often the case that wastewater containing boron discharged from several industries often includes fluoride ions, and tetrafluoroboric ion are produced by the reaction of boric and fluoride ions. This ion is very stable in the aqueous solution. The conventional detoxification methods, i.e. co-precipitation or lime precipitation method cannot apply to such wastewater. Furthermore, there is an acceptable limit of fluorine in water by its toxicity (Japanese standard of discharged water is 8 mg/dm^3, WHO standard of potable water is 1.5 mg/dm^3) [2].

Chapter 2 and 3 described that the precipitation recovery of boric and tetrafluoroboric ions as reusable natural mineral and detoxification of solution containing boric and tetrafluoroboric ions by hydrothermal mineralization method [3, 4]. As a result, it was found that the boric acid in aqueous media was precipitated as parasibirskite ($Ca_2B_2O_5 \cdot H_2O$) treated at 130 - 150 °C by using ordinary batch type treatment vessel (Figure 4-1-(a)). However, the boron concentration in the

treated-water was ca. 100 mg/dm^3. The cause of this result attributed to re-dissolution of parasibirskite during the cooling process to room temperature. Thus, H_3PO_4 was added to prevent the re-dissolution of parasibirskite by coating the surface of precipitates with calcium hydroxyapatite and to intercept the contact of $Ca_2B_2O_5 \cdot H_2O$ with H_2O. As a result, boron concentration reduced down to ca. 4 mg/dm^3 after 12 h treatment. But, contamination of phosphorous compound such as hydroxyapatite in the precipitate would be an inhibitation factor to reuse the formed mineral as reusable industrial resource. Additionally, the optimum treatment time to reduce boron concentration to less than the standard of discharged water was so long (12 h) that it was difficult to apply this ordinary batch type treatment to practical industries. It is expected from above results that the solubility of parasibirskite under hydrothermal condition was lower than that at room temperature. Therefore, separation of the precipitates from reacted solution in auqsi-equilibrium with hydrothermal conditions would be effective to reduce boron concentration in the treated-water.

In this study, in situ solid/liquid separation effect of the hydrothermally mineralized products from reacted solution by using a sampling-type autocrave (Figure 4-1-(b)) was demonstrated, in order to prevent the re-dissolution of borate mineral precipitated under hydrothermal conditions during cooling process. When hydrothermal mineralization treatment is carried out by using the ordinary pressure vessel shown in Figure 4-1-(a) (in this paper, this vessel is described as apparatus A), cooling process more than 1 h is necessary to separate precipitate from reacted aqueous solution because of its high temperature and pressure. On the other hand, the sampling-type hydrothermal treatment apparatus shown in Figure 4-1-(b) (apparatus B) can separate precipitate form solution in quasi-equilibrium state of the hydrothermal condition. The suspended product is led into the sampling tube by its own vapor

pressure, and the precipitates are then separated from suspension by a metal filter with 0.5 μm mesh. After that, the samples were immidiately cooled down to room temperature in cooling condenser. Thus, the collection of reacted solution at equilibrium state under hydrothermal condition can be accomplished by this apparatus B.

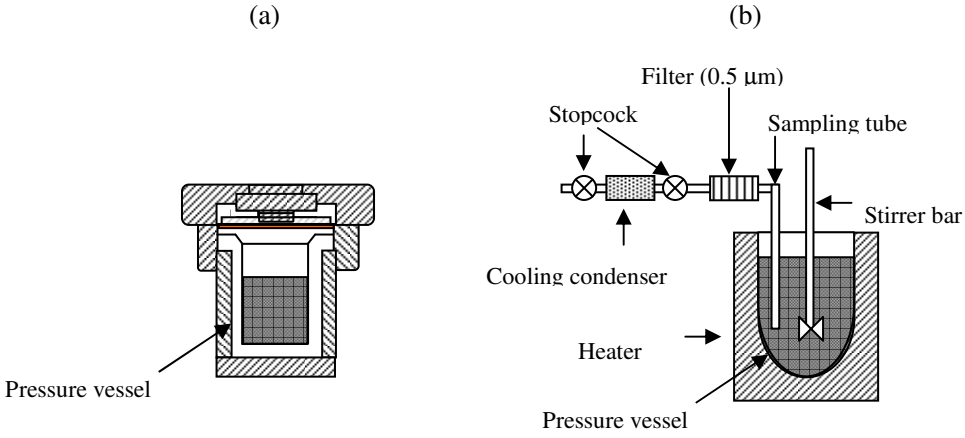

Figure 4-1. Schematic diagram of the ordinary (a; apparatus A) and sampling-type (b; apparatus B) hydrothermal treatment apparatus.

4.2. Experimental

4.2.1. Preparation of samples

The model wastewaters were prepared by dissolving B_2O_3 or diluting hydrofluoric acid (Wako Pure Chemical Industries, Ltd.) into distilled and deionized water. Model wastewater of boric acid solution contains 45.5 – 273 mmol/dm^3 (500 – 3000 mg/dm^3) of boron and that of tetrafluoroboric acid solution contains 45.5 mmol/dm^3 (500 mg/dm^3) of boron and 182 mmol/dm^3 (3500 mg/dm^3) of fluorine.

4.2.2. Sampling-type hydrothermal treatment

Model wastewaters of 60 mL were sealed in a pressure vessel with 2.0 or 6.0 g (27 or 81 mmol, respectively) of $Ca(OH)_2$ mineralizer. Thermal adjustment was carried

out by temperature controller (CHINO Corporation, DZ1000).

4.2.3. Ordinary batch-type hydrothermal treatment

Model wastewaters of 30 mL were sealed in a pressure vessel lined with a fluorocarbon resin along with 1.0 or 3.0 g (13 or 40 mmol, respectively) of $Ca(OH)_2$. Hydrothermal treatment was carried out by placing the vessel in a dry oven controlled at 150 °C for 2 – 6 h. After the hydrothermal treatment, the vessel was cooled in air for 1 h. The precipitates and solvents obtained by hydrothermal treatment were collected by using membrane filter (0.2 μm).

4.2.4. Analytical method

Quantitative elemental analysis of boron in the solvent, which was obtained after hydrothermal treatment, was carried out by using the inductively coupled plasma-atomic emission spectrometry (ICP-AES: Perkin-Elmer, Optima3300DV). Concentration of fluoride ion and tetrafluoroboric ion remaining in the treated-water was measured by using ion chromatograph (Shimadzu, CTO-20AC. Mobile phase; $NaHCO_3$ 0.1008 wt % and Na_2CO_3 0.0064 wt % aqueous solution, Column; Shim-Pack IC-SA2) with suppressor (Shimadzu, HIC-10Asp, type 312) and conductivity detector (Shimadzu, CDD-6A).

4.3. Results and Discussions

Firstly, we examined the solubility of $Ca(OH)_2$ under hydrothermal conditions. It is well known that it decreases with an increase in temperature under atmospheric pressure. However, there is no report on the solubility of $Ca(OH)_2$ under hydrothermal conditions. Figure 4-2 shows the variation of $Ca(OH)_2$ solubility in the autoclave in a temperature range of 25 to 175 °C, which was measured by using the

apparatus B. Solubility of $Ca(OH)_2$ decreased gradually with an increase in temperature, and the concentration of Ca^{2+} was lower than 20 mg/dm^3 at temperatures more than 125 °C. Thus, it is found that this appratus B can separate reacted solution and precipitate under hydrothermal conditions.

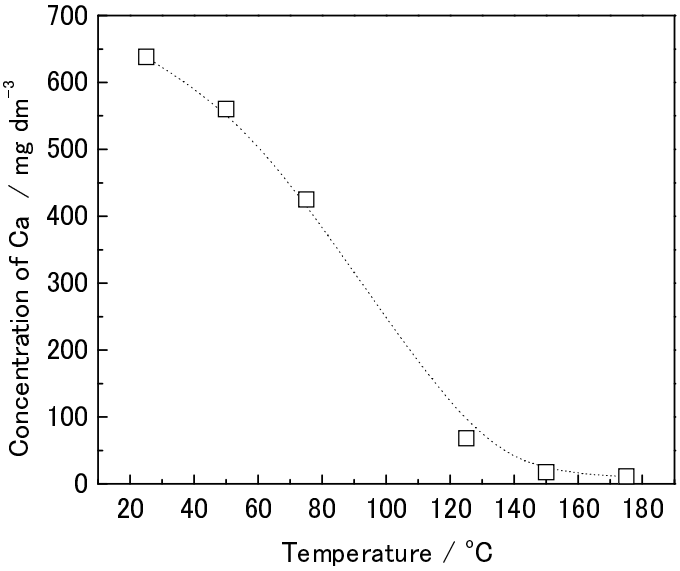

Figure 4-2. Dependence of the $Ca(OH)_2$ solubility on the temperature of the aqueous solution.

Figure 4-3 shows the result of hydrothermal mineralization treatment for the model wastewater containing 500 or 3000 mg/dm^3 of boric acid with $Ca(OH)_2$ mineralizer at 150 °C by using the apparatus A and B. The boron concentration decreased and parasibirskite ($Ca_2B_2O_5 \cdot H_2O$) was simultaneously formed by the treatment. XRD pattern of the precipitate obtained by this treatment using the apparatus B was shown in Figure 4-4. As a results of our previous study, parasibirskite formed by heterogeneous nucleation on the surface of $Ca(OH)_2$ [5]. However, boron concentration after the treatment by using the apparatus A was more than 100 mg/dm^3 for longer treatment time. This result was caused by re-dissolution

of borate mineral ($Ca_2B_2O_5 \cdot H_2O$) during cooling process for 1 h [5]. On the other hand, residual boron concentration in the water treated by the apparatus B was lower than 4 mg/dm^3. This result is one of the evidences that the solubility of borate mineral under hydrothermal condition is lower than that at ordinary temperature and puressure.

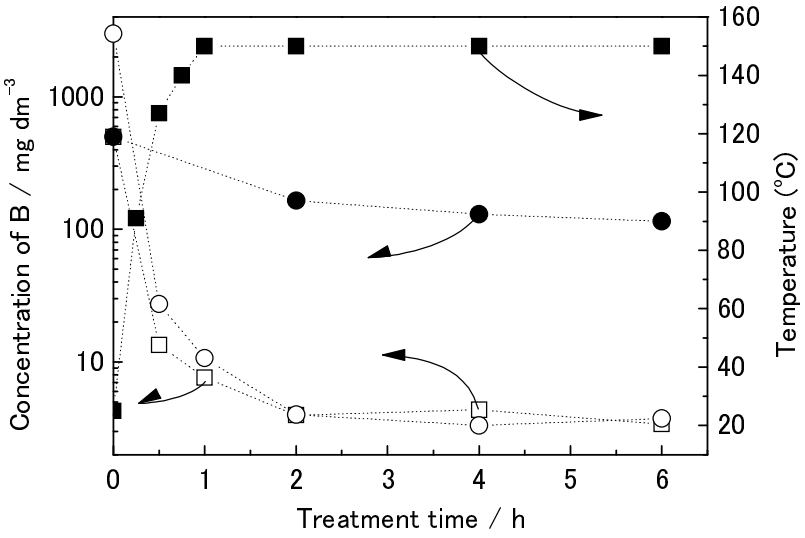

Figure 4-3. Dependence of the boron concentration on the treatment time. □: treated for aqueous media containing 500 mg/dm^3, ○: 3000 mg/dm^3, ●: 500 mg/dm^3 by using batch type apparatus, ■: temperature of the apparatus. All treatments were carried out with 6.0 g $Ca(OH)_2$.

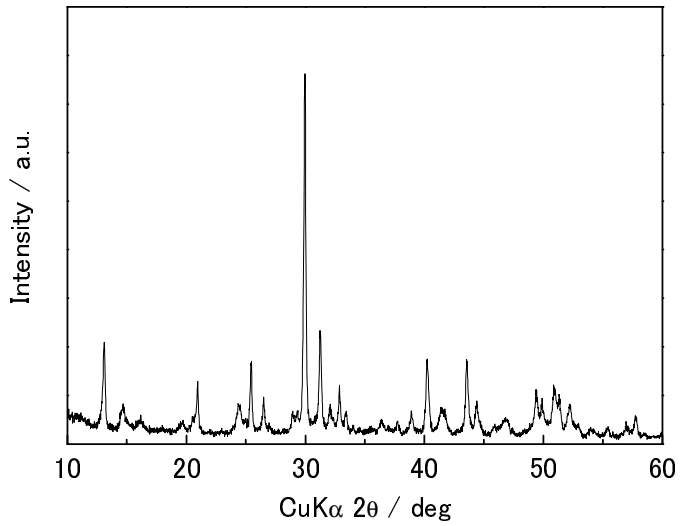

Figure 4-4. XRD pattern of the precipitate obtained by the treatment for 3 h with 1.0 g of $Ca(OH)_2$ mineralizer at 150 °C using quasi-flow type apparatus. All diffraction peaks are derived from $Ca_2B_2O_5 \cdot H_2O$.

Furthermore, boron concentration after the treatment is not influenced by varing the initial concentration of boron. Detailed initial concentration dependence are shown in Figure 4-5. Thus, the boron concentration in the treated-water is independent of the initial concentration, *i.e,* it depend only on the solubility of $Ca_2B_2O_5 \cdot H_2O$ under hydrothermal condition. This boron concentration in treated-water is lower than the standard of discharged water of Japan. Therefore, the separation of precipitate from solvent under hydrothermal condition enables effective recovery of boron and simultaneous detoxification of polluted water.

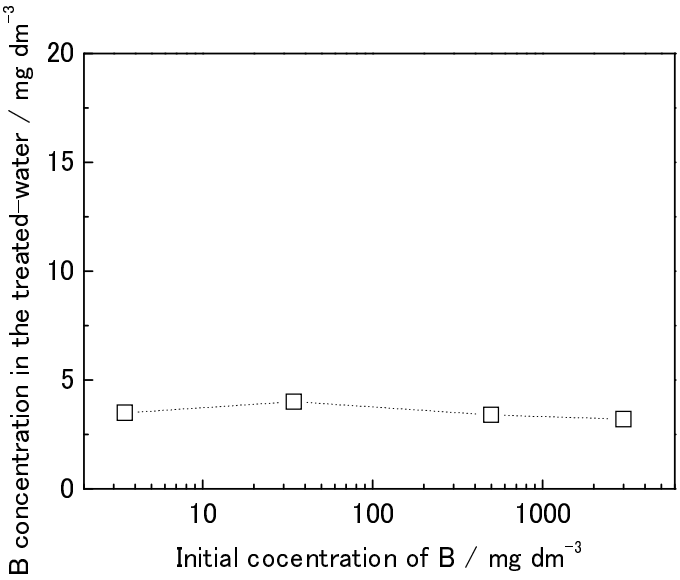

Figure 4-5. Initial concentration dependence of the boron concentration in the treated-water. Sample: 60 ml, $Ca(OH)_2$: 6.0 g, Treatment temperature: 150 °C, Treatment time: 4 h.

In addition, the total treatment time required for the reduction of boron concentration down to less than 10 mg/dm^3 shortened by using the apparatus B for 1 – 2 h compared with the apparatus A, which needed treatment time more than 12 h. This result suggests the detoxification and resource recovery are accomplished immediately when the treatment temperature of the treatment vessel for apparatus B reaches 150 °C. On the other hand, boron concentration by treating the apparatus A gradually decreased for more than 2 h (see Figure 4-3). It is expected that decrease of boron concentration for longer treatment time by using the apparatus A would cause the crystal and/or grain growth of borate mineral. Thus, the difference of treatment time between the apparatus A and B is responsible for that the re-dissolution rate of borate mineral must be controlled by the grain and/or crystal size in the high pressure vessel. Therefore, the improvement of yield recovery in the case of apparatus A with longer treatment time would be attained by the separation of the formed mineral from aqueous media before approaching the equilibrium state in the solution because the

re-dissolution rate of borate mineral is slow due to crystal and/or grain growth. In contrast, the crystal and/or grain growth of precipitate will not be required in case of the apparatus B, because this apparatus can invalidate the crystal and/or grain growth of precipitate of borate mineral by separation of the precipitate from the reacted suspension under hydrothermal condition. Therefore, it will be concluded that the separation of precipitate from reactive aqueous solution is effective for a prompt detoxification of wastewater polluted by boric acid and the recovery of boron as recyclable resource.

Results of the hydrothermal mineralization treatments by using the apparatus B in aqueous solutions containing 4000 mg/dm^3 of tetrafluoroboric acid (B: 500, F: 3500 mg/dm^3) with $Ca(OH)_2$ at 150 °C are shown in Figure 4-6 and Figure 4-7. A steady state of the residual concentrations of boron and fluorine was attained after the treatment time of 2 h and both boron and fluorine concentrations were ca. 4 mg/dm^3. Thus, this treatment is also applicable to the tetrafluoroboric ion. Residual concentration of tetrafluoroboric ion drastically decreased from the beginning of treatment and it was not detected after 2 h. Boric and fluoride ions were detected along with the decrease of tetrafluoroboric ion concentration. It is expected that the tetrafluoroboric ion would decompose under alkali, high temperature and pressure conditions and complete for 2 h. Thus, the slow decreasing rate of residual boron concentration as shown in Figure 4-7 depends on the decomposition rate of tetrafluoroboric acid. After that, the formation of borate mineral would occur on the surface of $Ca(OH)_2$ and the precipitation reaction completed at 2 h. In addition, 20 – 30 mg/dm^3 of fluoride ion was observed, which is higher than the value calculated from the solubility of CaF_2 at 25 °C at the treatment time range of 0.5 – 1 h (Figuire 4-6). Fluoride ion concentration increased from 0.5 to 1 h. The solubility of CaF_2 was found to decrease with an increase in temperature in our previous study[17]. Thus,

it was anticipated that the precipitation of fluoride ion would occur as soon as the tetrafluoroboric ion was decomposed. Excess amount of F^- generated by decomposition of tetrafluoroboric ion in a short time range of treatment in contrast to the Ca^{2+} (ca. 15 mg/dm^3) as shown shown in Figure 4-2. It is expected that the rate controlling factor to form CaF_2 is not the reaction between Ca^{2+} and F^-, but the dissolution process of $Ca(OH)_2$ by solution equilibrium and diffusion of dissolved Ca^{2+}. Therefore, F^- concentration increased at the treatment time between 0.5 and 1 h .

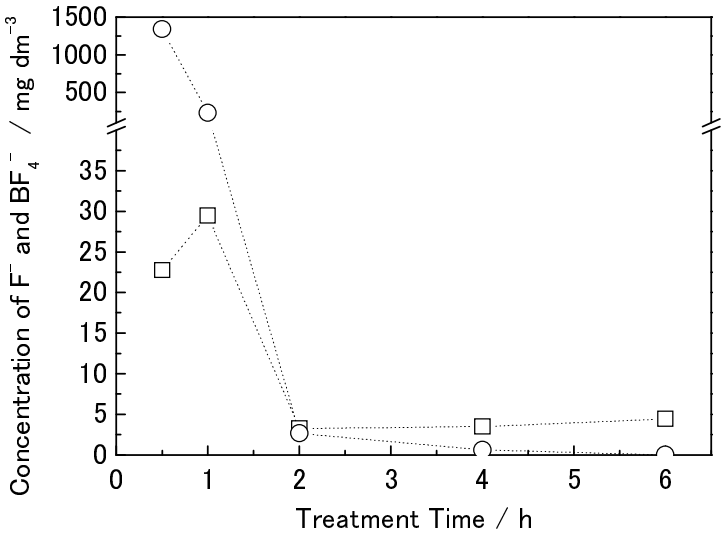

Figure 4-6. Dependence of the fluoride and tetrafluoroboric ion concentration on the treatment time. (a): Concentration of F^- (□) and BF_4^- (○). Treatment temperature: 150 °C, $Ca(OH)_2$: 2.0 g, BF_4^-: 4000 mg/dm^3.

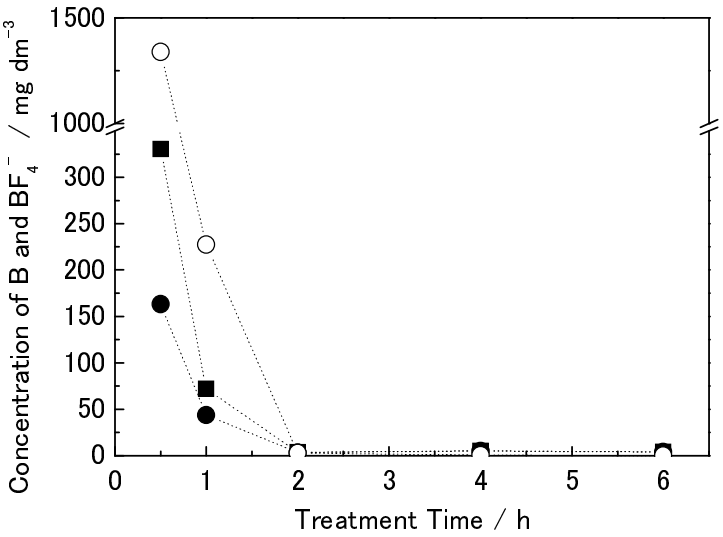

Figure 4-7. Dependence of the boron, boric ion and tetrafluoroboric ion concentration on the treatment time. Concentration of B (■), BF_4^- (○) and B exist as boric ion (●). Treatment temperature: 150 °C, $Ca(OH)_2$: 2.0 g, BF_4^-: 4000 mg/dm^3.

4.4. Conclusions

In conclusion, the detoxification of polluted water containing boric or tetrafluoroboric ions and the resource recovery by using the sampling-type hydrothermal mineralization treatment was investigated. As a result, effective recovery of boron and fluorine was successfully achieved at shorter treatment time throu in situ solid/liquid separation under quasi-equilibrium hydrothermal condtion. We obtained important information on decomposition of tetrafluoroboric ion and formation of fluorite by measuring solubility of $Ca(OH)_2$ under hydrothermal condition. Therefore, the hydrothermal mineralization treatment by using the flow-type apparatus would be effective method to detoxify the wastewater and ground water containing these ions and recoverions as recyclable mineral. These results suggest that large amount of wastewater containing boron and fluorine could be treated more effectively for shorter time by using the flowing-type hydrothermal apparatus.

References

1. S. Karahan, M. Yurdakoc, Y. Seki, and K. Yurdakoc, *Journal of Colloid and Interface Science* **293**, (1), (2006). 36-42

2. WHO, *Geneva: World Health Organization*, (1993).

3. T. Itakura, R. Sasai, and H. Itoh, *Water Research* **39**, (12), (2005). 2543-2548

4. T. Itakura, R. Sasai, and H. Itoh, *Bulletin of the Chemical Society of Japan* **79**, (8), (2006). 1303-1307

5. T. Itakura, R. Sasai, and H. Itoh, *Chemistry Letters* **35**, (11), (2006). 1270-1271

Chapter 5 Removal and recovery of arsenic from aqueous media containing arsenite and arsenate ions by hydrothermal mineralization

5.1 Introduction

Arsenic is one of the important resources for advanced electronic material production, and chemical species containing arsenic ions are contained in water discharged from petroleum refining plant or thermal power plant [1-5]. However, they have extremely high toxicity against human health and the environment especially in the case of trivalent arsenite ion ($As^{III}O_3^{3-}$). Thus, the national effluent standard of Japan (NESJ) was set at 0.1 mg/dm^3, which is the same as WHO guideline (the standard for environmental water is 0.01 mg/dm^3). An appropriate treatment should be employed for such wastewater to attain the environmental standard. Furthermore, serious environmental problems by arsenic pollution of groundwater have emerged in Asian countries, such as Bangladesh, India and China [6-13]. On the other hand, arsenic ore is less produced in Japan, where arsenic is expected to be recycled. Therefore, the establishment of the system for removing and recycling arsenic species from wastewater will be one of the world-important issues, also in Japan that is poor in natural minerals.

Several techniques to remove arsenic from aqueous media have been developed, for example, by adsorption, electro-coagulation [8, 14], membrane permeation [15, 16] and biological methods [10, 17, 18]. Especially, the adsorption methods using iron hydroxide and zero-valent irons were actively investigated [19-26]. However, these have the following problems. (1) Arsenic in aqueous media cannot be reused as resources. (2) The applicable concentration range is narrow. (3) Removal yield is low, especially, for arsenite ion ($As^{III}O_3^{3-}$). Thus, some oxidation techniques to remove arsenite ion from aqueous media are investigated [1, 27-32]. However, used

adsorbent or collected residues must be properly treated again as hazardous wastes. In order to solve these problems, it is expected that the formation method of insoluble and reusable precipitate containing As from aqueous media containing arsenite and arsenate ions is effective. But, it is difficult to form precipitate with low solubility in water because of high stability of arsenic oxoanins in aqueous media. Thus, it is much expected to develop a new technique to recover arsenic species as solid precipitates from aqueous media regardless of its concentration, oxidation number and ionic species.

Compounds that contain high arsenic concentrations and are insoluble in water, are frequently found in natural minerals, for example, Haidinglite ($Ca(AsO_3OH)\cdot(H_2O)$) and Johnbaumite ($Ca_5(AsO_4)_3(OH)$). This fact suggests that the earth has an ability to produce insoluble minerals containing arsenic under certain conditions in nature. Previous chapters described that the precipitation technique of boron and fluorine from aqueous media containing borate, fluoride and fluoroborate ions by imitating natural mechanism to form some minerals in hydrothermal water (by so-called "hydrothermal mineralization" technique) [33-35]. In this study, we investigated the precipitation recovery of arsenic from model wastewater containing arsenite ion ($As^{III}O_3^{3-}$) by using hydrothermal mineralization treatment, which was derived from earth-mimetic mineral precipitation phenomena caused by the activity of magma in the presence of water.

5.2. Experimental

5.2.1. Hydrothermal treatment

Model wastewaters with 1 - 2000 mg/dm^3 (0.013 – 26.7 mmol/dm^3) of arsenite and arsenate ions were prepared by dissolving As_2O_3 in 0.5 N NaOH solution, and neutralized by HCl or by dissolving Na_2HAsO_4 in distilled and deionized water (Wako Pure Chemical Industries, Ltd.), respectively. These model wastewaters (30 ml) were

sealed in a pressure vessel lined with fluorocarbon resin together with mineralizer $Ca(OH)_2$ and in some cases, with H_2O_2 added as oxidizer. Hydrothermal treatments were carried out by leaving the vessel in a dry oven for 2 – 96 h at a given temperature in the range of 100 – 200 °C. After the hydrothermal treatment, the vessels were cooled down in atmospheric air for 1 h. Precipitates obtained by the hydrothermal treatment were filtered and collected.

5.2.2. Sampling-type hydrothermal treatment

Model wastewater of 90 mL which containing 2000 mg/dm^3 (26.7 mmol/dm^3) As were sealed in a pressure vessel with 1.0 g of $Ca(OH)_2$ mineralizer. Thermal adjustment was carried out by temperature controller (CHINO Corporation, DZ1000).

5.2.3. Analytical method

The precipitates were identified by X-ray diffraction (XRD: RIGAKU Rint-2500) using CuKα radiation. The microstructural observation and qualitative elements analysis of the precipitates were performed by scanning electron microscopy (SEM: JEOL JSM-T20) equipped with energy dispersive X-ray spectrometry (EDS: JED-2140). Thermometric analyses of the precipitates were carried out by thermogravimetric and deferential thermal analyzers (TG-DTA: RIGAKU Thermo plus, TG-8120). Quantitative analysis of the arsenate ion in the solvent obtained after the hydrothermal treatment was carried out by molybdenum blue method [36]. In order to determine the total arsenic content in the solvent, oxidation by hydrothermal treatment in a solvent with concentrated HNO_3 (0.2 ml/10 ml of treated-water) was carried out at 200 °C for 12 h.

5.3. Results and Discussions

5.3.1. Hydrothermal mineralization treatment for arsenate ion ($As^{V}O_4^{3-}$) with $Ca(OH)_2$ mineralizer

Figure 5-1 shows the treatment time dependence of the arsenic concentration against the treatment time, when the initial concentration of As^{V} is 2000 mg / dm^3 with the mineralizer of 0.18 g $Ca(OH)_2$, and the treatment temperatures are 100 and 150 °C. The arsenic concentration reduced down to 1.8 mg / dm^3 only by addition of $Ca(OH)_2$ to the model wastewater, *i.e.*, before the hydrothermal mineralization treatment. Figure 5-2 shows the XRD patterns of the precipitates obtained before and after the treatment at 100 °C. Diffraction peaks derived from arsenic compound was not observed before the treatment (Figure 5-2-(a)). Thus, it is supposed that decrease of arsenic concentration only by addition of $Ca(OH)_2$ will be caused by the adsorption of the arsenate ion ($As^{V}O_4^{3-}$) to the hydroxyl group on the surface of $Ca(OH)_2$. But, the residual arsenic concentration before the hydrothermal mineralization is still higher than the value of NESJ. On the other hand, the arsenic content after hydrothermal mineralization treatment for more than 16 h was 0.02 mg / dm^3, which is lower than the NESJ value. The diffraction peaks of arsenate apatite ($Ca_5(AsO_4)_3(OH)$) were observed after the treatment (Figure 5-2-(b) or (c)). Therefore, the formation of arsenate apatite enables an effective recovery of arsenic because of its very low solubility in water (less than 0.2 mg As / 100 dm^3) [37, 38]. However, the residual arsenic concentration was lower than the above value in equilibrium with water at normal conditions. Thus, the solubility of arsenate apatite under hydrothermal conditions will be lower than that at room temperature and pressure, which promotes the crystal growth of the arsenate apatite. It was considered that the lower arsenic concentration was maintained even during the cooling process because large crystal sizes of arsenate apatite prevented re-dissolution into water.

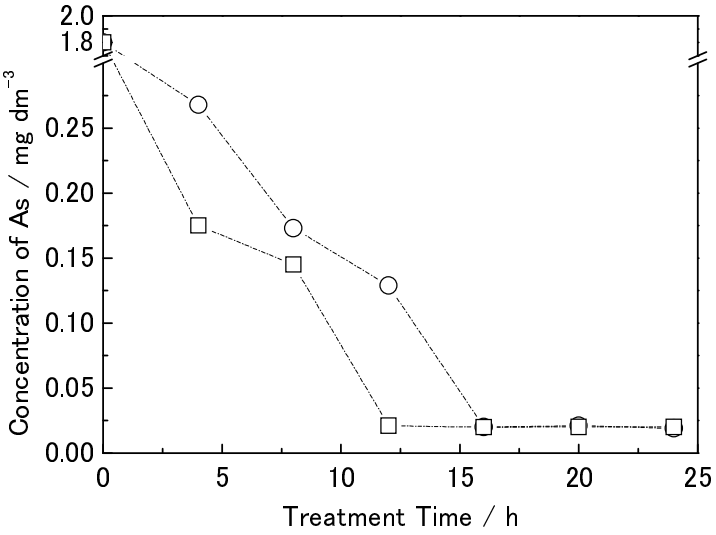

Figure 5-1. Dependence of concentration of As in the treated-water on the treatment time. As: 2000 mg/dm^3, □: 150 °C, ○: 100 °C.

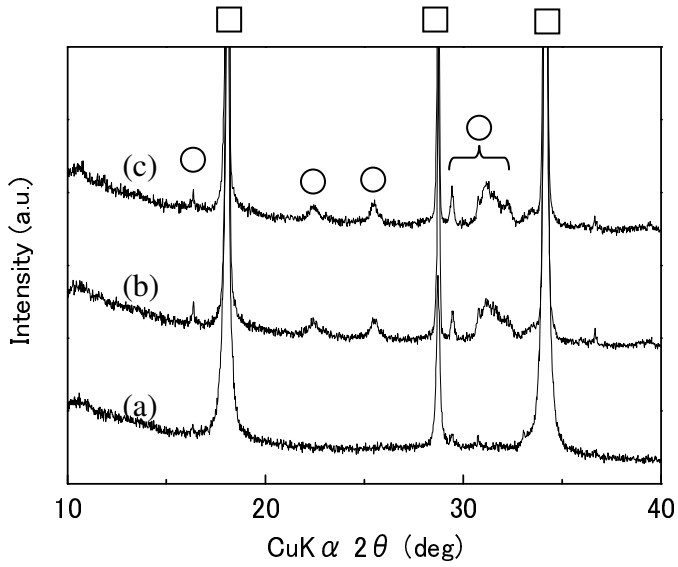

Figure 5-2. XRD patterns of the precipitates before (a) and after the treatment for 8 h (b) and 16 h (c) at 100 °C. □: $Ca(OH)_2$, ○: $Ca_5(AsO_4)_3(OH)$.

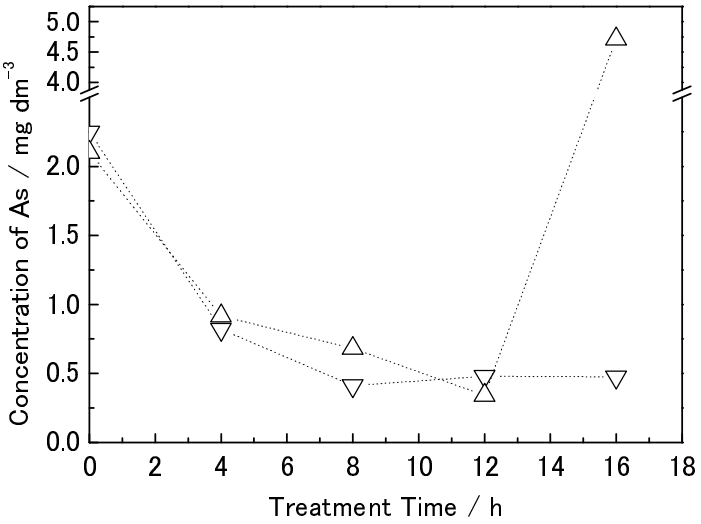

Figure 5-3. Dependence of the concentration of As in the treated-water on the treatment time. As(III): 2000 mg/dm^3, 100 °C. Amount of $Ca(OH)_2$ addition was ▽: 0.36 g, and △: 0.18 g.

5.3.2. Hydrothermal mineralization treatment for arsenate ion ($As^{III}O_3^{3-}$) with $Ca(OH)_2$ mineralizer

Treatment time dependence of the As concentration in the model wastewater (As^{III}: 2000 mg/dm^3) treated at 100 °C with $Ca(OH)_2$ is shown in Figure 5-3. The arsenic content decreased only by adding $Ca(OH)_2$ mineralizer to the model wastewater, and it was reduced down to 4 mg/dm^3 (even before the hydrothermal mineralization treatment). This decrease in As concentration is derived from formation of arsenic calcium compound as described later. However, this concentration does not meet NESJ (0.1 mg/dm^3). By performing the hydrothermal mineralization in the model wastewater added with $Ca(OH)_2$, As concentration draws concave curves against treatment time, i.e., a proper treatment time exists for decreasing As concentration. The increase of As concentration at longer treatment-time might be caused by the nature of As compound formed during the treatment. At the optimal treatment condition, the As concentration reduced down to ca. 0.4 mg/dm^3, which is one tenth of

As concentration before the hydrothermal treatment, but is still higher than the NESJ. It is apparent leastwise that the precipitate containing As can be formed by this hydrothermal treatment.

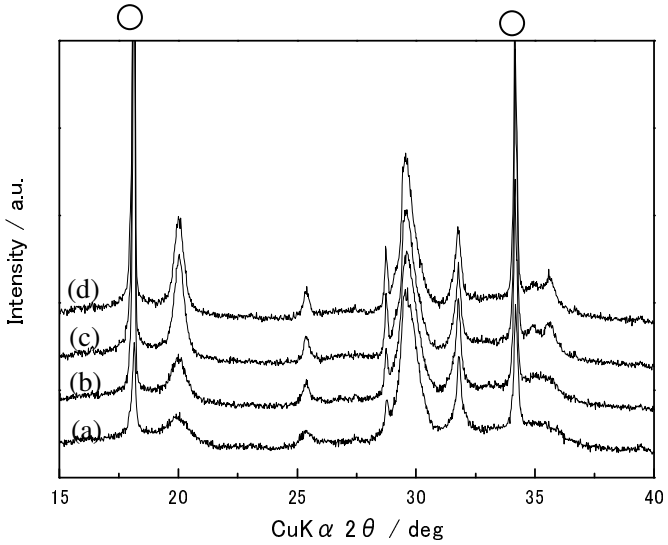

Figure 5-4. XRD patterns of the precipitates obtained before and after the treatment at 100 °C with 0.18 g of $Ca(OH)_2$. As(III): 2000 mg/dm^3, (a): before the treatment, (b): 4 h, (c): 12 h, (d): 16 h, ○: $Ca(OH)_2$. Other peaks were unassignable.

Figure 5-4 shows the XRD patterns of the precipitates before and after the treatments for arsenite ion containing model wastewater at 100 °C with $Ca(OH)_2$ mineralizer. Unassignable peaks were observed in the patterns before and after the treatments together with the diffraction peaks of $Ca(OH)_2$. According to the results of XPS, TG-DTA and SEM-EDS analyses, the chemical formula of this unassingable compound was estimated as $Ca_5(As^{III}O_3)_3(OH)\cdot 4H_2O$. Scheme 5-1 shows possible reactions in the hydrothermal mineralization treatment. The formation of $Ca_5(As^{III}O_3)_3(OH)\cdot 4H_2O$ would accomplish by the reaction Scheme 5-1-(e). Figure 5-5 shows the XRD patterns of the precipitates after the treatment at 200 °C and single phase crystals contained in the treated precipitates. Each precipitates in Figure 5-5 were prepared under the following conditions. Figure 5-5-(a): the precipitate before

the treatment. Figure 5-5-(b): $Ca_5(AsO_3)_3(OH)$ prepared by heat treatment of the precipitate before the treatment at 200 °C for 4 h in order to eliminate crystal water. Figure 5-5-(c): Arsenate apatite ($Ca_5(As^VO_4)_3(OH)$) formed by hydrothermal mineralization treatment of arsenate ion ($As^VO_4^{3-}$) with $Ca(OH)_2$ mineralizer at 200 °C for 24 h. Figure 5-5-(d): Precipitate after the hydrothermal treatment for the model wastewater containing arsenite ion ($As^{III}O_3^{3-}$) at 200 °C for 8 h. These results indicate that the precipitate after the treatment is a mixture of $Ca_5(As^{III}O_3)_3(OH)$ and $Ca_5(As^VO_4)_3(OH)$. Thus, crystal water of $Ca_5(AsO_3)_3(OH)\cdot 4H_2O$ would be removed during the hydrothermal mineralization treatment according to Scheme 5-1-(f). After that, As(III) in the precipitate were oxidized and formed $Ca_5(AsO_4)_3(OH)$. Figure 5-6 shows the XPS spectra of the precipitates obtained at the treatment temperature of 200 °C. Oxidation of As(III) progressed during the treatment and the ratio of trivalent and pentavalent As was ca. 1 : 0.9 after long term treatment (at 200 °C for 96 h). Gas analysis by GC-TCD suggested that the oxidizer was H_2O, because generation of hydrogen was confirmed. Thus, the oxidation of As(III) was accomplished by the reaction of AsO_3^{3-} and H_2O shown in Scheme 5-1-(j). After that, the formation of $Ca_5(As^VO_4)_3(OH)$ would occur by the reaction of AsO_4^{3-} and precipitate of $Ca(OH)_2$ (Scheme 5-1-(k)). Additionally, the solubility of $Ca_5(AsO_3)_3(OH)\cdot 4H_2O$ and $Ca_5(AsO_3)_3(OH)$ in water, which was measured by a simple solubility test, was 13.79 mg As/100 dm^3 and 29.10 mg As/100 dm^3, respectively. Therefore, the concave tendency in Figure 5-3 would be caused by the removal of crystal water from $Ca_5(AsO_3)_3(OH)\cdot 4H_2O$ and the formation of $Ca_5(AsO_3)_3(OH)$, which has higher solubility in water with an increase of treatment time. In contrast, the solubility of $Ca_5(As^VO_4)_3(OH)$ was less than 0.2 mg As/100 dm^3 that was very low compared with the above trivalent arsenic compounds. It is expected, therefore, that intentional oxidation of arsenite ion to form $Ca_5(AsO_4)_3(OH)$ would be effective for precipitation

of arsenic species.

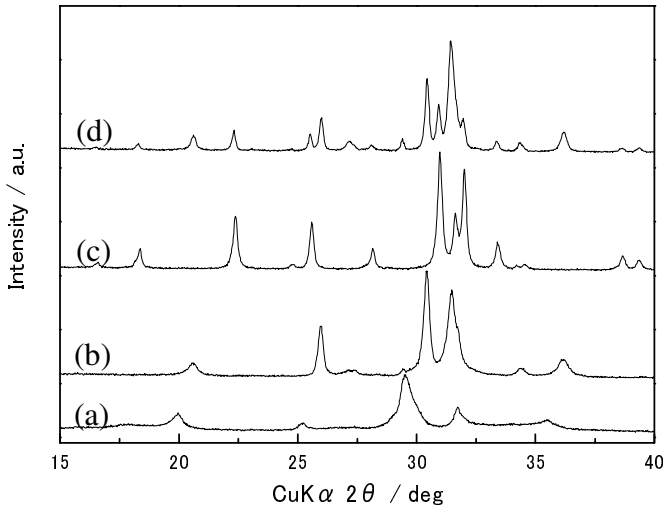

Figure 5-5. XRD patterns of the precipitates. (a): before the treatment ($Ca_5(AsO_3)_3(OH)\cdot 4H_2O$), (b): $Ca_5(AsO_3)_3(OH)$, (c): $Ca_5(AsO_4)_3(OH)$, (d): treated at 200 °C with 0.18g of $Ca(OH)_2$ for 8 h (As: 2000 mg/dm^3).

(a) $Ca(OH)_2 + H_2O_2 \rightarrow CaO_2 + 2H_2O$

(b) $2CaO_2 + 2H_2O \rightarrow 2Ca(OH)_2 + O_2$

(c) $H_2O_2 \rightarrow H_2O + O_2$

(d) $CaO + H_2O \rightarrow Ca(OH)_2$

(e) $3AsO_3^{3-} + 5Ca(OH)_2 + 4H_2O \rightarrow Ca_5(AsO_3)_3(OH)\cdot 4H_2O + 9OH^-$

(f) $Ca_5(AsO_3)_3(OH)\cdot 4H_2O \rightarrow Ca_5(AsO_3)_3(OH) + 4H_2O$

(g) $Ca_5(AsO_3)_3(OH)\cdot 4H_2O + 10H_2O_2 \rightarrow 5CaO_2 + 3AsO_3^{3-} + 11OH^-$

(h) $AsO_3^{3-} + CaO_2 \rightarrow AsO_4^{3-} + CaO$

(i) $AsO_3^{3-} + H_2O_2 \rightarrow AsO_4^{3-} + H_2O$

(j) $AsO_3^{3-} + H_2O \rightarrow AsO_4^{3-} + H_2$

(k) $3AsO_4^{3-} + 5Ca(OH)_2 \rightarrow Ca_5(AsO_4)_3(OH) + 9OH^-$

Scheme 5-1. Possible reactions in the hydrothermal mineralization treatment.

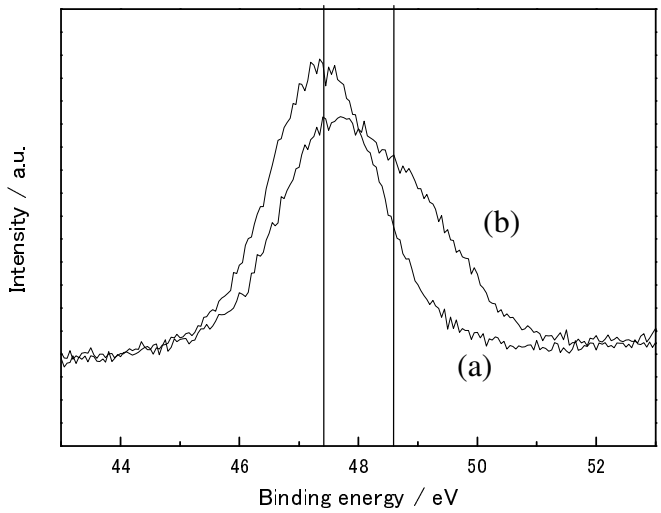

Figure 5-6. XPS spectra of As3d (a): before and (b) after the treatment, treated at 200 °C with 0.18g of $Ca(OH)_2$ for 96 h (As: 2000 mg/dm^3). Vertical lines of left side and right side mean the binding energies of As(III) and As(V), respectively.

5.3.3. Treatment for model wastewater containing arsenite ion ($As^{III}O_4^{3-}$) with $Ca(OH)_2$ mineralizer and H_2O_2 oxidizer

The effect of H_2O_2 addition on oxidation of arsenite ions and precipitation of $Ca_5(As^VO_4)_3(OH)$ was investigated. Figure 5-7 shows the dependence of concentration of As(III) on treatment time under the hydrothermal conditions for 0 – 16 h at 100 or 150 °C with the addition of 0.18 g $Ca(OH)_2$ and 3 % H_2O_2. This indicates that the residual concentration of As is 0.15 mg/dm^3 at the optimum treatment time of 12 h. Figure 5-8 shows the XRD patterns of the precipitates formed under the above hydrothermal conditions. Diffraction peaks of CaO_2 are observed at short treatment times (0 h to 8 h) and then the diffraction peaks of $Ca(OH)_2$ appear with decreasing the intensities of CaO_2 peaks. This result shows that the oxidation of $Ca(OH)_2$ occurred at the beginning of treatment (Scheme 5-1-(a)), after which it gradually reacts with H_2O to form $Ca(OH)_2$ (Scheme 5-1-(b)). High values of As

concentrations before the treatment (compared with the case of no H_2O_2 addition in Figure 5-3) would be caused by decomposition of $Ca_5(AsO_3)_3(OH)\cdot 4H_2O$ (Scheme 5-1-(g)) and CaO_2. On the other hand, only the diffraction peaks of $Ca_5(As^VO_4)_3(OH)$ was observed after the hydrothermal treatment. Therefore, the minimum value of As concentration at the optimum treatment time is attributed to the result of oxidation of arsenite (As(III)) to arsenate (As(V)) by H_2O_2 or CaO_2, and formation of $Ca_5(AsO_4)_3(OH)$ (Scheme5-1-(h), (i), (j), (k)). However, a concave curve tendency is still observed in Fig. 5-7 against the treatment time and the NESJ could not be overcome. Oxidation of arsenite ion would be insufficient, because arsenite ion still existed mainly in treated-water by detailed analysis shown in Table 5-1.

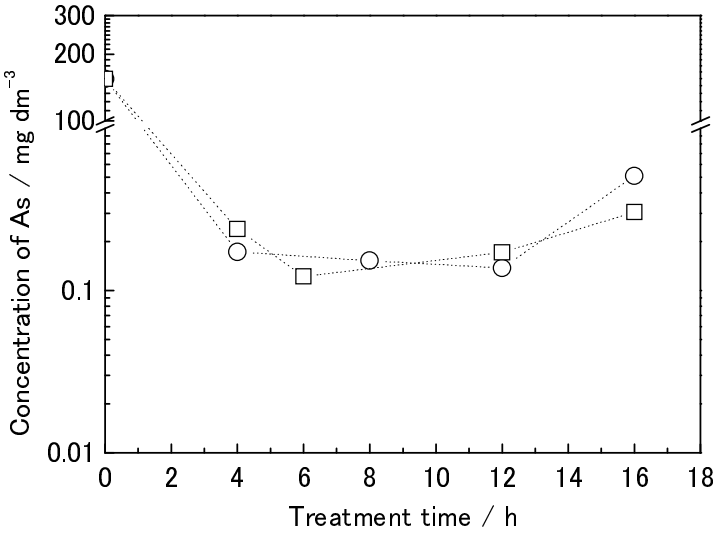

Figure 5-7. Dependence of As concentration on treatment time with 0.18 g of $Ca(OH)_2$ and 3 % H_2O_2. As(Ⅲ): 2000 mg/dm^3. ○: 100 °C, □: 150 °C.

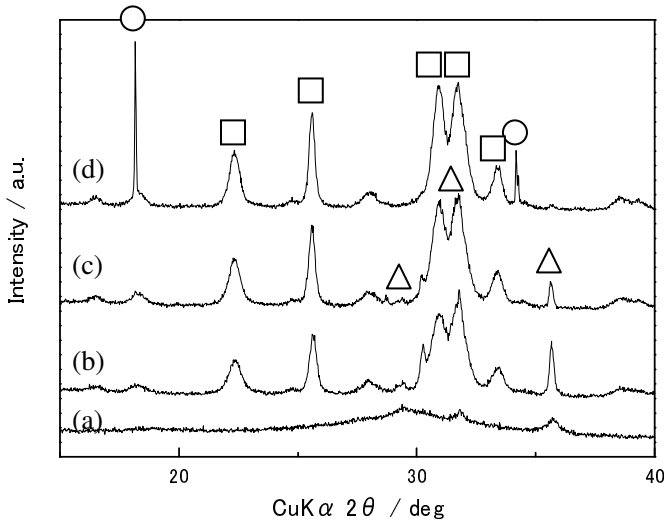

Figure 5-8. XRD patterns of the precipitates obtained by hydrothermal mineralization treatment with 0.18 g of $Ca(OH)_2$ and 3 % H_2O_2 at 100 °C, (a): before the treatment, (b): 4 h, (c): 8 h, and (d): 16 h. ○: $Ca(OH)_2$, □: $Ca_5(AsO_4)_3(OH)$, △: CaO_2.

Table 5-1. As(III) and As(V) concentrations in the treated-water with 3 % H_2O_2

	As(III) / mg/dm^3	As(V) / mg/dm^3	As / mg/dm^3
100 °C for 12 h	0.106	0.031	0.137
100 °C for 16 h	0.504	0.004	0.508
150 °C for 12 h	0.164	0.008	0.172
150 °C for 16 h	0.302	0.003	0.305

Figure 5-9 shows similar concave curves against treatment time in case of 5 % H_2O_2 addition at 100 °C and 150 °C, which means that arsenite ion also exists in the water. However, the As concentration was less than the value of NESJ, 0.1 mg/dm^3 at the optimum treatment conditions attained at 5 % H_2O_2 addition at 150 °C for 4-12 h. This result indicates that oxidation of 2000 mg/dm^3 of arsenite ion and the formation of $Ca_5(As^VO_4)_3(OH)$ were mostly accomplished by the hydrothermal treatment with H_2O_2 addition. Obviously, the optimum amount of H_2O_2 addition depends on the initial

concentration of arsenite ion, which needs at least 5 % H_2O_2 in this case to oxidize 2000 mg/dm^3 of arsenite ion to arsenate.

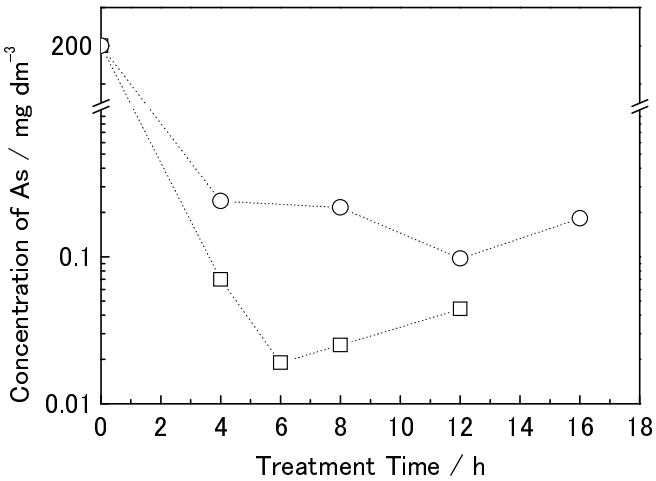

Figure 5-9. Dependence of the concentration of As in the treated-water on the treatment time with 0.18 g of $Ca(OH)_2$ and 5 % H_2O_2. As(Ⅲ): 2000 mg/dm^3. ○: 100 °C, □: 150 °C.

Oxidative conditions of arsenite to arsenate were investigated in order to search for more effective recovery of arsenite ion. Table 5-2 shows the As concentration dependence after the treatment as a function of initial concentration of As (1-2000 mg/dm^3) and the amount of H_2O_2 addition against 1 mmol of As. This result demonstrates that more than 50-66 times mole of H_2O_2 against the trivalent Arsenic are required to oxidize arsenite ion. The formation of CaO_2, the decomposition of CaO_2 to $Ca(OH)_2$ by reaction with H_2O and the decomposition of H_2O_2 to H_2O and O_2 would occur as shown in Scheme 5-1-(a), (b), (c), respectively.

Table 5-2. Dependence of As concentration in the treated-water on the initial As concentration and the amount of H_2O_2 addition

Initial concentration of As (mg/dm^3)	Amount of $Ca(OH)_2$ addition (g/30ml sample)	Amount of H_2O_2 addition (%)	Content of H_2O_2 (mmol/1 mmol As)	As concentration in the treated water
1	0.36	3.0	66000	0.06
10	0.36	3.0	6600	0.04
100	0.36	3.0	660	0.05
1000	0.36	3.0	66	0.06
2000	0.36	3.0	33	0.51
2000	0.36	5.0	55	0.04

5.3.4. Initial arsenate ion concentration dependence

Figure 5-10 shows the initial arsenate ion concentration dependence of the As concentration in the treated-water with $Ca(OH)_2$ mineralizer and 3 % H_2O_2 oxidizer. Dependence of As concentration was not observed on the initial concentration of arsenate ion. It is expected that the As concentration in the treated-water depends on only the solubility of formed mineral. Therefore, this hydrothermal mineralization treatment could be applied for various kind of contaminated water, *e.g.,* industrial wastewater, leachate from disposal site, and contaminated ground water.

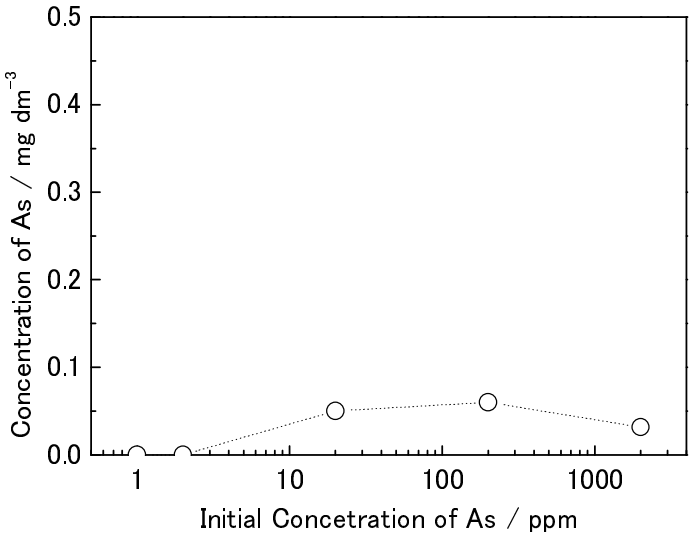

Figure 5-10. Initial concentration dependence of the As concentration in the treated-water treated for model wastewater containing arsenate ion at 150 °C with 3 % H_2O_2 oxidizer and 0.36 g $Ca(OH)_2$ mineralizer.

5.3.5. Initial arsenite ion concentration dependence

Initial arsenite ion concentration dependence of the As concentration in the treated-water is shown in Figure 5-11 with $Ca(OH)_2$ mineralizer and 3 % H_2O_2 oxidizer. Initial arsenite ion concentration dependence was not observed at concentration range 0.1 – 1000 mg/dm^3. On the other hand, As concentration treated for aqueous media containing 2000 mg/dm^3 of As was higher than that of the other conditions. However, As concentration of the treated-water obtained by the treatment for aqueous solution containing 2000 mg/dm^3 treated with 5 % H_2O_2 oxidizer was 0.02 mg/dm^3 (see Figure 5-9) which was same value with the other initial arsenite ion concentrations shown in Figure 5-11. This result verifies that the hydrothermal mineralization treatment is independent of the initial concentration of arsenite ion when the enough amount of H_2O_2 is added, because the residual As concentration in the treated-water depends only on the solubility of $Ca_5(AsO_4)_3(OH)$. Therefore, it is concluded that the hydrothermal mineralization treatment is effective precipitation technique for arsenic recovery from

wastewater containing arsenite ion.

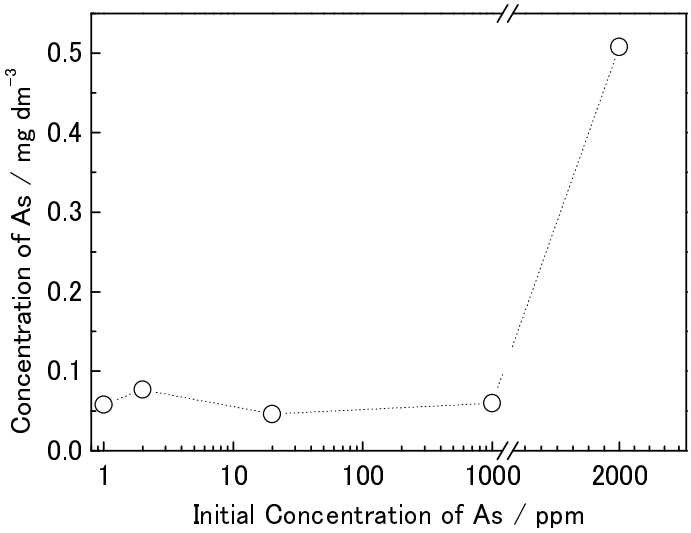

Figure 5-11. Initial concentration dependence of the As concentration in the treated-water treated for model wastewater containing arsenite ion at 150 °C with 3 % H_2O_2 oxidizer and 0.36 g $Ca(OH)_2$ mineralizer.

5.3.6. Treatment for model wastewater containing arsenate ($As^{V}O_4^{3-}$) and arsenite ions ($As^{III}O_3^{3-}$) with $Ca(OH)_2$ mineralizer

The result of hydrothermal mineralization treatment against model wastewater is shown in Figure 5-12, where a mixed aqueous solution of arsenate ($As^{V}O_4^{3-}$: 1000 mg / dm^3) and arsenite ion ($As^{III}O_3^{3-}$: 1000 mg / dm^3) is treated at 100 °C with $Ca(OH)_2$. The arsenic content decreased before the treatment (only by addition of $Ca(OH)_2$), though it was higher than that of model wastewater containing arsenate ion only. Additionally, majority of arsenic species in the model wastewater before the hydrothermal treatment was found arsenate ion by detailed analysis. The formation of $Ca_5(As^{III}O_3)_3(OH)\cdot 4H_2O$ occurred only by addition of $Ca(OH)_2$, as described in 5.3.2. Thus, adsorption site of arsenate ion would be decreased due to the formation of $Ca_5(As^{III}O_3)_3(OH)\cdot 4H_2O$ and the consumption of $Ca(OH)_2$. In contrast, the arsenic species in the model wastewater after the treatment were arsenite ion. By performing

the hydrothermal treatment, arsenic concentration draws a concave curve against the treatment time and the minimum value of arsenic was 0.3 mg / dm^3 when treated for 12 h. The tendency of the variation of arsenic concentration in treated-water is same as the treatment for the model wastewater containing arsenite ion only, as shown in our previous study . XRD patterns of the precipitates after the treatment showed diffraction peaks derived from arsenic compounds of $Ca_5(As^{V}O_4)_3(OH)$ and $Ca_5(As^{III}O_3)_3(OH)\cdot 4H_2O$. Thus, arsenate ions were precipitated as arsenate apatite by hydrothermal mineralization treatment as shown above. But, partial arsenite ions were still in the water because of the nature of precipitate ($Ca_5(As^{III}O_3)_3(OH)\cdot 4H_2O$) formed by this treatment. The solubilities of $Ca_5(As^{III}O_3)_3(OH)\cdot 4H_2O$ and $Ca_5(As^{III}O_3)_3(OH)$ in water, were 13.79 mg As/100 dm^3 and 29.10 mg As/100 dm^3, respectively, according to a simple solubility test. These values are higher than that of arsenate apatite. As we already reported, the crystal water of ($Ca_5(As^{III}O_3)_3(OH)\cdot 4H_2O$) was eliminated by a prolonged hydrothermal treatment. Therefore, the increase in residual As at more than 12 h in Figure 5-12 would be caused by the removal of crystal water from $Ca_5(AsO_3)_3(OH)\cdot 4H_2O$ and the formation of $Ca_5(AsO_3)_3(OH)$ which has higher solubility in water than $Ca_5(AsO_3)_3(OH)\cdot 4H_2O$. Therefore, it is expected that oxidation treatment of arsenite ion enables effective recovery of arsenic species finally to form $Ca_5(AsO_4)_3(OH)$.

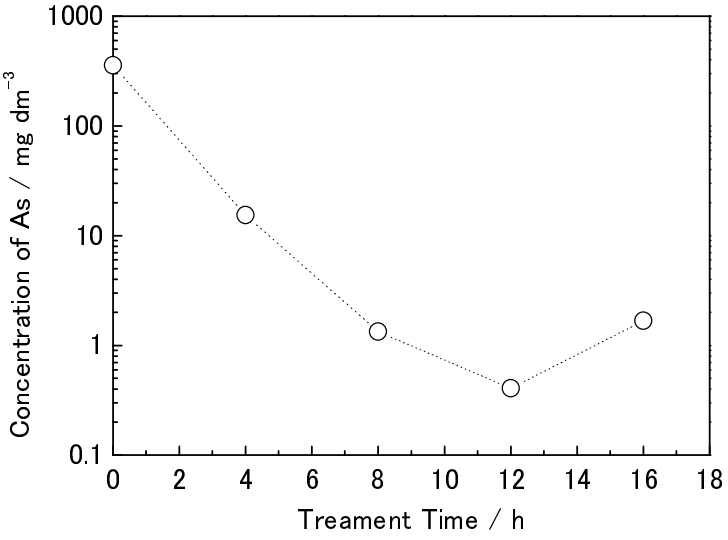

Figure 5-12. Dependence of concentration of As in the treated-water on the treatment time. As(III): 1000 mg/dm^3, As(V): 1000 mg/dm^3, $Ca(OH)_2$: 0.36g, 100 °C.

5.3.7. Treatment for model wastewater containing arsenate ($As^{V}O_4^{3-}$) and arsenite ions ($As^{III}O_3^{3-}$) with $Ca(OH)_2$ mineralizer and H_2O_2 oxidizer

Figure 5-13 shows the result of the hydrothermal treatment with $Ca(OH)_2$ and 3 % H_2O_2 against the model wastewater containing 2000 mg/dm^3 of arsenate ion. Arsenic concentration before the treatment was much higher than that without H_2O_2. XRD analysis of the precipitate before the treatment exhibited the existence of CaO_2 shown in Figure 5-16-(a). Thus, the formation of CaO_2 from $Ca(OH)_2$ would bring about the desorption of arsenate ion that adsorbed on the surface of $Ca(OH)_2$. On the other hand, arsenic concentration in the treated-water treated for more than 12 h was very low (0.02 mg/dm^3) which was the same value of the treatment without H_2O_2. Therefore, the addition of H_2O_2 is no interfering factor to form arsenate apatite from aqueous media containing arsenate ion. The treatment time dependence of arsenic treated for the mixed aqueous solution of arsenite (1000 mg/dm^3) and arsenate (1000 mg/dm^3) ions on the treatment time with $Ca(OH)_2$ and 3 % H_2O_2 is shown in Figure 5-14. Arsenic concentration decreased with an increase of treatment time and it was

0.02 mg/dm^3 at optimum treatment time (12 – 16 h). Thus, it was found that the hydrothermal mineralization treatment with $Ca(OH)_2$ and H_2O_2 enabled effective recovery of arsenic regardless of the model wastewater containing both arsenite and arsenate ions. Figure 5-15 shows the XPS spectra of As 3d orbital and Figure 5-16 shows XRD patterns of the precipitates before and after the treatment. The data indicate that the valence state change of arsenic species from three to five occurs at 4 – 12 h and the precipitate of the treatment after 12 h is a single-phase of arsenate apatite. Thus, the treatment with oxidizer H_2O_2 immediately oxidizes arsenite ion to arsenate ion and forms arsenate apatite. The low solubility of arsenate apatite was found to cause effective recovery of arsenic species from model wastewater.

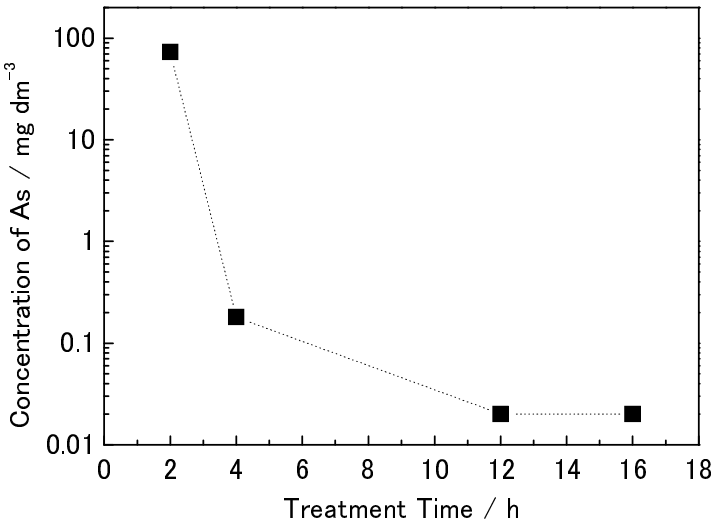

Figure 5-13. Dependence of concentration of As in the treated-water on the treatment time. As(V): 2000 mg/dm^3, $Ca(OH)_2$: 0.36g, H_2O_2: 3% 100 °C.

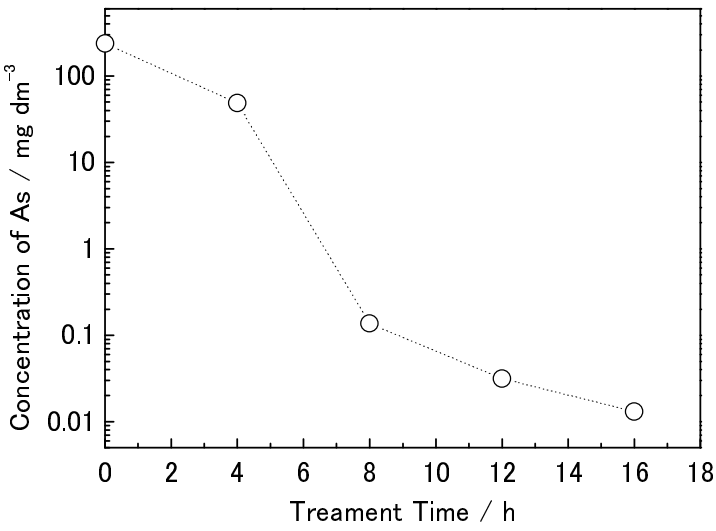

Figure 5-14. Dependence of concentration of As in the treated-water on the treatment time. As(III): 1000 mg/dm^3, As(V): 1000 mg/dm^3, $Ca(OH)_2$: 0.36g, H_2O_2: 3% 100 °C.

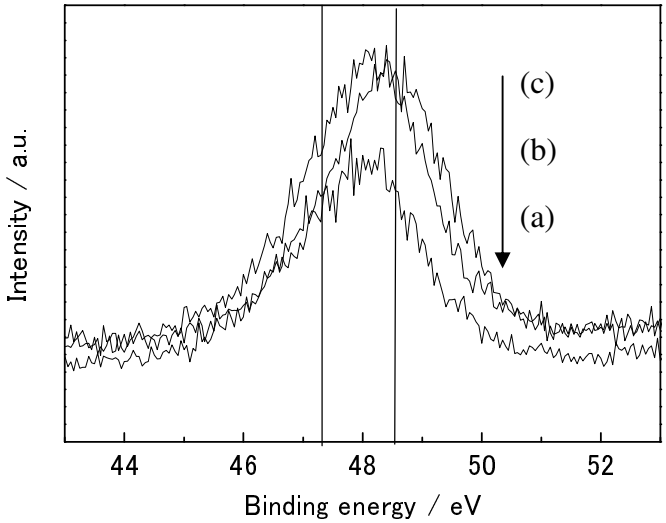

Figure 5-15. XPS spectra (vertical lines of left side and right side mean the binding energies of As(III) and As(V), respectively.) of the precipitates before (a) and after the treatment for 4 h (b) and 12 h (c). As(III): 1000 mg/dm^3, As(V): 1000 mg/dm^3, $Ca(OH)_2$: 0.36g, H_2O_2: 3% 100 °C.

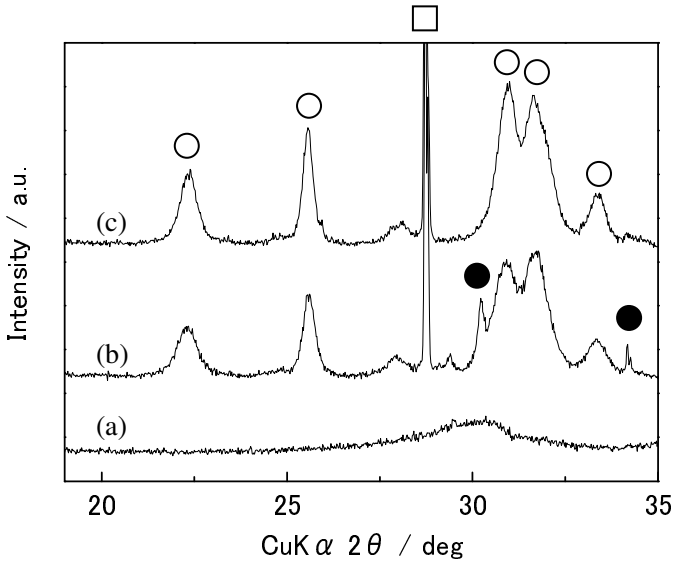

Figure 5-16. XRD patterns of the precipitates before (a) and after the treatment for 4 h (b) and 12 h (c). As(III): 1000 mg/dm^3, As(V): 1000 mg/dm^3, $Ca(OH)_2$: 0.36g, H_2O_2: 3% 100 °C. □: $Ca(OH)_2$, ○: $Ca_5(AsO_4)_3(OH)$, ●; $Ca_5(AsO_3)_3(OH) \cdot 4H_2O$.

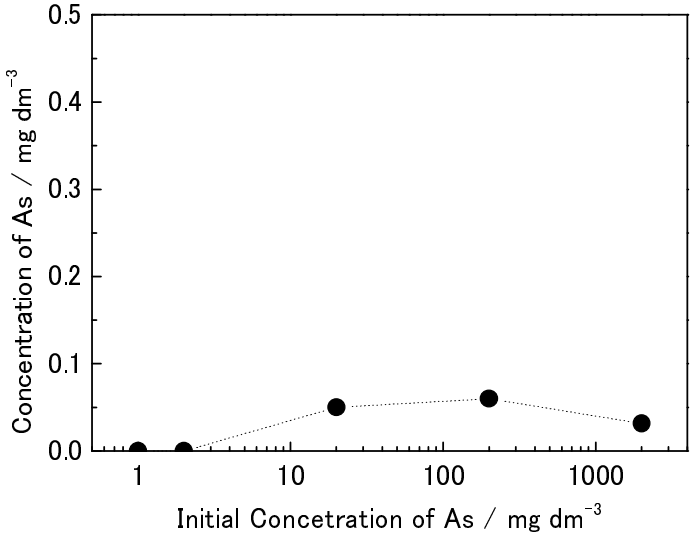

Figure 5-17. Dependence of concentration of As in the treated-water on the initial concentration of As. As(III): 1000 mg/dm^3, As(V): 1000 mg/dm^3, H_2O_2 3 %, 100 °C for 12 h.

Figure 5-17 shows the initial arsenic concentration dependence on the final arsenic concentration after the treatment time of 12 h with added $Ca(OH)_2$ and H_2O_2. Initial arsenic concentration dependence was not observed even when the treatment was

carried out for the arsenate and arsenite ions mixed aqueous solution. This result indicates that the arsenic concentration below NESJ value is attained regardless of the initial concentration of arsenic species, because the final concentration is responsible for only the solubility of formed minerals.

5.3.8. Effects of pH and added amount of $Ca(OH)_2$ mineralizer

The pH of the treated-water was 13 at any treatment condition, because it is saturated with $Ca(OH)_2$. The dependence of pH was investigated in the range of 6 – 12, controlled by addition of HCl to the model wastewater containing 2000 mg/dm^3 of arsenate ion. Arsenic concentration in the treated-water increased with a decrease of pH. Especially, in the treatment at pH 6, arsenic content in treated-water was 2000 mg/dm^3, which was the same value before the treatment. This result suggests that the existence of precipitated $Ca(OH)_2$ is essential in order to mineralize arsenic species under hydrothermal conditions. Figure 5-18 shows the As concentration dependence on the amount of $Ca(OH)_2$ added for 30 ml of model wastewater containing 1000 mg/dm^3 of arsenite and 1000 mg/dm^3 of arsenate ions along with 3 % H_2O_2. More than 0.36 g addition is required in order to meat the NESJ value. This amount of $Ca(OH)_2$ added is higher than the stoichiometric amount to form $Ca_5(AsO_4)_3(OH)$. Moreover, the concentration of Ca^{2+} in the solution and pH does not change at any amount of $Ca(OH)_2$ in Figure 5-18, because the solubility of $Ca(OH)_2$ is low (0.056 g / 30 dm^3 H_2O at 0 °C, 0.023 g / 30 dm^3 at 100 °C). These results suggest that the formation of arsenate apatite occurs by heterogeneous nucleation on the surface of $Ca(OH)_2$ under the hydrothermal conditions. Therefore, the increase of the amount of added $Ca(OH)_2$ means the increase of surface area of $Ca(OH)_2$ precipitates, i.e., the accommodation sites for deposition of $Ca_5(AsO_4)_3(OH)$ microcrystals.

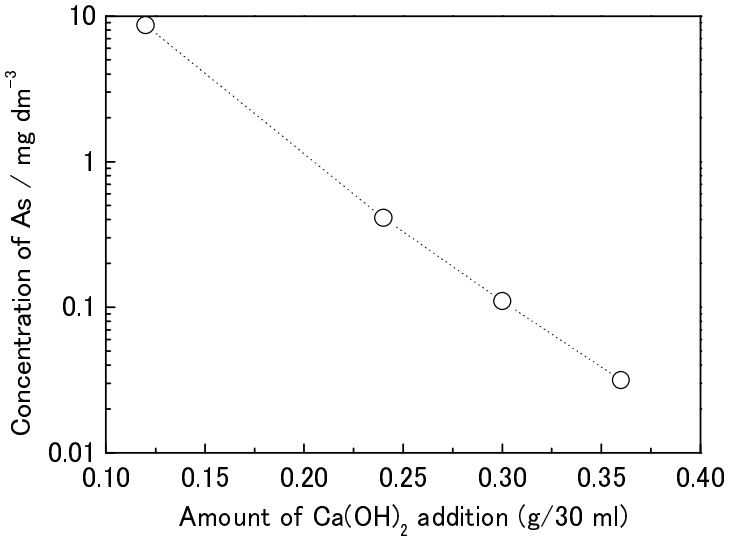

Figure 5-18. Dependence of the concentration of As in the treated-water on the amount of added $Ca(OH)_2$. As(III): 1000 mg/dm^3, As(V): 1000 mg/dm^3, H_2O_2 3 %, 100 °C for 12 h.

5.3.9. Hydrothermal mineralization treatment for model wastewater containing arsenate ion ($As^VO_4^{3-}$) by using sampling-type apparatus

Hydrothermal mineralization treatments by using the sampling-type apparatus, which is shown in Figure 5-19, were carried out in order to prevent re-dissolution of arsenate mineral precipitated under hydrothermal conditions in order to enhance treatment efficiency. During the hydrothermal treatment, the reactive suspension is led into the sampling tube by its own vapor pressure, and precipitates are separated from reaction suspension by 0.5 μm metal filter. After that, the samples were immediately cooled down at room temperature by cooling condenser. Thus, the collection of reaction solution during the hydrothermal treatment can be accomplished by the present sampling-type apparatus. The details of this hydrothermal treatment apparatus are described in Chapter 4.

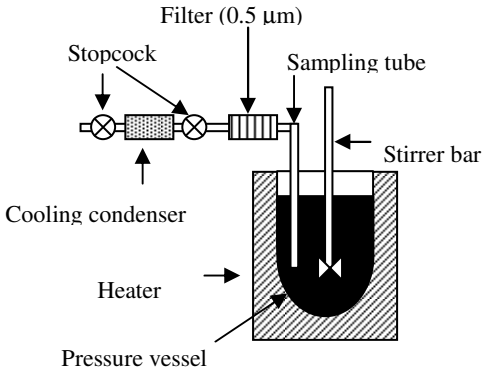

Figure 5-19. Schematic diagram of the sampling-type hydrothermal treatment apparatus.

Figure 5-20 shows the result of hydrothermal mineralization treatment by using ordinary batch type and sampling-type treatment apparatus. As a result, As concentration after the treatment for 3 h was c.a. 0.016 mg/dm^3. This result indicates that the separation of reaction solution from precipitate under hydrothermal condition brings not only improve yield recovery, but also shorten optimal treatment time. This shift of optimal treatment time is caused that crystal and/or grain growth of formed mineral is not necessary to decrease As concentration in the treated-water. The rate of re-dissolution of formed mineral comes under the influence of crystallinity and crystal radius. Therefore, it is expected that the decrease of As concentration at longer treatment time by using ordinary batch type hydrothermal apparatus (e.g. Figure 5-1) would be accomplished by crystal growth of $Ca_5(AsO_4)_3(OH)$. Larger crystal and/or grain size brings separation of solution from precipitate before dissolving great deal of $Ca_5(AsO_4)_3(OH)$ by its slow re-dissolution rate during the cooling process. On the other hand, crystal growth has not an effect for the As concentration in treated-water, when solutions are separated from precipitate under hydrothermal condition, because this treatment can completely prevent re-dissolution of formed minerals without crystal growth. Therefore, optimal treatment time to reduce As concentration was shortened by using sampling-type hydrothermal treatment apparatus.

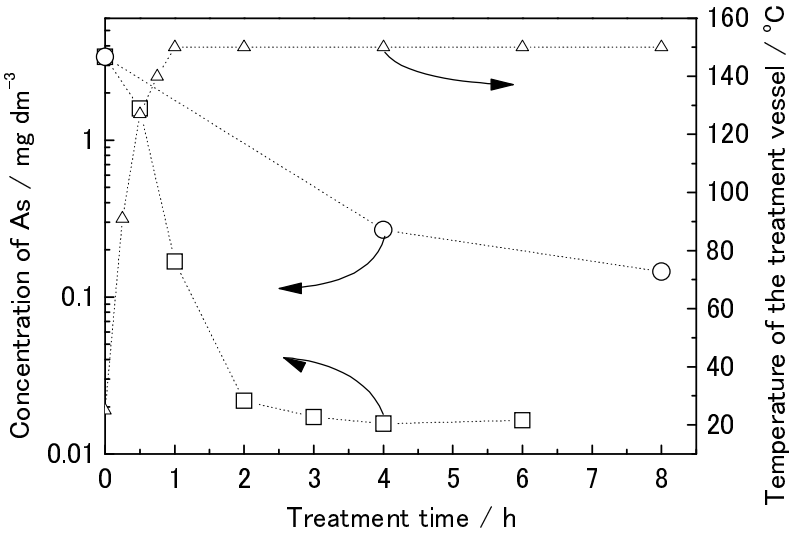

Figure 5-20. Dependence of the As concentration on the treatment time treated at 150 °C by using ○: ordinary batch type apparatus and □: sampling-type treatment apparatus. $As^{V}O_4^{3-}$: 2000 mg/dm^3, △: Temperature of treatment vessel at each treatment time.

5.4. Conclusions

Precipitation recovery of arsenic and detoxification of model wastewater containing arsenate, arsenite and mixture of each ions were investigated. In order to recover $As^{III}O_3^{3-}$, simultaneous oxidation and mineralization of arsenite were effective to precipitate arsenic as $Ca_5(AsO_4)_3(OH)$ mineral with high yield. The amount of H_2O_2 addition depends on the initial concentration of arsenite ion. The optimum treatment conditions were at 150 °C for 12 h with 5 % of H_2O_2 for the model wastewater, which contains 2000 mg/dm^3 of arsenite ion. The hydrothermal mineralization treatment with $Ca(OH)_2$ precipitates arsenate ions effectively as reusable arsenate apatite mineral ($Ca_5(AsO_4)_3(OH)$). The arsenic concentration of the treated-water was approximately 0.02 mg/dm^3 regardless of its initial concentration, but it depended on only the solubility of $Ca_5(AsO_4)_3(OH)$ and amount of added H_2O_2. As a result, arsenite ions were precipitated completely and the As concentration in treated-water was lower than the NESJ, 0.1 mg/dm^3. On the other hand, arsenate ion

was easily recovered as arsenate apatite ($Ca_5(AsO_4)_3(OH)$) by hydrothermal mineralization treatment. The arsenic concentration in the treated-water was 0.02 mg/dm^3 treated for the model wastewater containing 1 – 2000 mg/dm^3 of arsenate ion. In order to precipitate arsenic from mixed solution of arsenate and arsenite ions, simultaneous treatment with mineralization and oxidation by using H_2O_2 oxidizer was found effective. Formation of arsenate apatite was carried out by heterogeneous nucleation. Therefore, the precipitation of $Ca(OH)_2$ was essential to recover arsenic compounds from aqueous media by hydrothermal mineralization treatment.

The separation of aqueous solution from precipitate under hydrothermal condition could completely prevent re-dissolution of formed arsenate apatite. Additionally, it could avoid the treatment time to increase crystallinity and/or grain growth. As a result, yield recovery of As was increased and optimal treatment time was shortened. Therefore, the hydrothermal mineralization treatment would be more effective to precipitate arsenic species from aqueous media by constructing flow-type hydrothermal treatment apparatus.

References

1. M. Bissen, and F. H. Frimmel, *Acta Hydrochimica Et Hydrobiologica* **31**, (2), (2003). 97-107

2. M. Bissen, and F. H. Frimmel, *Acta Hydrochimica Et Hydrobiologica* **31**, (1), (2003). 9-18

3. U. K. Klaning, B. H. J. Bielski, and K. Sehested, *Inorganic Chemistry* **28**, (14), (1989). 2717-2724

4. U. K. Klaning, and K. Sehested, *Journal of Physical Chemistry* **90**, (21), (1986). 5460-5464

5. P. L. Smedley, and D. G. Kinniburgh, *Applied Geochemistry* **17**, (5), (2002).

517-568

6. P. Xu, S. B. Huang, Z. J. Wang, and G. Lagos, *Science of the Total Environment* **362**, (1-3), (2006). 50-55

7. K. S. Murray, D. T. Rogers, and M. M. Kaufman, *Journal of the American Water Resources Association* **42**, (3), (2006). 777-792

8. J. R. Parga, D. L. Cocke, J. L. Valenzuela, J. A. Gomes, M. Kesmez, G. Irwin, H. Moreno, and M. Weir, *J. Hazard. Mater.* **124**, (1-3), (2005). 247-254

9. M. A. Hossain, M. K. Sengupta, S. Ahamed, M. M. Rahman, D. Mondal, D. Lodh, B. Das, B. Nayak, B. K. Roy, A. Mukherjee, and D. Chakraborti, *Environ. Sci. Technol.* **39**, (11), (2005). 4300-4306

10. J. Akai, K. Izumi, H. Fukuhara, H. Masuda, S. Nakano, T. Yoshimura, H. Ohfuji, H. M. Anawar, and K. Akai, *Applied Geochemistry* **19**, (2), (2004). 215-230

11. M. Akcay, H. M. Ozkan, C. J. Moon, and B. Spiro, *Ore Geology Reviews* **29**, (1), (2006). 19-51

12. N. J. Cook, *Ore Geology Reviews* **11**, (5), (1996). 303-338

13. D. G. Rancourt, D. Fortin, T. Pichler, P. J. Thibault, G. Lamarche, R. V. Morris, and P. H. J. Mercier, *American Mineralogist* **86**, (7-8), (2001). 834-851

14. P. R. Kumar, S. Chaudhari, K. C. Khilar, and S. P. Mahajan, *Chemosphere* **55**, (9), (2004). 1245-1252

15. H. Gecol, E. Ergican, and A. Fuchs, *Journal of Membrane Science* **241**, (1), (2004). 105-119

16. Y. Sato, M. Kang, T. Kamei, and Y. Magara, *Water Res.* **36**, (13), (2002). 3371-3377

17. I. A. Katsoyiannis, and A. I. Zouboulis, *Water Research* **38**, (1), (2004). 17-26

18. M. X. Loukidou, K. A. Matis, A. I. Zouboulis, and M. Liakopoulou-Kyriakidou, *Water Res.* **37**, (18), (2003). 4544-4552

19. M. L. Pierce, and C. B. Moore, *Water Res.* **16**, (7), (1982). 1247-1253

20. S. Fendorf, M. J. Eick, P. Grossl, and D. L. Sparks, *Environ. Sci. Technol.* **31**, (2), (1997). 315-320

21. D. M. Sherman, and S. R. Randall, *Geochim. Cosmochim. Acta* **67**, (22), (2003). 4223-4230

22. S. Bang, M. D. Johnson, G. P. Korfiatis, and X. G. Meng, *Water Res.* **39**, (5), (2005). 763-770

23. B. A. Manning, M. L. Hunt, C. Amrhein, and J. A. Yarmoff, *Environ. Sci. Technol.* **36**, (24), (2002). 5455-5461

24. S. R. Kanel, B. Manning, L. Charlet, and H. Choi, *Environ. Sci. Technol.* **39**, (5), (2005). 1291-1298

25. F. S. Zhang, and H. Itoh, *Chemosphere* **60**, (3), (2005). 319-325

26. O. X. Leupin, and S. J. Hug, *Water Res.* **39**, (9), (2005). 1729-1740

27. S. J. Hug, and O. Leupin, *Environ. Sci. Technol.* **37**, (12), (2003). 2734-2742

28. S. J. Hug, L. Canonica, M. Wegelin, D. Gechter, and U. Von Gunten, *Environ. Sci. Technol.* **35**, (10), (2001). 2114-2121

29. A. J. Bednar, J. R. Garbarino, J. F. Ranville, and T. R. Wildeman, *Journal of Geochemical Exploration* **85**, (2), (2005). 55-62

30. J. Ryu, and W. Choi, *Environ. Sci. Technol.* **38**, (10), (2004). 2928-2933

31. G. Ghurye, and D. Clifford, *Journal American Water Works Association* **96**, (1), (2004). 84-96

32. C. Casiot, O. Bruneel, J. C. Personne, M. Leblanc, and F. Elbaz-Poulichet, *Science of the Total Environment* **320**, (2-3), (2004). 259-267

33. T. Itakura, R. Sasai, and H. Itoh, *Bulletin of the Chemical Society of Japan* **79**, (8), (2006). 1303-1307

34. T. Itakura, R. Sasai, and H. Itoh, *Water Res.* **39**, (12), (2005). 2543-2548

35. T. Itakura, R. Sasai, and H. Itoh, *Chemistry Letters* **35**, (11), (2006). 1270-1271

36. V. Lenoble, V. Deluchat, B. Serpaud, and J. C. Bollinger, *Talanta* **61**, (3), (2003). 267-276

37. J. V. Bothe, and P. W. Brown, *Environmental Science & Technology* **33**, (21), (1999). 3806-3811

38. J. V. Bothe, and P. W. Brown, *Journal of Hazardous Materials* **69**, (2), (1999). 197-207

Chapter 6 Hydrothermal mineralization treatment for removing/recovering antimonic ion in water

6.1. Introduction

There has been a growing concern over the adverse effect of antimony on human health due to its toxicity and increase in industrial use [1]. Antimony has been used in large quantities for fire retardants, ceramics and the other advanced material manufacturing. The World Health Organization (WHO) allows 5 μg/dm^3 for antimony by the guideline [2]. National drinking water contaminant standard of the United States is set at 6 μg /dm^3 and Japan is 2 μg/dm^3 [3]. Generally, the standard for effluent is set at ten times higher than that of drinking water ex. 20 μg/dm^3 in Japan. Therefore, establishment of the detoxification treatment for wastewater containing Sb is strongly desired.

It is well known that the dominant oxidation state of antimony in most oxygenated environmental water is Sb(V) from the examination to determine the type of antimony for estimation of health risk [4]. Various removal treatments for Sb from polluted water were investigated e.g. by adsorption [5-10], electro-coagulation [11], solvent extraction [12], and membrane methods [4, 13]. However, these methods have less removal ability, especially for treating heavily contaminated water. Additionally, chemical species collected by these methods cannot be reused as resources for production. In previous Chapters, we investigated the recovery of As from $As^{V}O_4^{3-}$/$As^{III}O_3^{3-}$, or B from $B(OH)_4^-$/BF_4^- contained in aqueous media as natural mineral by hydrothermal mineralization [14-16]. Properties of $Sb^{V}O_4^{3-}$ resemble to the same group elements in the periodic table, such as phosphoric acid ($P^{V}O_4^{3-}$) and arsenate ($As^{V}O_4^{3-}$) acid. Thus, it is expected that the hydrothermal mineralization

treatment can be applied to the contaminated water by $Sb^{V}O_4^{3-}$ for recovering Sb as precipitate and detoxify the polluted water.

6.2. Experimental

Model wastewaters containing 90 mg/dm^3 (0.74 mmol/dm^3) of pentavalent antimony (dissolved as $Sb^{V}O_4^{3-}$) were prepared by dissolving Sb_2O_5 in distilled and deionized water. Then, 30 dm^3 of the model wastewater was sealed in a pressure vessel lined with fluorocarbon resin together with mineralizer $Ca(OH)_2$. Hydrothermal mineralization treatments were carried out by leaving the vessel in a dry oven for 2 – 12 h at 150 – 230 °C. After the treatment, the vessel was cooled down in room temperature for 1 h or in ice water for 10 min. Determination of Sb concentration and the analysis of the precipitates before and after the treatment were carried out by inductively coupled plasma mass spectrometry (ICP-MS) and X-ray diffraction (XRD) respectively.

6.3. Results and Discussions

Figure 6-1 shows the treatment time dependence of the Sb concentration in the water treated at 150 – 230 °C with 0.05 – 0.3 g of $Ca(OH)_2$ mineralizer. Sb concentration only by addition of $Ca(OH)_2$ (i.e. before the hydrothermal treatment) did not reduce. However, it decreased drastically by applying the hydrothermal mineralization treatment. Residual Sb concentrations were decreased with an increase of treatment temperature and it was 0.06 mg/dm^3 at 230 °C for 12 h with 0.3 g of $Ca(OH)_2$. Therefore, the hydrothermal mineralization treatment is definitely effective for reducing Sb in aqueous media. Figure 6-2 shows the XRD pattern of the precipitate obtained by the treatment with 0.05 g $Ca(OH)_2$ at 200 °C for 12 h. The

precipitate formed by the treatment was $Ca_2Sb_2O_7$, which has the structure similar to Monimolite ($(Pb,Ca)_2Sb_2O_7$). The recovered $Ca_2Sb_2O_7$ would be easily reused by the conventional resource manufacturing process. Although, residual Sb concentration did not vary drastically by changing the added $Ca(OH)_2$ amount in the range of 0.1 – 0.3 g, it was gradually decreased. As the solubility of $Ca(OH)_2$ into water is constant at a given hydrothermal condition, Ca^{2+} concentration in solution does not vary by changing the added amount of $Ca(OH)_2$, even when the added amount of $Ca(OH)_2$ is 0.05 g which showed low recovery rate of Sb (Figure 6-1-(b)). Thus, it is expected that the formation reaction of the $Ca_2Sb_2O_7$ may occur between SbO_4^{3-} and the precipitate of $Ca(OH)_2$ mineralizer. Improvement of yield recovery of Sb would be attained by increasing the surface area of $Ca(OH)_2$ precipitate used for the formation reaction of $Ca_2Sb_2O_7$. Furthermore, residual concentration decreased to 0.05 mg/dm^3 by rapid cooling in ice water (see in Figure 6-1-(b)) which is lower than the Sb concentration treated with 0.3 g of $Ca(OH)_2$ at 230 °C. This result indicates that the solubility of $Ca_2Sb_2O_7$ under hydrothermal condition is lower than that under ordinary temperature and pressure. In this study, a batch type of pressure vessel was cooled down to room temperature for 1 h after the treatment. During this process, re-dissolution of $Ca_2Sb_2O_7$ would occur and Sb concentration increase. On the other hand, a rapid cooling of the vessel prevented the re-dissolution of $Ca_2Sb_2O_7$ in shorter cooling process (typically for 10 min). Decrease of Sb concentration was achieved through the separation of the solvent from precipitate before re-dissolving a large amount of $Ca_2Sb_2O_7$ into treated-water. This result suggests that every Sb concentration after the treatment in this study would be higher than that in-situ under hydrothermal condition. Therefore, the system construction to separate reaction solution from precipitate in-situ under hydrothermal condition would improve the efficiency to remove and recover Sb by hydrothermal mineralization.

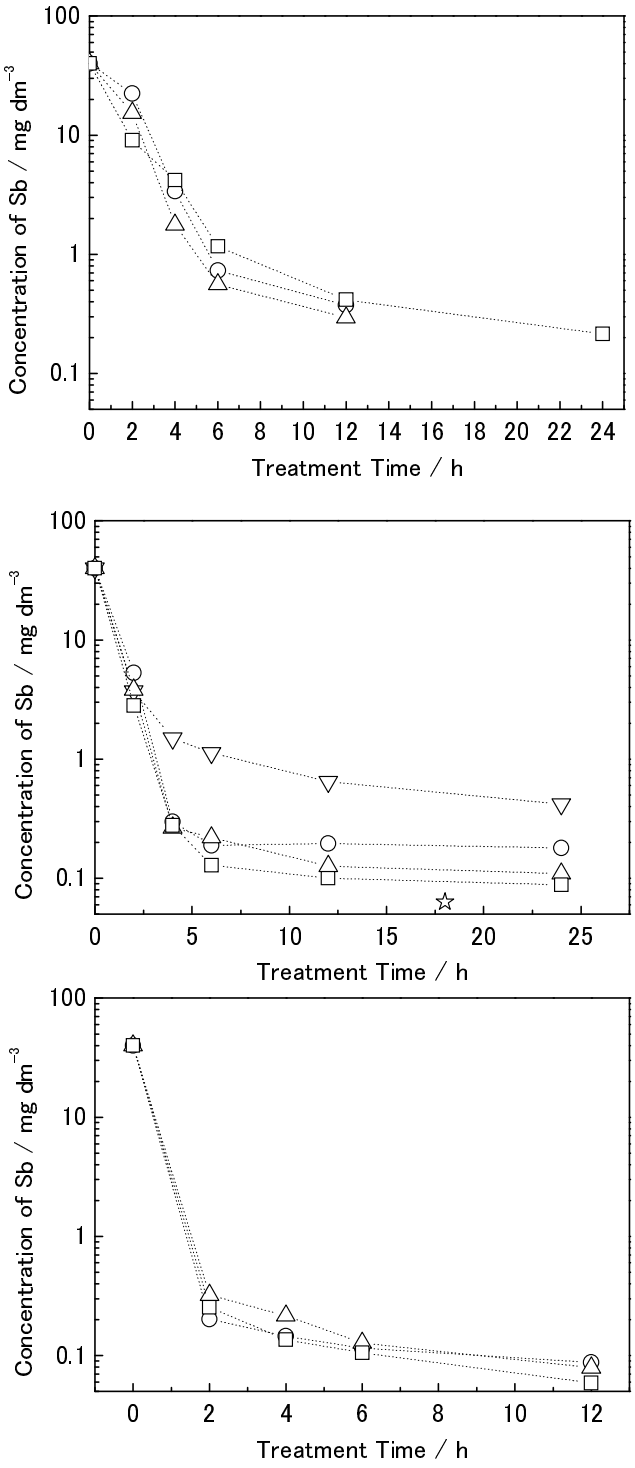

Figure 6-1. Dependence of the Sb on the treatment time with ▽; 0.05 g, ○; 0.1 g, △; 0.2 g, □ and ☆; 0.3 g $Ca(OH)_2$ mineralizer. (a); 150 °C, (b); 200 °C, (c); 230 °C. ☆; rapidly cooled down by ice water for 5 min.

From this consideration, all of Sb concentration after the treatment shown in this study would be higher than that of under hydrothermal condition. Therefore, system construction to separate reaction solution from precipitate under hydrothermal condition would improve efficiency of removal and recovering Sb by hydrothermal mineralization treatment.

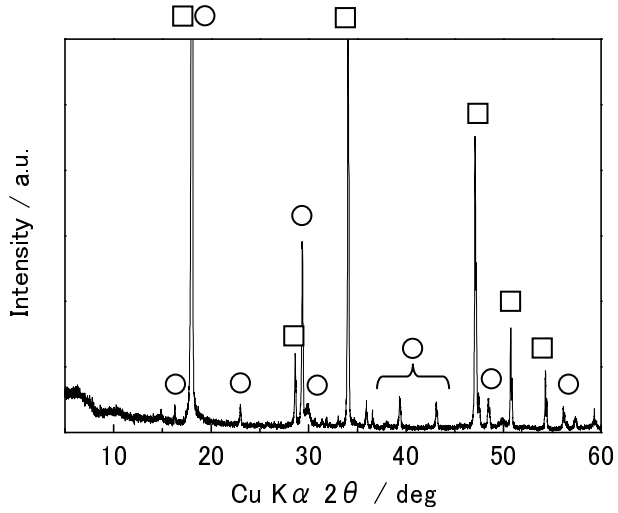

Figure 6-2. XRD pattern of the precipitate obtained by hydrothermal treatment at 200 °C for 24 h with 0.05 g of $Ca(OH)_2$. ○: $Ca_2Sb_2O_7$, □: $Ca(OH)_2$.

6.4. Conclusions

It is concluded that the hydrothermal mineralization treatment is effective for recovering SbO_4^{3-} from aqueous media. The recovered mineral was $Ca_2Sb_2O_7$, which had a structure similar to Monimolite. Thus, reuse of the formed precipitate would become possible by incorporating this process into the traditional resource manufacturing process. Rapid cooling test showed that the solubility of $Ca_2Sb_2O_7$ under hydrothermal condition was lower than that under room temperature and pressure. Therefore, it is expected that the separation of reaction solution and precipitate *in-situ* under hydrothermal condition bring about the improvement of higher yield recovery of Sb.

References

1. N. Khalid, S. Ahmad, A. Toheed, and J. Ahmed, *Applied Radiation and Isotopes* **52**, (1), (2000). 31-38

2. WHO, *Geneva: World Health Organization*, (1993).

3. Y. Nakamura, and T. Tokunaga, *Water Science and Technology* **34**, (7-8), (1996). 133-136

4. T. Saito, S. Tsuneda, A. Hirata, S. Nishiyama, K. Saito, K. Saito, K. Sugita, K. Uezu, M. Tamada, and T. Sugo, *Separation Science and Technology* **39**, (13), (2004). 3011-3022

5. B. B. Tewari, and M. Boodhoo, *Journal of Colloid and Interface Science* **289**, (2), (2005). 328-332

6. M. Kang, T. Kamei, and Y. Magara, *Water Research* **37**, (17), (2003). 4171-4179

7. P. Navarro, and F. J. Alguacil, *Hydrometallurgy* **66**, (1-3), (2002). 101-105

8. A. G. Leyva, J. Marrero, P. Smichowski, and D. Cicerone, *Environmental Science & Technology* **35**, (18), (2001). 3669-3675

9. N. V. Deorkar, and L. L. Tavlarides, *Hydrometallurgy* **46**, (1-2), (1997). 121-135

10. S. M. Hasany, and M. H. Chaudhary, *Applied Radiation and Isotopes* **47**, (4), (1996). 467-471

11. A. S. Koparal, R. Ozgur, U. B. Ogutveren, and H. Bergmann, *Separation and Purification Technology* **37**, (2), (2004). 107-116

12. P. Navarro, J. Simpson, and F. J. Alguacil, *Hydrometallurgy* **53**, (2), (1999). 121-131

13. M. Kang, M. Kawasaki, S. Tamada, T. Kamei, and Y. Magara, *Desalination*

131, (1-3), (2000). 293-298

14. T. Itakura, R. Sasai, and H. Itoh, *Chemistry Letters* **35**, (11), (2006). 1270-1271

15. T. Itakura, R. Sasai, and H. Itoh, *Water Research* **39**, (12), (2005). 2543-2548

16. T. Itakura, R. Sasai, and H. Itoh, *Bulletin of the Chemical Society of Japan* **79**, (8), (2006). 1303-1307

Chapter 7 Detoxification of wastewater containing ionic liquid by combination of hydrothermal mineralization and photocatalytic decomposition

7.1. Introduction

Ionic liquids (ILs), which exist in a stable liquid phase at room temperature, have been increasingly studied recently as environmentally benign, or "green" solvents [1, 2]. They are generally composed of organic cations (e.g., ammonium, imidazolium, phosphonium or pyridinium ions) and inorganic or organic anions (e.g., Cl^-, BF_4^-, PF_6^- or $TFSI^-$ ions). Figure 7-1 shows the chemical structures of imidazolium cation, PF_6^- and TFSI anions. The nature of ILs are largely determined, in particular, on microscopic nature of the mixture with water. For instance, ILs based on hydrophilic counter-anions, like Cl^- or BF_4^-, are soluble into water, but ILs with hydrophobic counter-anions like PF_6^- or $TFSI^-$ anions are hardly soluble. The most commonly used ILs are made up of a dialkylimidazolium cation and hydrophobic anions such as PF_6^-. The feature can be exploited for liquid-liquid-separation, the efficiency of which is generally superior to the traditional organic liquids because of their physical properties such as non-volatility, chemical stability and easy tunability [3-8].

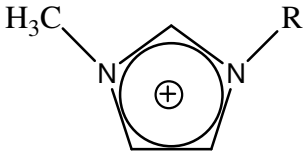

BMI^+: R= C_4H_9

1-butyl-3-methyl-imidazolium (BMI)

EMI^+: R= C_2H_5

1-ethyl-3-methyl-imidazolium (EMI)

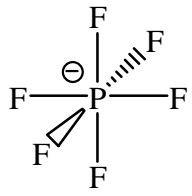

PF_6^-

Hexafluorophosphate

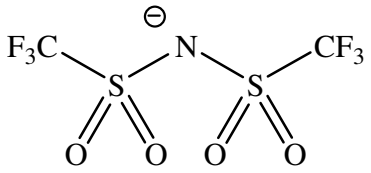

$TFSI^-$

Bis(trifluoromethylsulfonyl)imide

Figure 7-1. The BMI^+, EMI^+, PF_6^- and $TFSI^-$ ions.

Therefore, one of the most important factors for the actual application of ILs consists in their high stability. However, these physical properties of ILs have a negative aspect for decomposition treatment of ILs in order to prevent their emission into the environment. Dissolution of ILs into water would be slightly possible when they are subject to liquid-liquid extraction. Thus, it is anticipated to be effluent in the environment. The environmental risk of commercially available ILs and detoxification of aqueous solutions containing ILs have been discussed recently [3, 9]. However, these reports focus entirely on only the decomposition of organic cations, but do not refer the detoxification of inorganic anion parts. ILs have anion parts containing P, B, F and the other elements, which are inhibited to discharge owing to the environmental and effluent water quality standards. Therefore, the detoxification treatment for both organic cations and inorganic anions is required, when wastewater containing these ILs is discharged to the environment.

In Chapter 3 is described that the hydrothermal mineralization treatment is effective to remove and recover BF_4^- anion from aqueous media. Thus, it is expected that the hydrothermal mineralization treatment would be a capable method for removing these counter anions such as PF_6 and BF_4 in ILs On the other hand, the decomposition of organic cation parts in ILs would be so difficult under subcritical hydrothermal conditions that we focused on the photocatalytic oxidation and decomposition treatment for organic parts. Therefore, we investigated in this chapter the detoxification of aqueous media containing various kinds of ILs ((EMI)PF_6, (BMI)BF_4, (EMI)Br and (EMI)TFSI) by applying hydrothermal mineralization for recovering inorganic anion part, and photocatalytic oxidation for decomposing organic cation part.

7.2. Experimental

7.2.1. Hydrothermal treatment

Model wastewater with 200 mg/dm^3 of each ionic liquid (Nippon gousei Co. Ltd.) was prepared by dissolving each IL in distilled and deionized water. Each model wastewater (30 ml) was sealed in a pressure vessel lined with fluorocarbon resin together with mineralizer $Ca(OH)_2$ and oxidizer H_2O_2. Hydrothermal treatment was carried out by leaving the vessel in a dry oven for 2 – 24 h at 150 - 200 °C. After the hydrothermal treatment, the vessel was cooled down in atmospheric air for 1 h. Precipitates obtained by the hydrothermal treatment were filtered and collected.

7.2.2. Photocatalytic oxidation

TiO_2 (JRC-TIO-8, anatase type, 338 m^{2}g^{-1}) was supplied from the Catalyst Society of Japan, and Pt/TiO_2 (335 m^{2}g^{-1}) was prepared from the TiO_2 and an aqueous H_2PtCl_6 solution with 50% methanol by photodeposition method [10]. Photodecomposition reaction was carried out by irradiating the UV light from 300 W Xe lamp to the quartz reactor set in a closed photocatalytic reaction system. Model wastewaters with 20 mg/dm^3 of ILs were prepared by dissolving them in distilled and deionized water. The TiO_2 or Pt/TiO_2 was suspended in model wastewater under O_2 atmosphere, stirred and photoirradiated at room temperature.

7.2.3. Analytical method

The precipitates were identified by X-ray diffraction (XRD: RIGAKU Rint-2500) using CuKα radiation. Quantitative elemental analysis of phosphorous and boron in the solvent, which was obtained after the hydrothermal treatment, was carried out by using the inductively coupled plasma-atomic emission spectrometry (ICP-AES: Perkin-Elmer, Optima3300DV). Ion chromatograph analysis with suppressor (CSRS

ULTRA II 4-mm Auto Suppression External Water Mode) and conductivity detector were performed before and after the treatment for measurements of the concentrations of EMI^+ and BMI^+ (Column: Dionex IonPac CS12A + CG12A, Mobile phase 30 mmol/dm^3 Methanesulfonic acid / 15 (v/v)% Acetonitrile aq), and PF_6^-, BF_4^- and $TFSI^-$ (Column: Dionex IonPac AS12A + AG12A, 1.35 mmol/dm^3 Na_2CO_3 / 50 (v/v)% Acetonitrile aq). Quantitative and qualitative measurements of the organic compounds formed after the treatment, were carried out by GC-MS (Shimadzu, GCMS-QP5050A).

7.3. Results and Discussion

7.3.1. Hydrothermal mineralization treatment

$NaBF_4$ contained in aqueous solution was effectively decomposed and removed as precipitate by hydrothermal mineralization treatment with $Ca(OH)_2$ mineralizer as described in Chapter 3. Thus, we examined firstly the precipitation removal of $NaPF_6$ from aqueous media by hydrothermal mineralization treatment, because PF_6^- counter anion is included in commonly used ILs. Table 7-1 shows the removal yield of phosphorous by the treatment at 150 or 200 °C for 8 h with $Ca(OH)_2$ mineralizer and H_2O_2 oxidizer. More than 99.9 % of phosphorous was removed by the treatment at 200 °C regardless of the addition of H_2O_2. At the early stage of the treatment, decomposition of PF_6^- would occur by alkali, high temperature and high pressure conditions to form PO_4^{3-} and F^-. The precipitation removal of F^- and PO_4^{3-} by using hydrothermal mineralization treatment at lower treatment temperature, e.g., at 150 °C was already mentioned in Chapters 2 and 3. Thus, low removal yield of phosphorous treated at 150 °C would cause the low decomposition rate of PF_6^- by the treatment. Therefore, higher temperature treatment would be required in order to decompose PF_6^-. Figure 7-2 shows the removal yield of phosphorous by hydrothermal mineralization

treatment of the aqueous solution containing 200 mg/dm^3 of (BMI)PF_6 with $Ca(OH)_2$ oxidizer at 150 or 200 °C. Removal yield of phosphorous from (BMI)PF_6 showed the same behavior as the treatment of $NaPF_6$ aqueous solution. Figure 7-3 shows the XRD pattern of the precipitate after the treatment of the solution containing (BMI)PF_6 with $Ca(OH)_2$ mineralizer at 200 °C. Diffraction peaks of CaF_2 and $Ca_5(PO_4)_3(OH)$ were observed. As shown in Chapters 2 and 3, these compounds were formed by the reaction of $Ca(OH)_2$ and HPO_4^{2-}/F^- under hydrothermal conditions. This result is one of the evidences that decomposition reaction of PF_6^- in (BMI)PF_6 contained in the (BMI)PF_6 would occur by this treatment and form F^- and PO_4^{3-} ions formed. Therefore, the essential step for decomposition is not to dissociate the anion part PF_6^- from (BMI)PF_6, but to decompose directly PF_6 and generate PO_4^{3-} and F^- to form precipitate. $CaCO_3$ observed in Figure 7-3 would be formed by the reaction of $Ca(OH)_2$ with CO_3^{2-} which generated by decomposition of organic part in (BMI)PF_6. However, decomposition yield of imidazolium cation part was not enough to detoxify model wastewater completely (36.1 %) even when the hydrothermal mineralization treatment time was 24 h (see Table 7-2). Thus, we investigated the photocatalytic oxidation in order to decompose cation part by using Pt/TiO_2 and TiO_2.

Table 7-1. Phosphorous removal yield by hydrothermal mineralization treatment of aqueous media containing PF_6^- (Initial concentration of PF_6^- was 200 mg/dm^3)

Temperature / °C	H_2O_2 addition / %	Treatment time / h	P removal / %
25	0	0	0.6
25	3	0	13.8
150	0	8	27.5
150	3	8	30
200	0	8	99.9
200	1	8	99.9

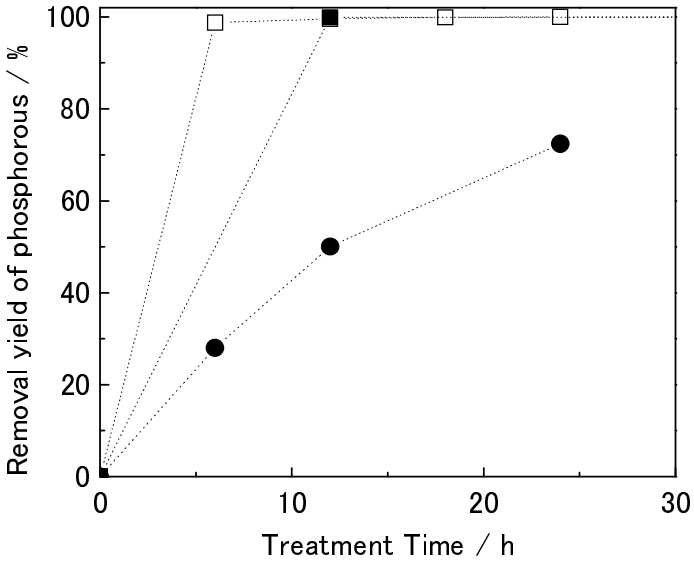

Figure 7-2. Removal yield of phosphorous by hydrothermal mineralization treatment of the model wastewater containing 200 mg/dm^3 of (BMI)PF_6 with $Ca(OH)_2$ mineralizer. ●: 150 °C with 3 % H_2O_2, ■: 200 °C with 3 % H_2O_2 and □: 200 °C without H_2O_2.

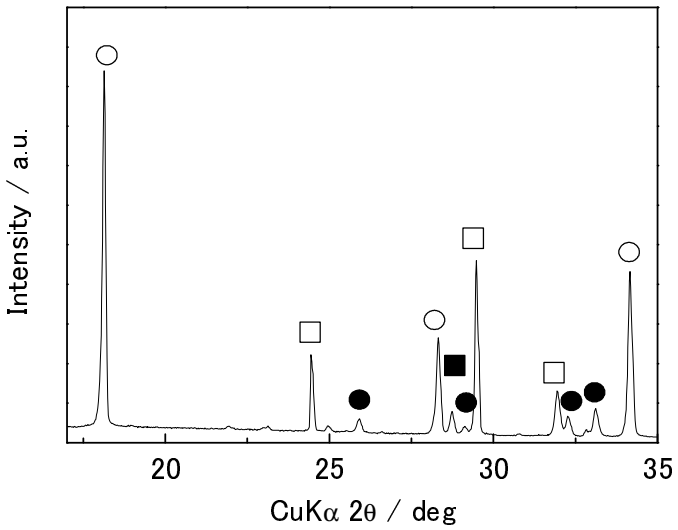

Figure 7-3. XRD pattern of the precipitate obtained by the hydrothermal mineralization treatment at 200 °C for 12 h for the model wastewater containing 200 mg/dm^3 of (BMI)PF_6 with $Ca(OH)_2$. ●: $Ca_5(PO_4)_3(OH)$, ■: CaF_2, ○: $Ca(OH)_2$ and □: $CaCO_3$.

7.3.2. Photocatalytic Decomposition

The photocatalytic oxidation was performed in order to decompose cation part completely by using the photocatalysts Pt/TiO_2 and TiO_2. Table 7-2 shows the decomposition rate and removal rate of anion and cation parts of ILs treated by 24 h UV irradiation with TiO_2 or Pt/TiO_2 and/or hydrothermal mineralization treatment for aqueous solutions containing 20 mg/dm^3 of ILs. As a result, cation parts of all ILs were effectively decomposed by the photocatalytic oxidation. The anion part of PF_6^- cannot be decomposed by photocatalytic oxidation, while BF_4^- contained in (BMI)BF_4 was decomposed mostly by photocatalytic treatment. As shown in the removal rate after the photocatalytic treatment only, however, boron and fluorine still exist in aqueous solution as H_3BO_4 and F^-. In order to remove the cation part, the photocatalytic decomposition was followed by hydrothermal mineralization treatment at 200 °C for 24 h in the aqueous solution containing 20 mg/dm^3 (EMI)PF_6. As a result, all of chemicals composing ILs were mostly decomposed and removed. Thus,

detoxification treatment of aqueous media containing (EMI)PF_6 was finally achieved. This result indicates that the aqueous media containing (BMI)BF_4 would be detoxified by the combination treatment of hydrothermal mineralization and photocatalytic oxidation, because both cation and anion parts are already removed or decomposed by each treatment (see Table 7-2 and Chapter 3). On the other hand, the decomposition of $TFSI^-$ by using both photocatalytic decomposition and hydrothermal mineralization treatment cannot be accomplished even by using both photocatalytic decomposition and hydrothermal mineralization treatments (Table 7-2). Therefore, the other decomposition or removal treatment is necessary for treating (BMI) or (EMI)-TFSI.

Table 7-3 shows the inversion rate to CO_2 and carbon balance treated in aqueous solution containing 20 mg/dm^3 (EMI)Br with Pt/TiO_2 for 24 h UV irradiation. Approximately 70 % of carbon was discharged as CO_2 into gas phase and the residual carbon was detected as ethyl-amine in the treated-water. The carbon balance derived from generated CO_2 and residual ethyl-amine was 97.8 % (see Table 7-3), so that ethyl-methyl-imidazolium cation in the model wastewater was considered to decompose to CO_2 via ethyl-amine intermediate compound.

Table 7-2. Decomposition rate of anion and cation parts of each ILs, and removal rate of anion part treated by hydrothermal treatment and/or photocatalytic decomposition

ILs	Treatment method	Decomposition rate of anion part / %	Removal rate of anion part / %	Decomposition rate of cation part / %
(EMI)Br	Pt/TiO_2	-	0	87.8
(EMI)PF_6	Pt/TiO_2	20.5	0	99.9
	TiO_2	24	0	99.9
	Hydrothermal treatment	99.8	99.8	36.1
	Pt/TiO_2 after hydrothermal treatment	99.8	99.8	99.9
(BMI)BF_4	Pt/TiO_2	99.9	0	99.9
	Hydrothermal treatment	99.9	99.9	36.3
(EMI)TFSI	Pt/TiO_2	21.3	0	99.9
	Hydrothermal treatment	0	0	25.1

(Irradiated light intensity was 19 mW/cm^2 (220-300 nm), 71 mW/cm^2 (310-400 nm) and 175 mW/cm^2 (360-470 nm). Treatment time was 24 h.)

Table 7-3. Amount of CO_2 generated, inversion rate and carbon balance

(EMI)Br concentration	Amount of CO_2 / μ mol	Inversion rate of CO_2 / %	Carbon balance / %
20 mg/dm^3	38.8	69	97.8

(Irradiated light intensities were 19 mW/cm^2 (220-300 nm), 71 mW/cm^2 (310-400 nm) and 175 mW/cm^2 (360-470 nm). Treatment time: 24 h.)

7.4. Conclusions

Detoxification method of aqueous media containing ionic liquids (ILs) by the combination of the hydrothermal mineralization and the photocatalytic decomposition was investigated. Anions contained in the ILs such as PF_6, BF_4 were effectively removed by the hydrothermal mineralization treatment with $Ca(OH)_2$ mineralizer. On the other hand, photocatalytic oxidation by using TiO_2 or Pt/TiO_2 decomposed organic cation parts completely. Therefore, the detoxification of aqueous solutions containing PF_6^- and BF_4^- anions was accomplished. However, both hydrothermal and photocatalytic treatments could not remove and/or decompose $TFSI^-$. Thus, further investigation for decomposing $TFSI^-$ and removing fluorine contained in the $TFSI^-$ would be required in order to meet the standard for discharged water of fluorine.

References

1. R. D. Rogers, and K. R. Seddon, *Science* **302**, (5646), (2003). 792-793

2. G. Chevrot, R. Schurhammer, and G. Wipff, *Physical Chemistry Chemical Physics* **8**, (36), (2006). 4166-4174

3. K. J. Baranyai, G. B. Deacon, D. R. MacFarlane, J. M. Pringle, and J. L. Scott, *Australian Journal of Chemistry* **57**, (2), (2004). 145-147

4. S. Busi, M. Lahtinen, M. Karna, J. Valkonen, E. Kolehmainen, and K. Rissanen, *Journal of Molecular Structure* **787**, (1-3), (2006). 18-30

5. A. G. Glenn, and P. B. Jones, *Tetrahedron Letters* **45**, (37), (2004). 6967-6969

6. W. W. Liu, T. Y. Zhao, Y. M. Zhang, H. P. Wang, and M. F. Yu, *Journal of Solution Chemistry* **35**, (10), (2006). 1337-1346

7. C. F. Poole, *Journal of Chromatography A* **1037**, (1-2), (2004). 49-82

8. U. Domanska, *Thermochimica Acta* **448**, (1), (2006). 19-30

9. A. W. Morawski, M. Janus, I. Goc-Maciejewska, A. Syguda, and J. Pernak, *Polish Journal of Chemistry* **79**, (12), (2005). 1929-1935

10. B. Kraeutler, and A. J. Bard, *Journal of the American Chemical Society* **100**, (13), (1978). 4317-4318

Chapter 8 Summary and perspective

This thesis deals with the research on feasibility of detoxification method of polluted water and resource recovery by hydrothermal mineralization treatment. As a result, hydrothermal mineralization treatment enables not only the detoxification of wastewater polluted by various oxoanions that have no effective removal method for removal, but also the precipitation recovery of resources in the wastewater as natural minerals. This treatment method is independent of the initial concentration of pollutants and the kind of ionic species. It is effective for treating various kinds of wastewaters. Furthermore, in situ solid/liquid separation enabled to improve yield recovery and to shorten optimal treatment time. These results expected that the establishment of a flow-type apparatus for hydrothermal mineralization treatment would contribute to achieve an effective resource circulation and to avoid environmental pollution problems.

The theoretical treatment of hydrothermal mineralization for the polluted water, in other ward, the precipitation mechanism of minerals under hydrothermal conditions could be thermodynamically described as follows. All the minerals formed in this work have negative solubility curves against the increase of temperature. The property of these formed minerals is essential to precipitate harmful oxoanions from polluted water by hydrothermal mineralization. The equation to derive temperature dependence of equilibrium constant is shown in Equation 8-1.

$$K_{T2} = K_{T1}\exp\left(\frac{\Delta_{sol}H^{\circ}(T_2 - T_1)}{RT_1T_2}\right) \tag{8-1}$$

where T_1 and T_2 are the temperatures of solution, R is the gas constant, $\Delta_{sol}H^{\circ}$ is the enthalpy change of dissolution, and K_{T1} and K_{T2} is the equilibrium constants of the temperatures at T_1 and T_2, respectively.

This equation indicates that the compound which has negative standard dissolution enthalpy change shows negative solubility curve against the increase in temperature. All the oxoanions treated in this work had negative enthalpy change due to the stabilization by hydration. This consideration suggests that the other compounds, which have negative enthalpy, would also precipitate by the hydrothermal mineralization treatment. For example, oxoanions such as chromate and selenate have negative standard dissolution enthalpy change. This fact means that the hydrothermal mineralization treatment has the potential to be applied to all kind of precipitation of dissolved oxoanions in water. Table 8-1 shows such compounds which have negative standard dissolution enthalpy change [1]. These data indicate that the hydrothermal mineralization treatment would be effective to precipitate carbonate and nitrate. Therefore, this treatment can be applied not only to wastewater treatment, but also to immobilization of the carbon dioxide and/or nitrogen oxide. However, the solubility of compounds into water is generally determined by standard dissolution enthalpy and entropy change. Thus, the investigation on such data is important to choose cationic species to form minerals. Equation 8-2 shows the equilibrium constant derived from its standard dissolution enthalpy and entropy change.

$$\Delta_{sol}G^\circ = -RT\ln K = \Delta_{sol}H^\circ - T\Delta_{sol}S^\circ; \tag{8-2}$$

where $\Delta_{sol}G^\circ$ is the free energy for dissolution, R is the gas constant, T is temperature, $\Delta_{sol}H^\circ$ is the standard enthalpy change of dissolution, and $\Delta_{sol}S^\circ$ is the standard entropy change of dissolution.

The equation indicates that the standard dissolution entropy change should be negative to achieve low solubility of the formed mineral into water. The amount of

standard dissolution entropy change directly affects the recovery yield and the concentration of hazardous elements contained in the treated-water. Thus, the investigation of cationic species to accomplish the lowest standard dissolution entropy change is necessary in order to form hardly soluble or insoluble minerals. Therefore, the hydrothermal mineralization treatment would be effective treatment method for aqueous media containing various chemicals by further investigations.

Table 8-1. Standard dissolution enthalpy change

Compound	$\Delta solH°$ / kJ mol^{-1}	Compound	$\Delta solH°$ / kJ mol^{-1}
$Ca(NO_3)_2$	-19.16	$Ca_5(PO_4)_3(OH)$	-75.7
$CaCO_3$	-13.08	Na_2CO_3	-26.7
$CaSO_4$	-26.9	Na_2SO_4	-2.43
$CaHPO_4$	-20.59	Na_2HPO_4	-24.06

The experimental results and discussion obtained in this thesis are summarized as follows according to the conclusions of each chapter.

Chapter 1 described the general introduction about the research background on treatments of wastewater and environmental water. The mineralogy and chemistry of elements, which are related to this work are also described. Subsequently, the purposes of the present study were stated followed by description of hydrothermal mineralization treatment and its advantage for treating industrial wastewater.

Chapter 2 described the development of a novel technique for removing boron species from wastewater by hydrothermal mineralization. The present technique made it possible not only to remove the dissolved boron species from wastewater, but also to recover the calcium borate mineral ($Ca_2B_2O_5 \cdot H_2O$) by the addition of $Ca(OH)_2$ and/or H_3PO_4 to wastewater, where $Ca(OH)_2$ and H_3PO_4 were mineralizer and

re-dissolution suppressor of the calcium borate mineral, respectively. More than 99% of boron dissolved into the model wastewater (boron concentration: 500 mg/dm^3) was recovered as the precipitate of $Ca_2B_2O_5 \cdot H_2O$ by the hydrothermal treatment at 130 °C for 14 h with 3.0g of $Ca(OH)_2$ and 1.5g of H_3PO_4. The recovered $Ca_2B_2O_5 \cdot H_2O$ precipitate in the present treatment could be used in the borax production process along with the natural ore of boron, because this compound has a similar crystal structure to colemanite which is natural mineral used for resource manufacturing.

Chapter 3 described the treatment of aqueous media containing fluoride and tetrafluoroboric ions. Fluoride ion included in the model wastewater was collected completely by hydrothermal treatment with $Ca(OH)_2$ at 150 °C for 4 hours. The amount of added $Ca(OH)_2$ was much lower than the conventional lime precipitation method. Recovery of boron and fluorine from model wastewater containing tetrafluoroboric ion was successfully accomplished by hydrothermal mineralization at 150 °C for more than 36 h. Formation of fine particles of CaF_2 by decomposition of BF_4^- had an excellent effect on inhibiting re-dissolution of borate mineral by settling down the particles and forming dense layer on the surface of precipitate. The recovery yield of fluorine and boron was 99.9 % and 98 %, respectively.

Chapter 4 described the detoxification of polluted water containing boric or tetrafluoroboric ions and the resource recovery by in situ solid/liquid separation hydrothermal mineralization treatment. As a result, effective recovery of boron and fluorine was achieved at shorter treatment time (2 h) than ordinary batch-type treatment (12 h) from aqueous solution containing in either case boric or tetrafluoroboric ions. Both boron and fluorine concentrations after the treatment were 4 mg/dm^3 for any model wastewater containing 5 - 3000 mg/dm^3 of boric ion or 8000 mg/dm^3 of tetrafluoroboric ion. Some information was obtained on the decomposition of tetrafluoroboric ion and the formation of fluorite (CaF_2) by

measuring solubility of $Ca(OH)_2$ under hydrothermal condition. The results of this chapter's experiments suggested that the hydrothermal mineralization treatment by using a flow-type apparatus would be effective for treating wastewater and ground water containing these ions.

In chapter 5, the precipitation recovery was investigated for arsenic detoxification by using model wastewaters containing arsenate, arsenite and the mixture of these ions. In order to recover $As^{III}O_3^{3-}$, simultaneous oxidation and mineralization treatments of arsenite were effective to precipitate arsenic as $Ca_5(AsO_4)_3(OH)$ mineral with high yield. The amount of H_2O_2 addition, which is added as oxidant for arsenite ion, depended on the initial concentration of arsenite ion. The optimum treatment conditions were at 150 °C for 12 h with 5 % of H_2O_2 for the model wastewater, which contains 2000 mg/dm^3 of arsenite ion. The arsenic concentration of the treated-water was approximately 0.02 mg/dm^3 regardless of its initial concentration, but it depended on the solubility of $Ca_5(AsO_4)_3(OH)$ and the amount of added H_2O_2. On the other hand, arsenate ion was easily recovered as arsenate apatite ($Ca_5(AsO_4)_3(OH)$ by hydrothermal mineralization treatment. The arsenic concentration in the treated-water was 0.02 mg/dm^3 for the model wastewaters containing 1 - 2000 mg/dm^3 of arsenate ion. In order to precipitate arsenic from mixed solution of arsenate and arsenite ions, simultaneous treatment with mineralization and oxidation by using H_2O_2 oxidizer was found effective. In situ solid/liquid separation effect under hydrothermal condition was also investigated, which resulted in that the yield recovery of As was increased and optimal treatment time was shortened. Therefore, it was found that the hydrothermal mineralization treatment is effective to precipitate arsenic species.

Chapter 6 described the results of the hydrothermal mineralization treatment for antimonic ion. This ion (SbO_4^{3-}) in aqueous media was effectively precipitated as

$Ca_2Sb_2O_7$, which had similar structure to Monimolite. Thus, the reuse of the formed precipitate would be easily attained by incorporating traditional resource manufacturing process.

Chapter 7 described the detoxification treatment for aqueous media containing various kinds of ionic liquids (ILs) by using both hydrothermal mineralization and photocatalytic decomposition. Cation parts of ILs investigated in this study consisted of butyl methyl or ethyl methyl imidazolium, while the anion parts were PF_6, BF_4, Br and TFSI. A series of experiments verified that anions contained in ILs such as PF_6, BF_4, etc. were effectively removed by the hydrothermal mineralization treatment with $Ca(OH)_2$ mineralizer. On the other hand, the organic cation parts were found to be decomposed by the photocatalytic oxidation of TiO_2. Therefore, the detoxification of aqueous solution containing ILs was accomplished.

References

1. *Handbook of the Chemistry fifth edition,* 2004, Maruzen, (In Japanese).

Acknowledgements

This work was carried out at Division of Environmental Research, EcoTopia Science Institute as a doctoral candidate enrolled in the Graduate School of Engineering at the Department of Applied Chemistry, Nagoya University.

I would like to express my sincere gratitude to my supervisor Professor Hideaki Itoh for his pertinent guidance, encouragement and valuable suggestions throughout this work. I also wish to express my gratitude to Professor Hiroki Haraguchi and Assistant Professor Eiji Fujimori for their cooperation to determine the Sb concentration in aqueous media. I would like to express many thanks for Professor Hiroki Haraguchi, Professor Toshiharu Fujisawa, and Professor Hitoki Matsuda and Associate Professor Hisao Yoshida for their reviewing and comments on this thesis.

I am deeply grateful to Associate Professor Hisao Yoshida, and Assistant Professor Ryo Sasai for their valuable comments and discussions in the study.

Special thanks must be expressed to Ms. Reiko Itoh and Mrs. Shinobu Nakao and the other members in Itoh's laboratory for their kind helps in my life and work during this study.

Finally, I express special thanks to my parents Osamu and Sayoko for their constant helps which enabled to continue this work.

Academic Achievements

(a) Original papers

1) “Recovery of Nd from sintered Nd-Fe-B permanent magnet by hydrothermal treatment”, Takeshi Itakura, Ryo Sasai, Hideaki Itoh, *Journal of Alloys and Compounds*, vol. 408-412, 2006, pp. 1382-1385

2) “Precipitation recovery of boron from wastewater by hydrothermal mineralization”, Takeshi Itakura, Ryo Sasai, Hideaki Itoh, *Water Research*, vol. 39, Issue 12, 2005, pp. 2543-2548

3) “A Novel Recovery Method for Treating Wastewater Containing Fluoride and Fluoroboric acid”, Takeshi Itakura, Ryo Sasai, Hideaki Itoh, Bull. *Chem. Soc. Jpn*, vol 79, No. 8, 2006, pp 1303-1307

4) “Arsenic Recovery From Water Containing Arsenite ions by Hydrothermal Mineralization”, Takeshi Itakura, Ryo Sasai, Hideaki Itoh, *Chemistry Letters*, vol 35, No. 11, 2006, 1270-1271

5) “Arsenic Recovery from Water Containing Arsenite and Arsenate ions by Hydrothermal Mineralization”, Takeshi Itakura, Ryo Sasai, Hideaki Itoh, *Journal of Hazardous Materials*, In Press

6) ”A Precipitation Method for Arsenite Ion in Aqueous Solution as Natural Mineral by Hydrothermal Mineralization”, Takeshi Itakura, Ryo Sasai, Hideaki Itoh, Submitted

7) “In Situ Solid/Liquid Separation Effect for High Yield Recovery of Boron and Fluorine from Aqueous Media Containing Boric or Fluoroboric ions” Takeshi Itakura, Ryo Sasai, Hideaki Itoh, Submitted

8) “Detoxification of antimonic contaminated water and precipitation recovery of antimony by hydrothermal mineralization” Takeshi Itakura, Ryo Sasai, Hideaki

Itoh, Submitted

(b) Proceedings

1) ”Resource Recovery from Nd-Fe-B permanent magnet by hydrothermal treatment”, Takeshi Itakura, Ryo Sasai, Hideaki Itoh, Proc. Waste Management in Japan, pp. 41-50, 2004

2) “Resource Recovery from Wastewater Containing Hazardous Oxoanions by Hydrothermal Mineralization”, Takeshi Itakura, Ryo Sasai, Hideaki Itoh, Proc. Waste Management 2006, pp. 201-210, 2006

(c) Reviews

1) 「環境水のヒ素汚染とその無害化技術」, 伊藤秀章、板倉剛(名古屋大学), 化学, 最新のトピックス, 2006 年 12 月号

(d) International meetings (or conferences)

1) “Recovery of Nd from sintered Nd-Fe-B permanent magnet by hydrothermal treatment”, Takeshi Itakura, Ryo Sasai, Hideaki Itoh, The 5th International Meeting of Pacific Rim Ceramic Societies (Pac Rim 5, Nagoya), (2003.10)

2) “Resource Recovery from Nd-Fe-B Permanent Magnet by Hydrothermal Treatment”, Takeshi Itakura, Ryo Sasai, Hideaki Itoh, Waste management2004 (Rhodes, Greece), (2004, 09)

3) “Recovery of Nd from Nd-Fe-B sintered magnet by hydrothermal treatment”, Takeshi Itakura, Ryo Sasai, Hideaki Itoh, Rare Earths '04 in Nara, (2004, 11)

4) “Detoxification and resource recovery of arsenic from wastewater by hydrothermal mineralization”, Takeshi Itakura, Ryo Sasai, Hideaki Itoh, Pacifichem 2005 (Hawaii, USA), (2005, 12)

5) “Resource Recovery from Wastewater Containing Hazardous Oxoanions by Hydrothermal Mineralization”, Takeshi Itakura, Ryo Sasai, Hideaki Itoh, Waste management 2006 (Malta), (2006,06)

(e) Domestic meetings

1）水熱処理によるNd‐Fe‐B系希土類焼結磁石スクラップからのNdの回収, 板倉剛、笹井亮、伊藤秀章, 平成15年度粉体および粉末冶金協会秋期年会, 早稲田大学, (2003.9)

2）水熱処理を用いた Nd-Fe-B 焼結磁石スクラップからの資源回収, 板倉剛、笹井亮、伊藤秀章, 第 29 回東海若手セラミスト懇話会, (2004.05), ポスター

3）水熱鉱化法による工業廃水中のホウ素含有アニオンの無害化と再資源化, 板倉剛、笹井亮、伊藤秀章, GSC シンポジウム 2005 (2005.03), ポスター

4）水熱鉱化法によるホウ素、フッ素含有廃水の無害化と再資源化, 板倉剛、笹井亮、伊藤秀章, 日本化学会第 85 回年会 (2005.03), 口頭

5）水熱鉱化法によるホウ素、フッ素含有工業廃水からの資源回収と再生, 板倉剛、笹井亮、伊藤秀章, 廃棄物学会 2005 年秋期年会 (2005.09), 口頭

6）水熱鉱化法を用いたヒ酸および亜ヒ酸含有排水の無害化, 板倉剛、笹井亮、伊藤秀章, GSC シンポジウム 2006 (2006.03), ポスター

7）水熱鉱化法による排水中のヒ酸および亜ヒ酸イオンの沈殿回収, 板倉剛、笹井亮、伊藤秀章, 日本化学会第 86 回年会 (2006.03), 口頭

8）水熱鉱化法による水溶液中のヒ酸、亜ヒ酸の沈殿回収, 板倉剛、笹井亮、伊藤秀章, 廃棄物学会 (2006.11), 口頭